AN INVESTIGATION OF
BLOCK-FORMED STRUCTURAL
MEMBERS

A Thesis presented
to the Faculty of Civil Engineering
The University of Manitoba

In Partial Fulfillment
of the Requirements for the Degree
Master of Science in Civil Engineering

by
Richard Linton Vere Edghill
January 1971

FACULTY OF GRADUATE STUDIES AND RESEARCH

Report of Thesis Examiners

THIS IS TO CERTIFY THAT the members of the examining committee of the Master's (X) Ph.D. ( ) thesis of:

Richard L. V. Edghill

Major Subject Structural Engineering

Thesis Title An Investigation of Block-Formed Structural Members

have read the thesis and are unanimously agreed that it should be graded

Approved
(approved or rejected)

Date January 26, 1971

Chairman

B.

ACKNOWLEDGEMENTS

The author wishes to express his sincere appreciation to the following for their help in the preparation of this thesis:

R. Lazar, Associate Professor, Department of Civil Engineering, the University of Manitoba, for his interest and advice in carrying out this thesis.

Dr. A. M. Lansdown, Head of the Civil Engineering Department, University of Manitoba, for his advice on the presentation of this thesis.

Mr. Ben Amos for his interest and assistance in obtaining the materials.

The technicians in the Civil Engineering laboratory, Mr. Eduard Lemke and Mr. Jan Rodenhuis in particular, for their assistance in the construction and testing of the members.

Kornovski and Keller Masonry Ltd., for their generous grant which made this thesis possible.

Tallcrete, Supercrete and Dominion Bridge, for donating the materials.

TABLE OF CONTENTS

LIST OF TABLES

LIST OF FIGURES

FIGURE PAGE

FIGURE PAGE

LIST OF SYMBOLS

a'	=	length of region of constant shear
α	=	angle between web reinforcement and axis of beam.
A_v	=	cross-sectional area of web reinforcement
A_s	=	cross-sectional area of longitudinal reinforcement
b	=	width of beam
d	=	depth from compression face to centroid of longitudinal reinforcement
$\Delta(max)$	=	maximum allowable beam deflection
f_c (test)	=	ultimate compressive stress of wall section
f_c (calc.)	=	theoretical ultimate compressive stress of wall section
f'_c	=	ultimate compressive unit strength of concrete cylinder
f'_m	=	ultimate compressive unit strength of mortar cube
f_v	=	tensile yield stress of web reinforcement
f_y	=	tensile yield stress of longitudinal reinforcement
h	=	height of wall section
L	=	length of beam
M	=	moment
p	=	ratio of longitudinal steel to area of concrete section
P(test)	=	applied load on beam at failute
P_f(calc.)	=	load at theoretical flexural capacity of beam

P_v(calc.) = load at theoretical shear capacity of beam

r = percentage of web reinforcement

s = horizontal spacing of web reinforcement

t = thickness of wall section

v = shear

V_c = theoretical shear capacity of concrete section

V_w = theoretical shear capacity of web reinforcement

w = width of wall section

1. INTRODUCTION

In recent years the concrete block has played an important role in most types of construction. The block was initially used as a cladding in steel and reinforced concrete construction. It carried no load but served as an attractive wall or partition with good accoustic qualities.

Engineers soon began to utilize them in load-bearing wall construction. With the advent of the two-core block, it was found that by constructing the wall in running bond, the cores lined up vertically. These cores could be reinforced and filled with concrete at little extra cost. This resulted in a wall inherently stronger under axial load with a capacity to resist bending and shear stresses, thus constituting a shear wall. These advances allowed designers to introduce load-bearing block walls into high-rise construction.

Using the shear-wall technique, structures were designed and built with concrete-filled reinforced block-walls without any other structural framing. With the increase in ductility due to the reinforcement, these methods were also introduced into seismic areas. These structures are now common up to twelve stories in height in earthquake zones such as southern California.

Additional use of concrete blocks have been made in single course lintel beams over door and window openings. Concrete blocks can be built to almost any shape or size. There is no reason why they cannot be used as a permanent form for any type of reinforced concrete structural member. In addition to providing the outer shell, it is assumed that composite action would exist between the shell and concrete fill in resisting stresses. It is hoped that this report will shed some light on the behavior of such members.

Object and Scope of Investigation

This investigation was conducted at the Civil Engineering Testing Laboratory of the University of Manitoba in 1970.

The purpose of the study is to compare, on an experimental basis, the behavior of concrete block-formed reinforced concrete members, to that of a "normal" reinforced concrete member.

Block-formed components differ primarily from reinforced concrete in that the "concrete" is supplied in three different and distinct ways - the precast concrete in the block units, the mortar, and the concrete fill. In contrast, only one more or less homogeneous concrete is used in Reinforced Concrete construction.

To compare these two types of construction, the validity of certain assumptions must be verified:

1. Unity of action exists between the block, concrete fill and the reinforcement in properly built block-formed structural elements.
2. Each individual component of the construction - blocks, concrete fill, masonry and reinforcement - contributes to the ultimate strength of the composite construction.

The last assumption permits the author to design and analyse the test specimens according to current codes on Reinforced Concrete. In the analysis, the presence of the block form is neglected and the concrete fill assumed to cover the overall section.

Scope of the work is limited to beams and wall sections. The flexural and shear capacities of the beams are investigated along with the axial load capacity of the wall sections.

It is beyond the scope of this preliminary type of investigation to subject the elements to all structural conditions. However, it is the intention of the author to present results that could be used for continued investigation into all types of block-formed structural elements.

History of Masonry Construction

Masonry construction is perhaps the oldest form of construction known to civilized man. Masonry structures, built by the ancient Egyptians, are still standing today. The craftsmanship demonstrated by these people is truly a wonder in itself. One such structure recorded in history is the "Pharoh of Alexandria," the lighthouse that stood watch over navigators of the Mediterranean Sea, guiding them to safe harbour. This structure was 550 feet high and the fire that burned at the top could be seen for 35 miles. An ancient description of construction mentions that the masonry courses were made of excellent stone and were united by molten lead. The landmark, buffeted by the elements, stood for 1500 years before being destroyed by an earthquake in the 13th century.[11]

The dark ages of Western Civilization were enhanced by the beauty of castles and cathedrals, some of which took over a century to build. On the one hand, castles were designed to repel assaults rather than for structural strength. These monsters of elegance must also have been status symbols because history seldom recorded an instance wherein a castle fell through the destruction of the outer walls. Castles with walls six to seven feet thick contribute little to the knowledge of the behavior of masonry structures. On the other hand, cathedrals were designed to display majestic beauty. These towers of grandeur must also have been status symbols.

Old cathedrals are true masonry structures; that is, they are completely devoid of metal or wood for structural support. They stand as evidence that builders began to understand stress transfer, at least qualitatively if not quantitatively. The world sees only the edifices that have been built and that have withstood the ravages of time and the elements. Little or nothing is known about those that have failed during the construction or soon after completion. With the passing of time, successes and failures have molded the state of the art of masonry construction.

The genesis of the science of structures was with Aristotle who correctly explained the action of the keystone of the arch as "resisting opposing forces on all sides".

Leonardo de Vinci gave impetus to the science by explaining the interacting of the elements of the arch as "a strength developed by two weaknesses, for the arch is composed of two segments of a circle, each of which, being weak in itself, tend to fall; but each opposes this tendency in the other with the two weaknesses combining to form one strength". The classic explanation has roots in the assumed triangular type loading of masonry over lintels and also in the concept of load redistribution as the materials in composite construction.

The combination of arches and columns was the essence of past construction. Criteria for construction of load bearing masonry in modern times evolved from the traditional arch as it passed through the centuries.

Only in recent times were scientific bodies established to guide the design of structures. Official building codes made their appearance before the turn of the twentieth century. Comparing early codes with the present U.S.A. Standard Building Code Requirements for masonry show little change in requirements in 70 years. The 1902 edition of the District of Columbia Building Code and the U.S.A. Standard have essentially the same wall height-to-thickness requirements; namely, at least 12 inches for the uppermost 25 feet and increasing 4 inches in thickness for each additional 35 feet in height. This is the present day wall design criteria. Not one single mathematical formula pertaining to masonry design is to be found in either publication.

Reinforced masonry has been used for over 100 years. However, it has been only during the past 30 years that the design procedure has been developed to any extent. Reinforced masonry has been widely adopted in two forms - reinforced brick masonry and reinforced concrete masonry.

Reinforced brick masonry is the technique of laying exterior and interior wythes with a grout collar joint in which reinforcement is placed. It provides masonry surfaces of elements of different heights, types, and coursing, all incorporated into a homogeneous structure. Reinforced concrete masonry is a type of construction in which solid or hollow concrete masonry units are assembled in such a way as to form continuous vertical and/or horizontal cavities within the construction. Steel bar reinforcement is then placed in these cavities and the cavities filled with grout or concrete so as to form a bonded composite construction, which will act as a unit in resisting load and stress.

As the name implies, reinforced concrete masonry is similar in most respects to reinforced concrete. It differs from reinforced concrete primarily in that the "concrete" is supplied in three different and distinct forms - the precast concrete in the masonry units, the mortar, and the grout or concrete fill. In contrast, only one more or less homogeneous concrete is used in reinforced concrete construction.

Earthquake Resistance of Reinforced Masonry

Masonry construction has a poor image in many locales because of the poor performance of some unengineered,unreinforced or unanchored masonry. Some unreinforced structures have shown satisfactory performance e.g., some of the massive or conservatively built structures.

However, reinforced masonry has performed quite well in even the most severe quakes. For example, 85% of the masonry buildings that were reinforced and properly tied showed no damage in the major earthquake in Anchorage, Alaska.[10] A good structural comparison was found at Elmandorf Air Force Base near Anchorage. A series of concrete masonry warehouses, 30 feet high with four foot spacing of reinforcement, showed no structural distress whatsoever. However, adjacent to the masonry structures, stood several tilt-up warehouses of similar size. Two segments of the tilt-up buildings collapsed and three were seriously damaged, confirming that the quake was catastrophic, at least to those buildings. Interior partitions and exterior non-load-bearing and load-bearing walls were very common in that area. It is of interest to compare the performance of these walls in Anchorage with masonry walls that were observed in the city of Skopje after the July, 1963 Yugoslavian earthquake.

Extensive loss of life and property was experienced in Skopje due to collapse of load-bearing masonry walls that were not reinforced and were not tied structurally to the slabs they supported. For the most part, these walls were built with lime mortar. In contrast, code requirements in force in Anchorage require that masonry walls be properly reinforced.

In 140 years of organized European settlement, New Zealand has experienced 17 destructive earthquakes.[9] The earthquake of 1931, in particular, showed those concerned with building that the simple load-bearing structures, traditional in Europe, were inadequate to resist earthquake shock. There were many brick buildings in Napier in 1931, and those were largely responsible for the loss of life. Not only were they inadequate in their design, but also in many cases they exhibited inadequate workmanship and poor supervision of construction.

For many years after the 1931 earthquake load-bearing masonry was not allowed in New Zealand. However, a revision of July, 1959 reintroduced the concept of load-bearing masonry, but this time replacing the old rule-of-thumb methods with rational design by elastic analysis. Designers found new allowable stresses for unreinforced masonry limiting. At the same time, earthquake theory was teaching the lesson of ductility and the value of reinforcing for prolonging the load deflection curve. Reinforced masonry, even for panels, seemed inevitable. To date, several load-bearing masonry structures have been designed and built.

A popular form of construction in New Zealand is the cavity wall which consists of an inner and outer leaf separated by a cavity of about 2 inches. The two leaves are connected by galvanized wire ties. The cavity wall has valuable properties for:excluding weather, thermal insulation, and sound insulation. Reinforcement is invariably deformed bars. It is used vertically in low stressed walls; and vertically and horizontally in high stress walls. Reinforcement is spaced at 16 inches to 32 inches on centre.

There are a few overall factors which enhance the behavior of reinforced masonry in seismic areas:

(1) Properly designed buildings perform in a dramatically more satisfactory manner compared to unanchored, undesigned

buildings of low factors of safety to lateral loads.

(2) The damping characteristics of masonry reduce the response to quakes.

(3) The natural frequency of these stiff structures may place them in the short period range where they have less response to quakes.

(4) Failures in reinforced masonry are of a ductile type which is a very effective type of resistance in catastrophic quakes. The avoiding of brittle or sudden complete failures is regarded as very important.

Finally, the confidence with which reinforced masonry is used by designers in high seismic areas is related to the confidence in their design methods, in their detailing for ductility, in the quality of the available materials and in the quality of the supervision and workmanship.

Advantages of Reinforced Masonry

The advantages of brick and concrete masonry are numerous. Some important ones are:

(1) Structural members are constructed in place, which eliminates heavy duty hoisting equipment and permits flexibility in construction due to last minute changes in design.

(2) All construction can generally be performed by masons without the need for other trades.

(3) All materials can usually be supplied locally.

(4) There is no need for watertight forms, only simple supports.

(5) The use of reinforced concrete masonry lintel beams and columns in masonry structures provides a pleasing continuity

in appearance.

(6) Structural members can be tied in with the remainder of the masonry structure through continuity of reinforcement and concrete fill.

(7) Reinforced concrete masonry offers as good or better fire protection than most other types of construction.

(8) There is excellent resistance to cracking and differential settlement.

(9) Reinforced masonry walls have good accoustic qualities, with high resistance to earthquakes and atomic blasts.

Experimental Background

Over the last thirty years, a number of tests have been performed on reinforced masonry structural members. They include beams, columns, piers and walls under various types of loading, using both brick and concrete block as the masonry component. The results of such tests have generally shown that the masonry unit acts together with the fill in resisting loads. Results have been compared with existing codes on Reinforced Masonry and adequate factors of safety established.

The use of Masonry beams in the construction industry has been largely limited to lintels over door and window openings. The loads and spans involved are usually small. Consequently, research in the field of masonry beams has been limited to short span, single course lintel beams.

Several tests of this nature have been conducted by investigators such as, Converse,[4] Mayrose[13] and Saemann.[18] Their results indicated that, in general, the behavior of reinforced concrete masonry beams under loading to failure was similar to that of reinforced concrete beams. To the best of the author's knowledge, there have been no studies involved with beams of over one course. This leaves a large field of study open for beams of any depth.

Reinforced concrete block walls have only become popular since the advent of the two-core block. This is understandable since the three-core block would be quite difficult to grout, especially in a full depth wall. However, reinforced grouted brick walls have been used for many years. Thus most of the research up to 1950 has been focused on reinforced brick walls and columns. Investigators such as Lyse,[12] Plummer,[16] Witney[22] and Bradshaw[1] have tested such members for lateral loads, static racking loads and crushing loads.

Concrete block walls have been subjected to similar tests by such researchers as Saemann, Schneider,[19] Scrivener,[20] Hedstrom,[7] Richart[17] and Cox.[5] These have involved both reinforced and unreinforced block walls. However, all research in concrete filled block walls has been concerned with lateral loads and racking loads. To the author's knowledge, there has been no research into the behavior of such walls under axial loads.

Although all researchers have agreed that reinforced masonry members do in fact behave similarly to reinforced concrete members, there has been no attempt to analyse them as such.

II. THE TEST PROGRAM

Selection of Members

(a) Beams:

There were two main factors governing the size of beams. The handling and testing facilities available were of primary concern. The modular size of the blocks available controlled the length in increments of 16 inches and the depth in increments of 8 inches. The width of the block could be varied from 6 inches to 12 inches in increments of 2 inches. It was decided to use an 8 inch wide block throughout as this was most readily available. Beam details are shown in Figure 1.

The lengths of all beams were set at 160 inches, comprising ten blocks per course. The heights varied from one to five courses.

Ten beams were initially built. The first two were single course beams. The next eight were 2-course beams, the only variable being the type of block used on the second course. From these initial tests, the H-block (see Figure 3) was chosen for the continuation of the beam tests.

The remaining beams varied from 2 to 5 courses, with the percentage of longitudinal reinforcement varying from the minimum to the maximum allowed by the "A.C.I. Code on Reinforced Concrete".

The web reinforcement generally consisted of 3/8 inches diameter, single leg stirrups at 8 inches on centre. This

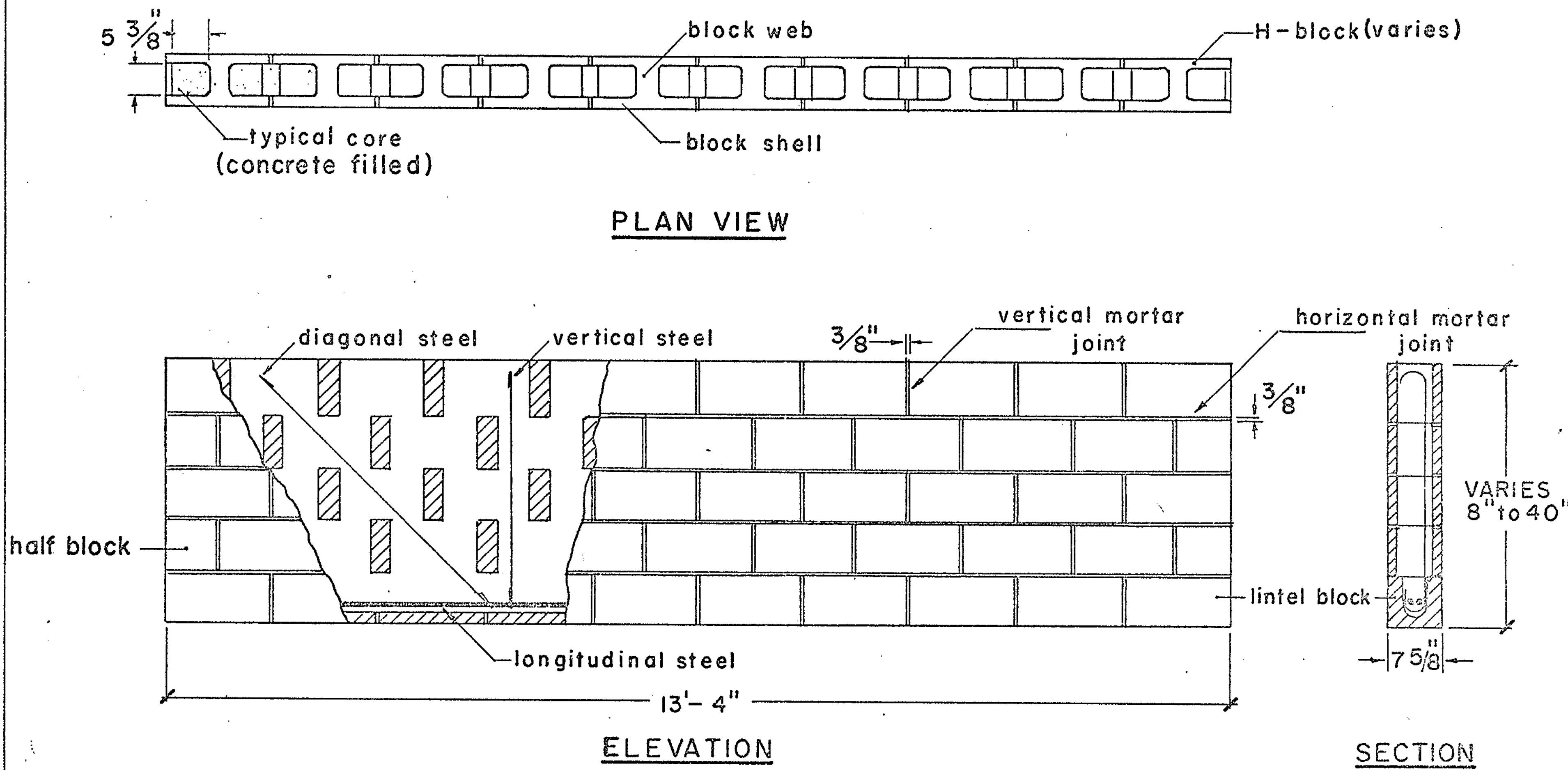

figure 1: beam details

reinforcement was placed in the shear zones only.

A total of 26 beams were tested. Generally, every two beams were identical. Beam properties and dimensions are listed in Table VIII (Page 74).

(b) Wall Sections:

The size of the sections was limited by the load capacity and clear depth of the test frame. Since the number of sections that could be built were limited, one size was chosen throughout. Six sections were tested.

The sections were all 12 ft. high, 8 in. thick and 16 in. wide. This size constituted a true section, in that by constructing a wall in running bond with blocks 16 in. long, this section would repeat itself every 16 in. There was no steel reinforcement in the wall sections, Wall section details are shown in Figure 2.

Material Properties

(a) Beams:

The blocks used were supplied by a local manufacturer. Nominal outside dimensions were 8"x8"x16" while the actual dimensions were 7 5/8"x7 5/8"x15 5/8", to allow for the 3/8in. thick mortar joint. Details and a photograph of the blocks used are shown in Figure 3. Compression tests were carried out on all blocks. Results are listed in Table 1 (Page 40) and a photograph of the test is shown in Figure 4.

For the bottom course, the 8 in. lintel block was used throughout. For the upper courses, four different type

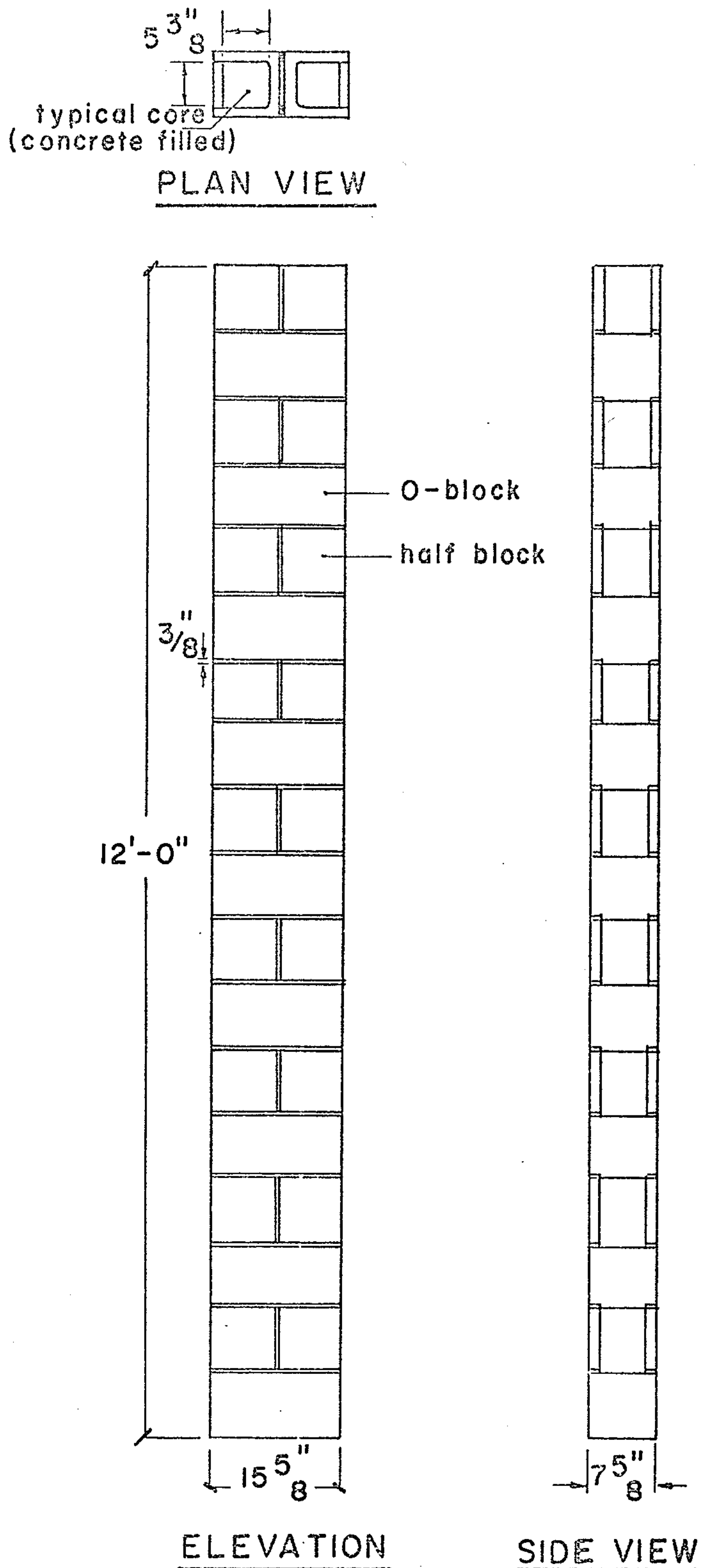

figure 2: wall section details

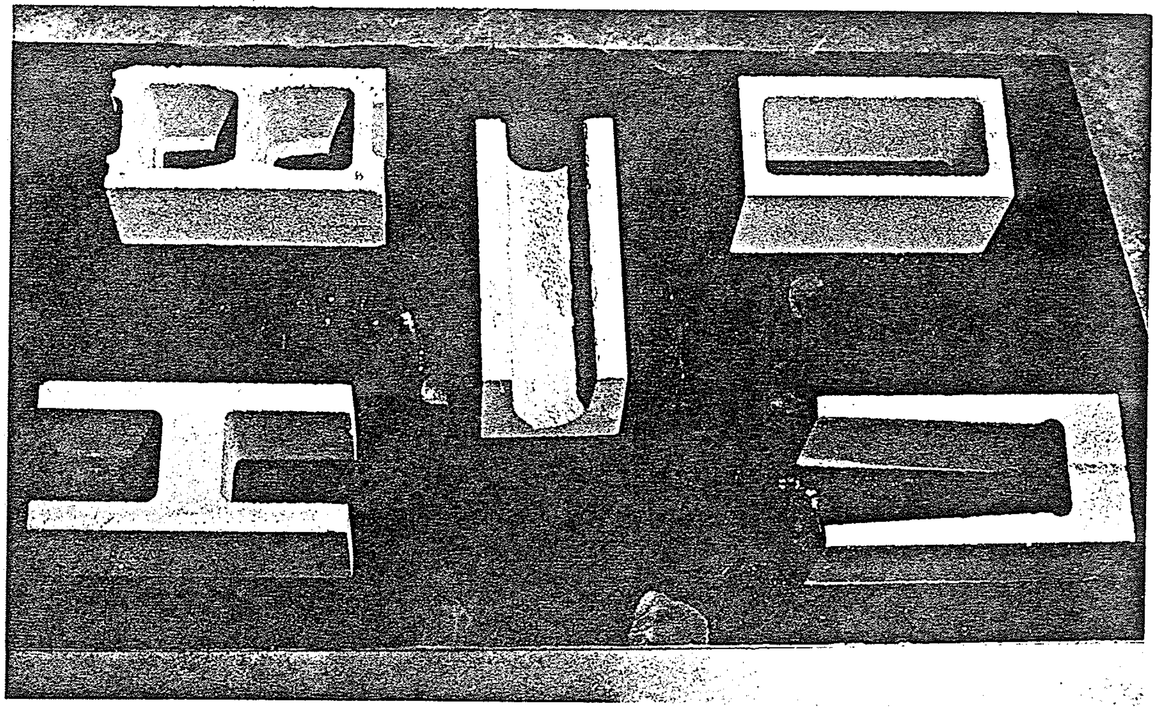

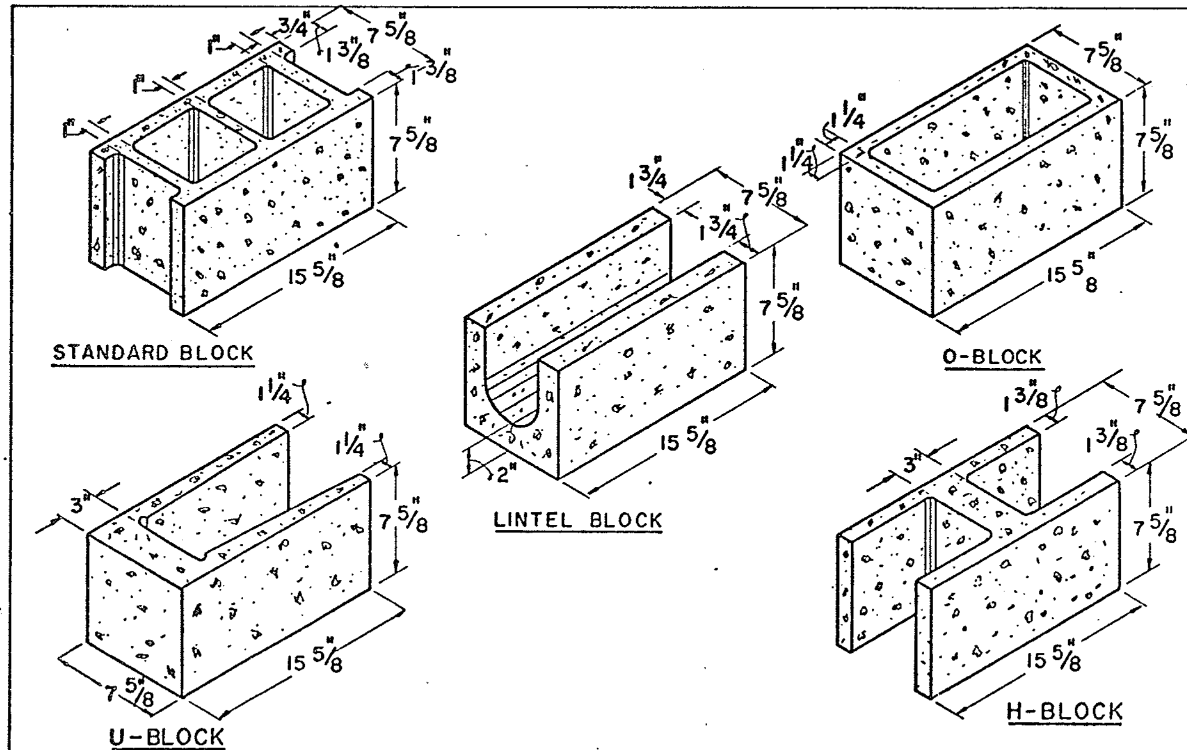

figure 3: block details and photograph

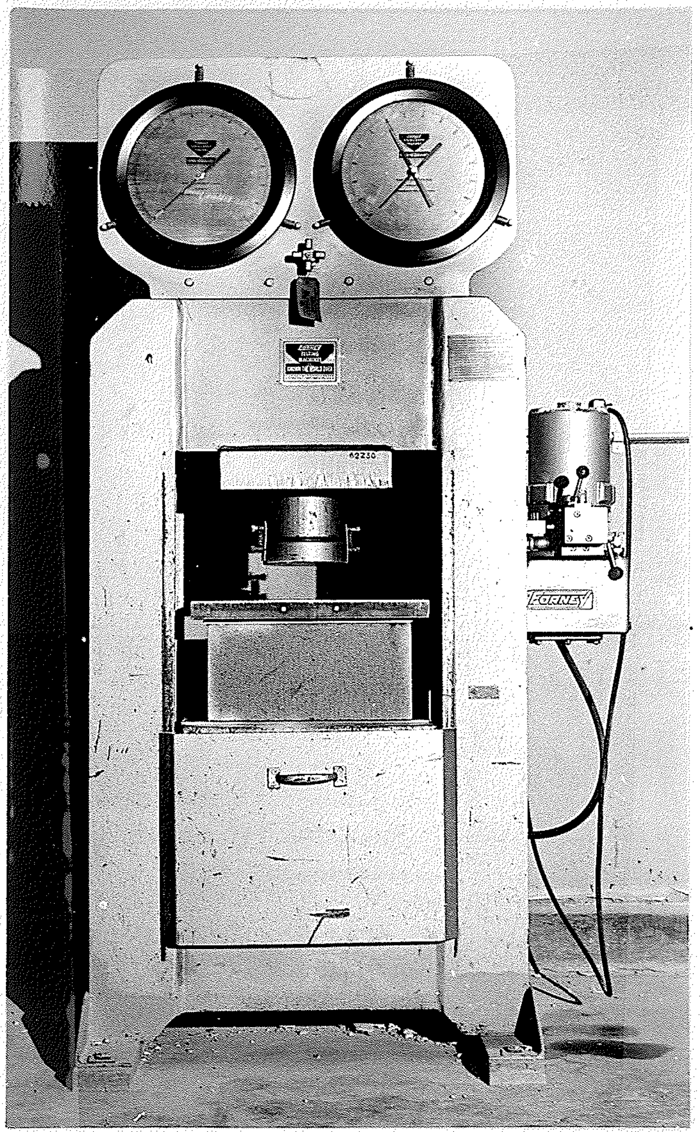

CONCRETE BLOCK IN 300,000 # TESTING MACHINE

FIGURE 4

units were used, one for each beam type. They were the standard block, U-block and O-block. The names of the latter three blocks were derived from their shape in plan. With one exception, all units conformed to ASTM Standard Specification (C90) for hollow, load-bearing, normal weight masonry units. The exception was that the total web thickness of the O-block was 2 1/2 in., 1/2 in. less than required by specifications. The cores in the blocks occupied approximately 50% of the total volume.

Concrete was supplied through a local manufacturer. Strengths between 2500 and 3000 p.s.i. were specified with a 3/4 in. maximum size aggregate and a 4 to 5 in. slump.

From each beam casting, two compression cylinders, 6 in. in diameter by 12 in. long, were taken. The cylinder compression tests were performed on the same day as the corresponding beam test in accordance with ASTM designation C39-64. A photograph of a cylinder test is shown in Figure 5 and the results listed in Table II (Page 41)

Mortar was mixed by a shovel in 50 lb. batches. Type N mortar was specified as in N.B.C. 65, with a minimum compressive strength of 750 p.s.i. at 28 days. The mortar was proportioned one part masonry cement to three parts sand. Water was added until good working consistency was achieved. The results of a sieve analysis on the sand are listed in Table III (Page 40).

From each batch, two 4 in. cubes were taken. The cube compression tests were performed on the same day as

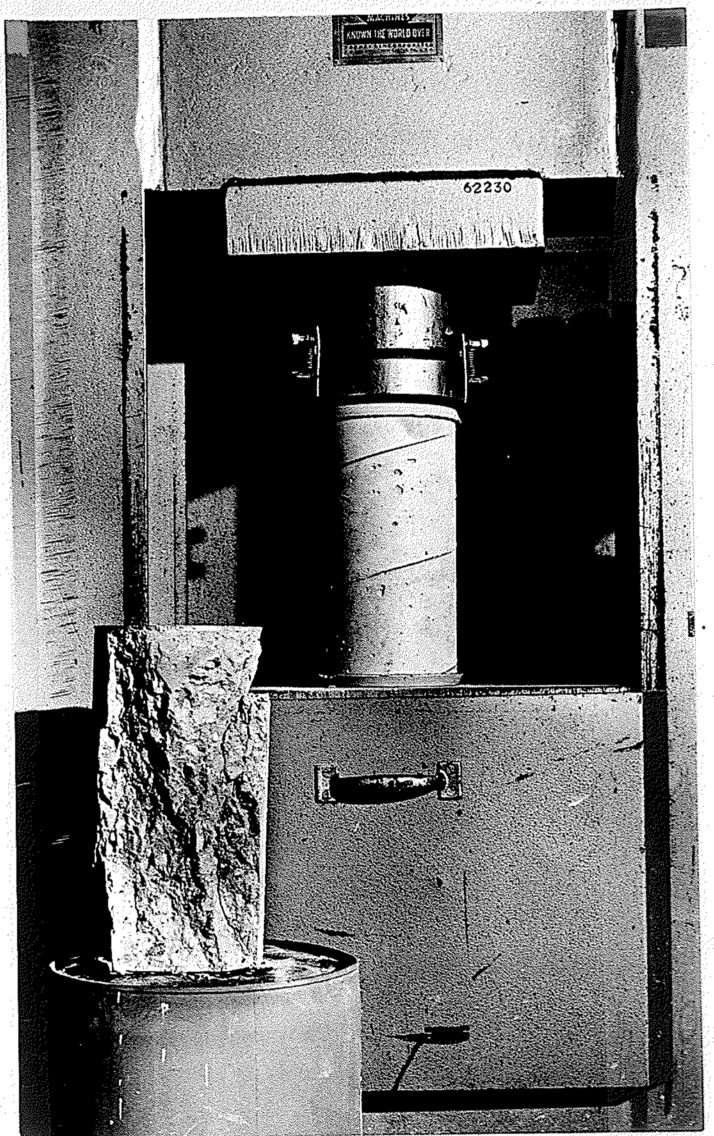

CONCRETE CYLINDER IN 300,000 # TESTING MACHINE

FIGURE 5

the corresponding beam test. A photograph of the cube test is shown in Figure 6 and the results listed in Table IV (Page 42).

The joint reinforcement consisted of two #9 gage (0.148 in. diameter) deformed steel wires with cross ties at 15 in. on centre.Yield strength of each wire was 1380 lb.

The grade of steel specified in ordering the reinforcement was Intermediate Grade Billet Bars in accordance with ASTM specifications A15 - 62T, with deformed section conforming to ASTM specification A - 305 - 56T.

Test coupons, approximately 24 in. long were sampled from the reinforcement for each bar size. Each coupon was tested for yield point, ultimate tensile strength, and percent elongation per 8 in. length. Figure 7 shows a coupon under test in the 200,000 lb. Riele testing machine and Table V (Page 43) lists the test results.

All longitudinal bars had standard 90^{0} bends at both ends. All stirrups had single legs and standard hooks at both ends. The spacing for the longitudinal steel was limited to two layers of two bars each. A complete reinforcing bar schedule is listed in Table VI (Page 44).

(b) Wall Sections:

The materials used for the wall sections were generally similar to the beams. However, the O-block was used exclusively in constructing the sections.

The concrete mix was designed to yield a compressive strength of 3000 p.s.i. at 28 days. The water-cement

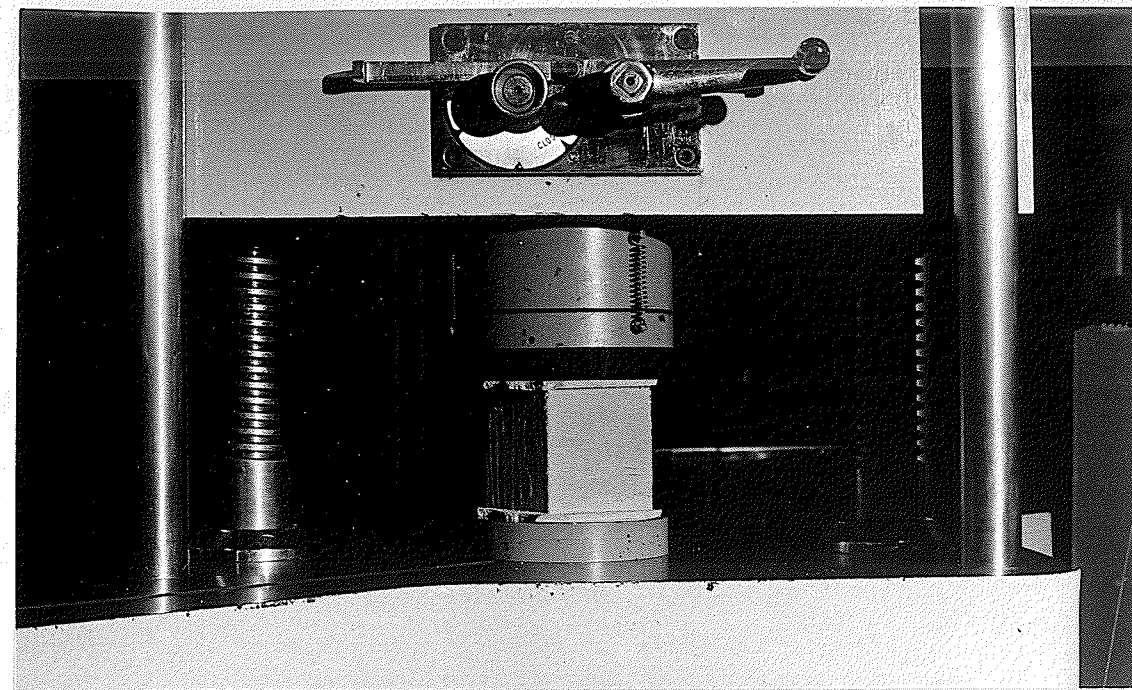

MORTAR CUBE IN 60,000 # TESTING MACHINE

FIGURE 6

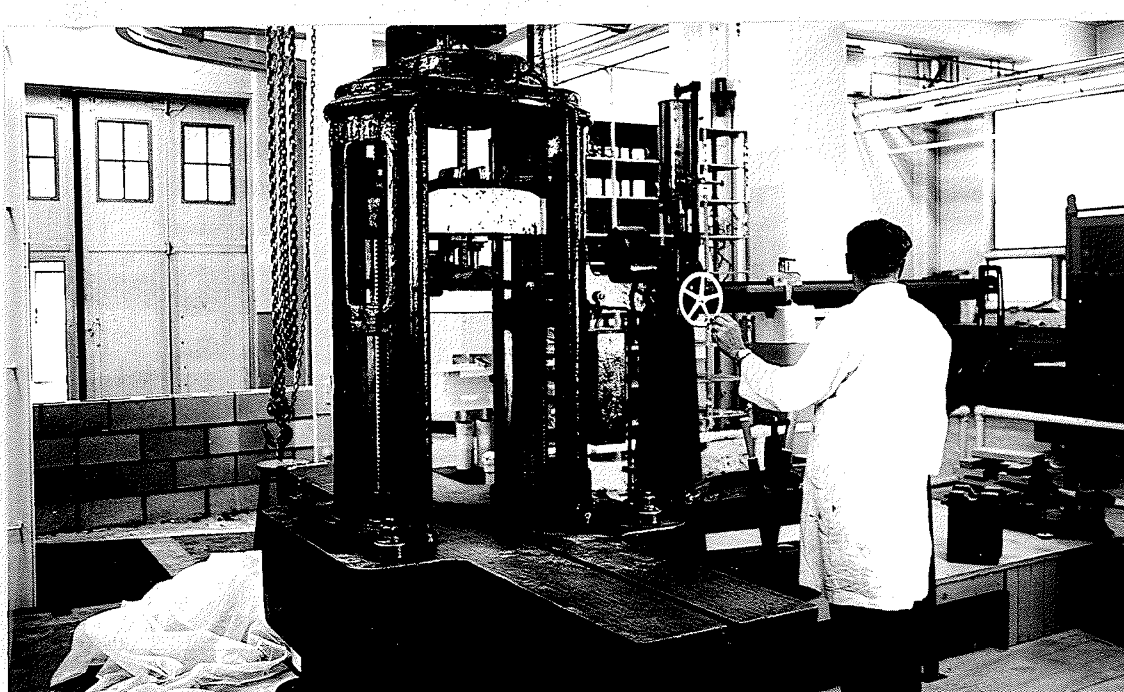

STEEL REINFORCEMENT UNDER TENSION TEST IN 200,000 #

RIELE TESTING MACHINE

FIGURE 7

ratio was 0.57 and the maximum aggregate size was 3/4 in. The batch properties were:

Normal-Strength Portland Cement	Aggregate Fine	Aggregate Course	Water
75 lb.	150 lb.	182 lb.	43 lb.

This batch yielded 3 1/2 cubic feet of concrete. Two batches per section were mixed, using mixing times of about 10 minutes. The slump measured 8 in. to 9 in. each time. The concrete was mixed in the laboratory using a rotating horizontal tub Eirich Machine. Concrete and mortar strengths are listed in Table VII (Page 45).

Construction of Members

(a) Beams:

Two stages were required in constructing the beams. The first stage involved the construction of the permanent form with concrete blocks and placing of the reinforcing bars. The second stage consisted of filling the cores of the form with concrete.

The beams were constructed on the level floor by an experienced bricklayer, along with the author, using ordinary construction methods and workmanship. A polyethelyne sheet was laid to prevent mortar from bonding to the floor. The bottom course lintel blocks were laid in sequence starting from one end using a steel angle guide to maintain alignment. Abutting ends of the blocks were well filled with mortar and shoved up tight to form joints approximately 3/8 inches thick. Excess mortar was cleaned from the interior joints at all times.

With the bottom course completed, the longitudinal steel was placed inside the form. Spacers were provided so that the reinforcing bars were exposed on all sides. However, in the cases where two layers of bars were required the two bars of the bottom layer were placed in a bundle. This was necessary because of the limited space available. For beams of only one course, the first stage was now completed.

Successive courses were laid in similar manner for deeper beams. All horizontal joints were approximately 3/8 inches thick and contained joint reinforcement. As these courses were set into a bed of mortar, a level was used in setting them. A half-block was used at the ends of alternate courses so the vertical joints would be staggered. The exterior joints on one side were pointed and coated with a white latex flat paints. This was done to improve fine crack detection. After the last course was completed, the stirrups, where required, were placed in the cores and hooked under the longitudinal reinforcing bars.

The forms were filled with concrete three days after they were built. A wooden trough was placed on top of the forms to prevent spilling as the cores were filled. A high-frequency internal vibrator, with a 3/4 inch head was used to consolidate the concrete.

About 8 inches of concrete was first placed and vibrated to ensure filling of all voids around the reinforcing bars.

The concrete was leveled with the top of the form. Soon after the cores were filled, the mortar joint became damp indicating that water from the concrete fill was being absorbed by the joints.

The beams were cured in the laboratory at 70^{0} F. The exposed concrete was covered with wet burlap for four days after casting.

Figure 8 shows a beam under construction with positions of joint, vertical and longitudinal reinforcement. Figures 9 and 10 show the interior of a four-course beam, before concrete placement with the block cores aligning vertically and diagonally respectively.

(b) Wall Sections:

The wall sections were constructed in a pit adjacent to the test frame using methods of workmanship similar to the beams. Since the size of the sections were only 8x16 inches in cross section, one O-block constituted the bottom course. For the second course, an O-block was cut in half and laid back to back in a bed of mortar. Both horizontal and vertical joints were made 3/8 inch thick. Figure 11 shows a photograph of a section under construction.

As in the beams, the excess mortar was cleaned from the joints and the exterior joints pointed. This sequence was continued up to 18 courses making the section 12 feet high. All mortar droppings were then cleaned out from the bottom of the section. As there was no joint reinforcing or reinforcing bars used in the wall sections,

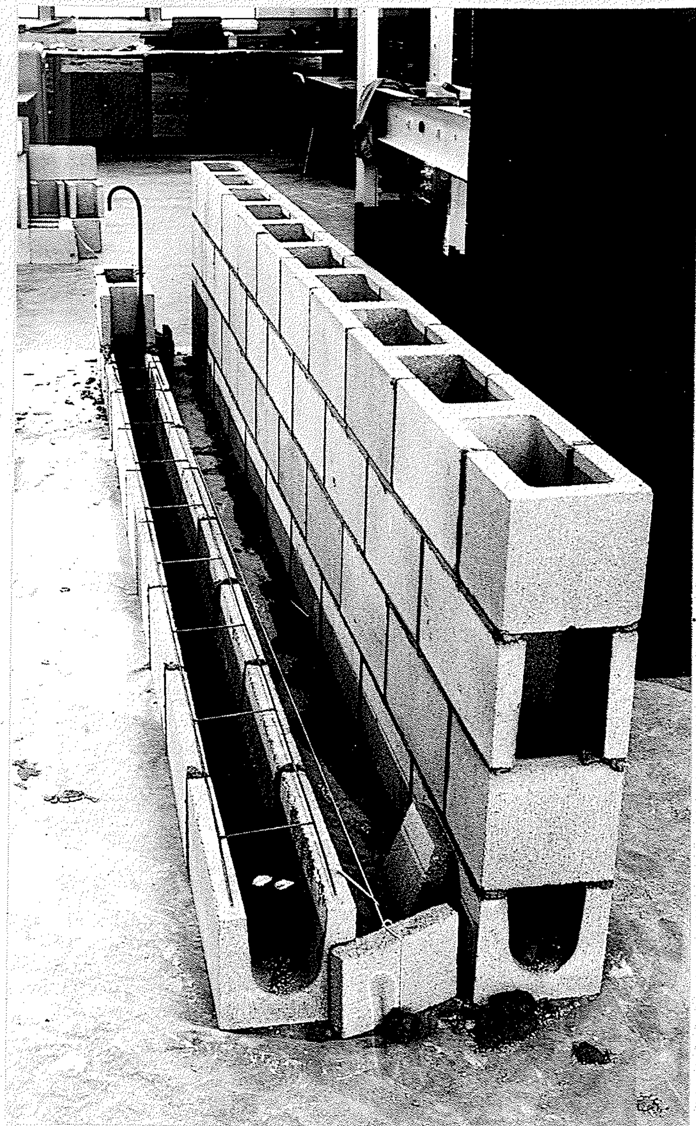

BEAM UNDER CONSTRUCTION SHOWING STEEL REINFORCEMENT

FIGURE 8

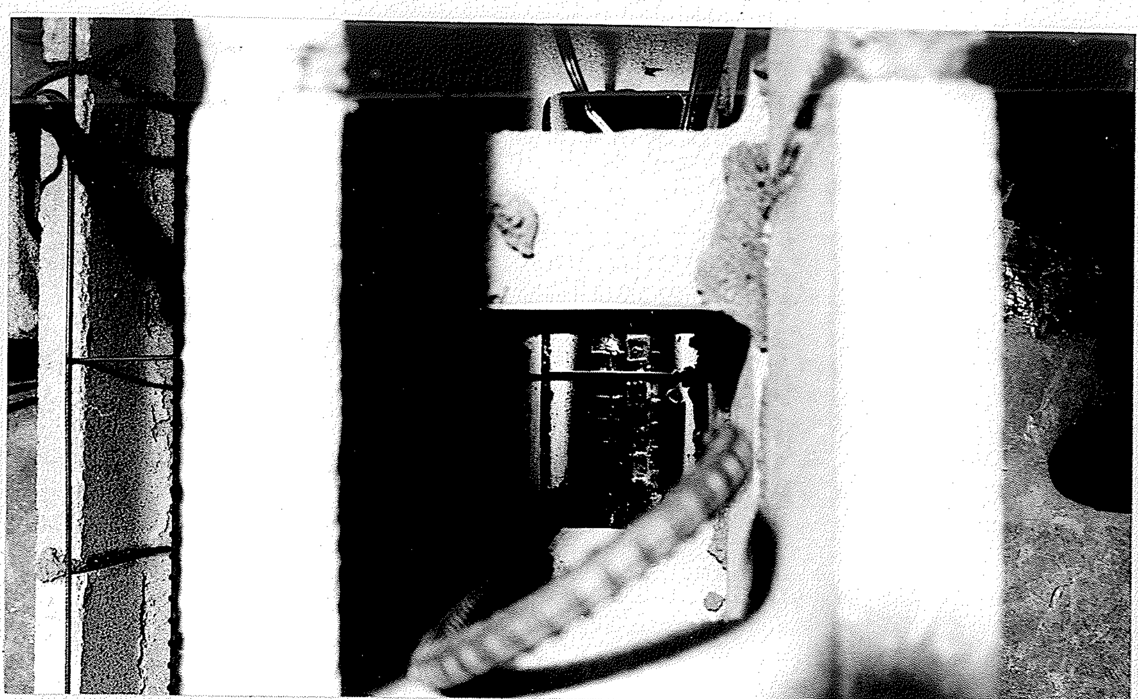

INTERIOR OF BEAM SHOWING CORES ALIGNING VERTICALLY

FIGURE 9

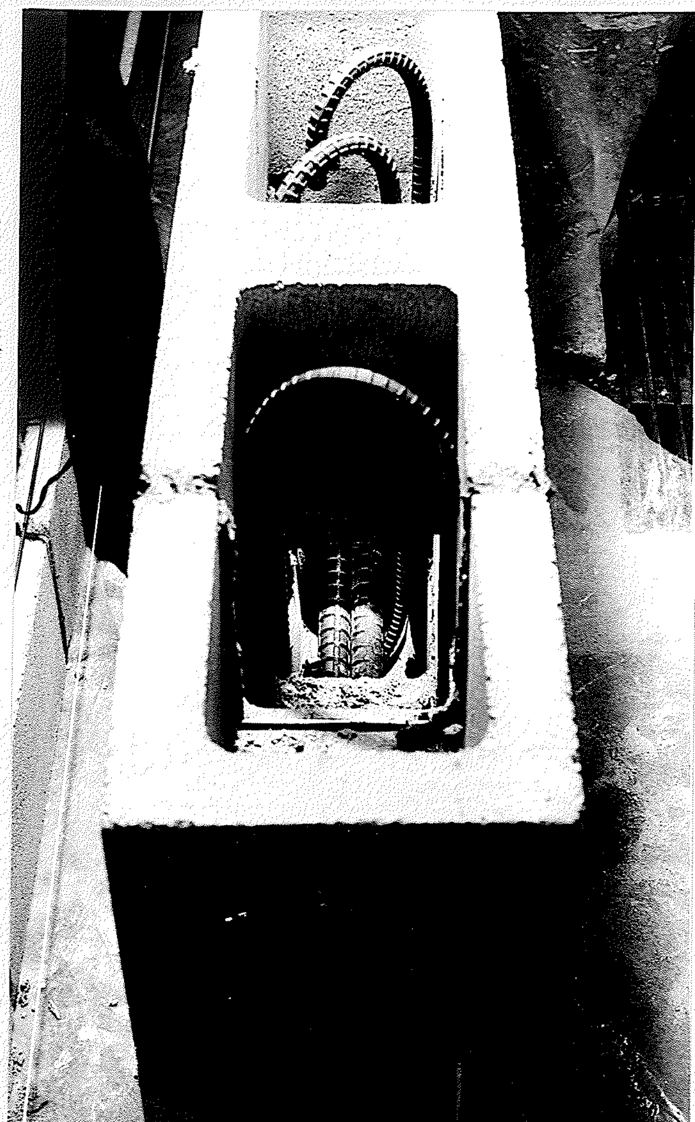

INTERIOR OF BEAM SHOWING CORES ALIGNING DIAGONALLY

FIGURE 10

WALL SECTION SHOWING METHOD OF CONSTRUCTION

FIGURE 11

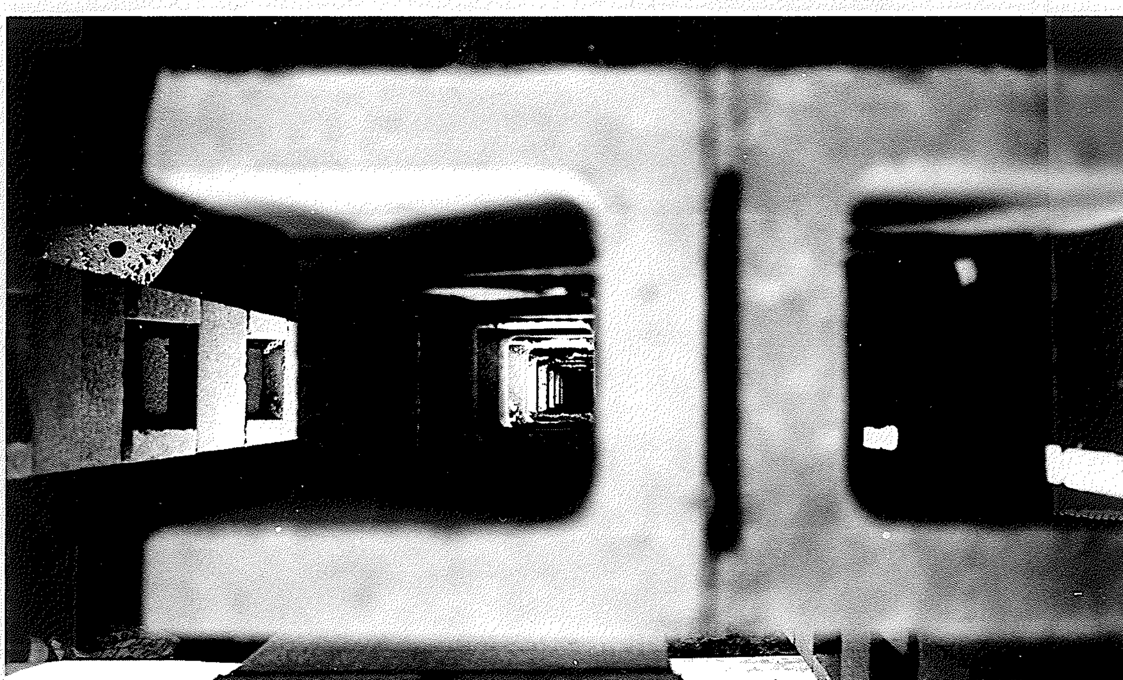

INTERIOR OF WALL SECTION SHOWING CORES ALIGNING VERTICALLY

FIGURE 12

the construction procedure was simplified. Figure 12 shows the interior of a section, before concrete placement, with the block cores aligning vertically.

Since the cores were open at every second course, it was necessary to form the sides of the section. This was done by attaching 3/4 inch thick plywood 8 inches wide by 12 feet high to both sides of the section. Figure 13 shows a completed section with open cores.

Three days after mortaring the blocks together, the cores were filled. The filling was done in 4 ft. lifts with approximately 10 minutes between lifts. Figure 14 shows the method of concrete placement.

There were two methods used in consolidating the concrete. For sections 1, 2 and 3, the concrete was consolidated by rodding with a 3/8 inch diameter reinforcing bar. For sections 4,5 and 6, a high frequency internal vibrator, with a 3/4 inch head was used.

On reaching the top, a trowel was used to bring the level of concrete flush with the top block. The wall sections were cured in the laboratory air at 70°F.

Testing Arrangement and Procedure

(a) Beams:

All beams were tested between two weeks and two months after the concrete had been poured. A 12 foot simply-supported span with third-point loading was used throughout. Figure 15 shows a loading diagram with resulting shears and bending moments across the beam.

WALL SECTION SHOWING HORIZONTAL CORE OPENINGS

FIGURE 13

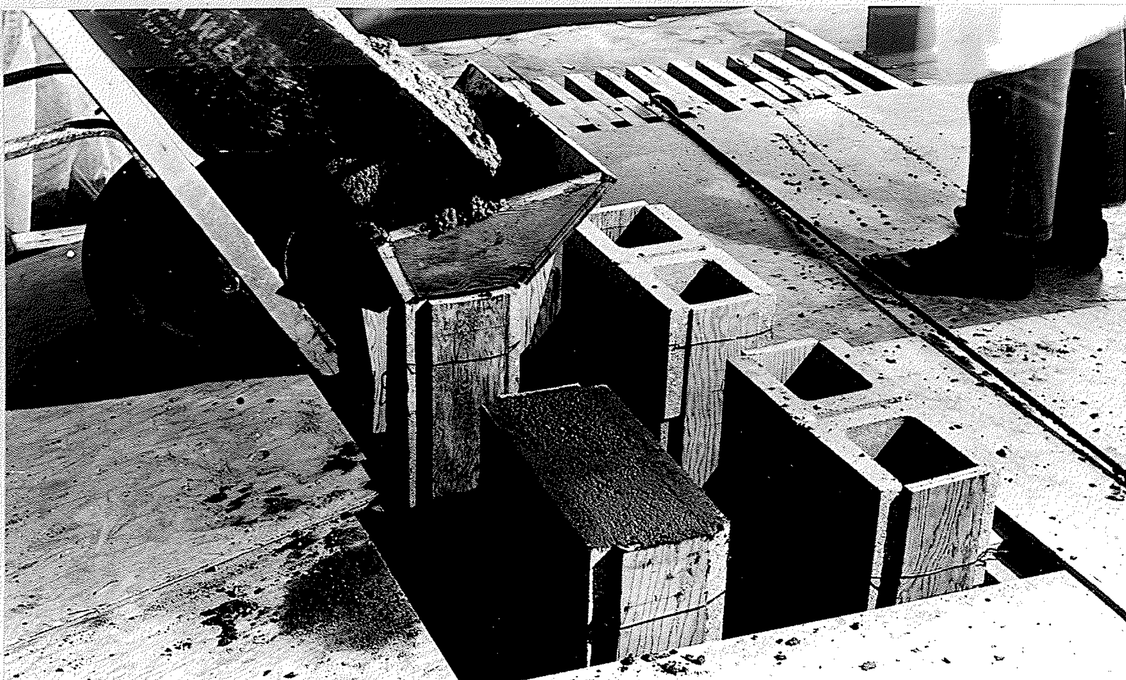

WALL SECTION SHOWING METHOD OF CONCRETE PLACEMENT

FIGURE 14

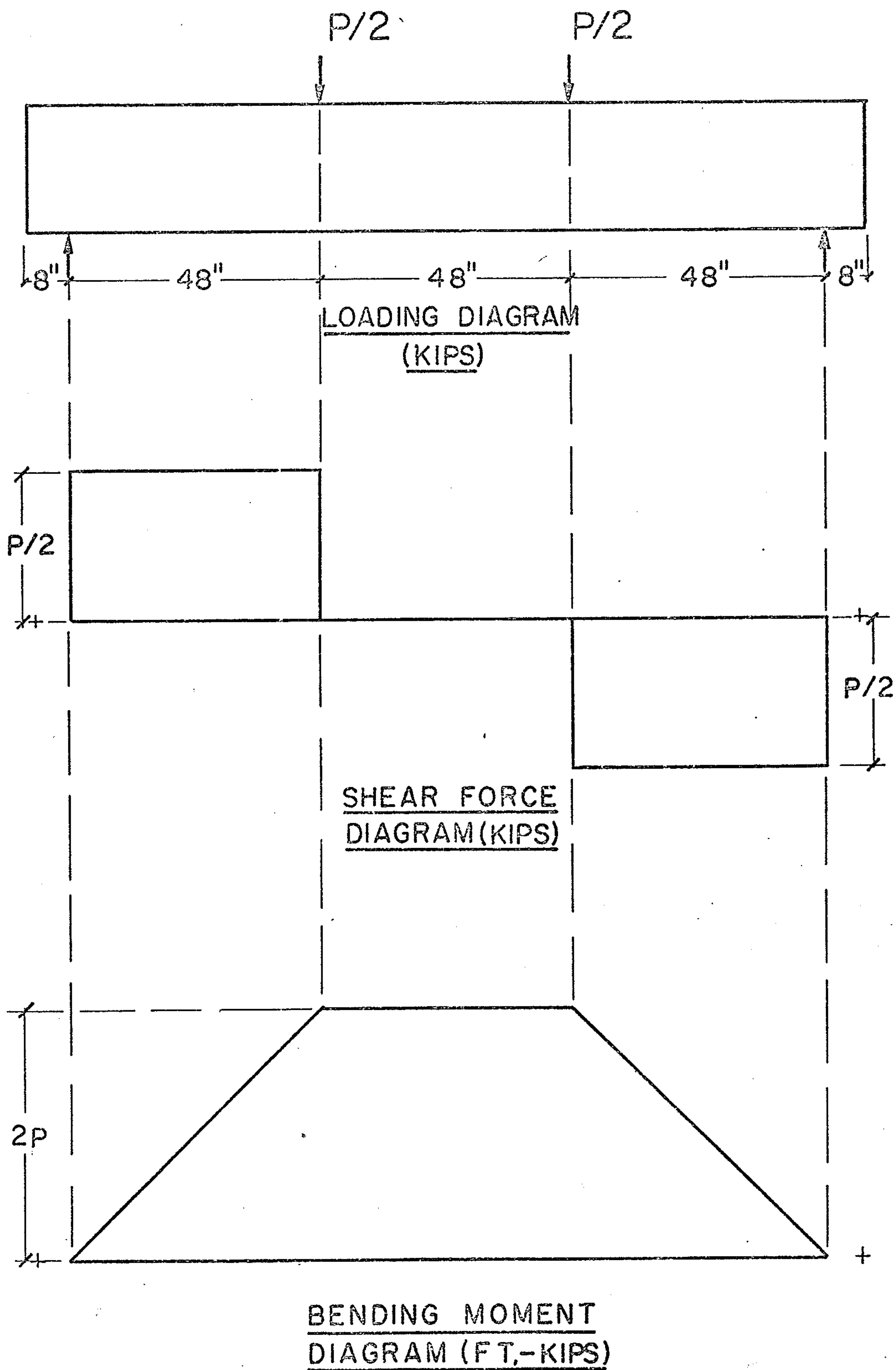

figure 15: beam loading, shear force and bending moment diagrams

The beams were tested in a closed frame. The load was supplied through 200,000 lb. hydraulic jack and recorded with a 200,000 lb. load cell. Figure 16 shows a photograph of the jack, load cell and load-bearing supports.

The beams were placed in a test frame by two hoists, running on an overhead track, connected to steel hooks embedded in the beams. Alignment of the beams in the test frame was simplified by the use of a transit set in line of the longitudinal axis of the beam. Ball and roller bearings were used at the load and beam supports. This gave the beam free end rotation and horizontal displacement. Bearing plates, 4"x4" in cross-section with a 1/8 in. thick birch veneer cushion, distributed the end reactions uniformly. Capping was not necessary due to the smoothness of the block surfaces. Bearing plates, 4"x4" in cross-section and capped to the beams with plaster, distributed the loads uniformly over the breadth of the beam.

A "Mercer" dial gauge was set under the beam to measure the vertical midspan deflection. For beams of four and five courses similar gauges were set at the top, centre and ends to measure lateral deflection. The "Mercer" dial gauges read to the nearest thousandth of an inch, having a maximum travel of two inches. Figures 17 and 18 give photograph and details of the test frame with a beam in position. The gauges are denoted by numbers 1 through 4 shown on the beam in their actual reading positions.

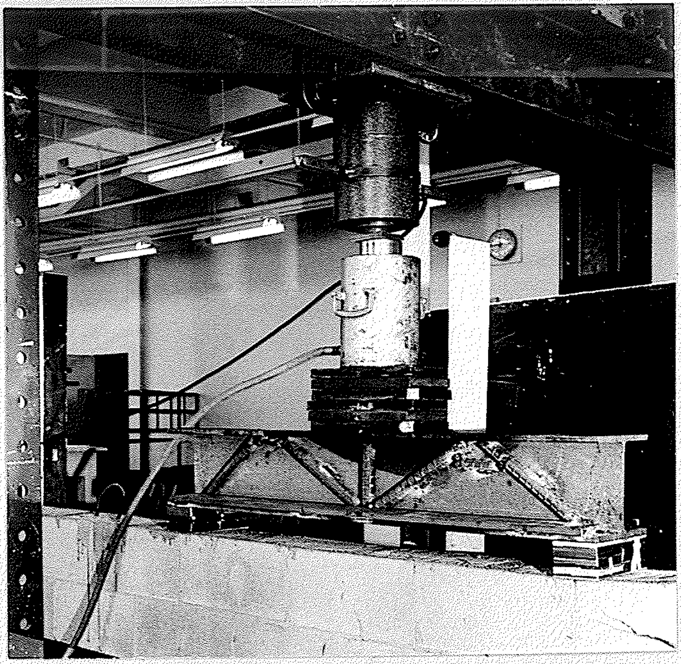

JACK, LOAD CELL AND LOAD-BEARING SUPPORTS IN POSITION

FIGURE 16

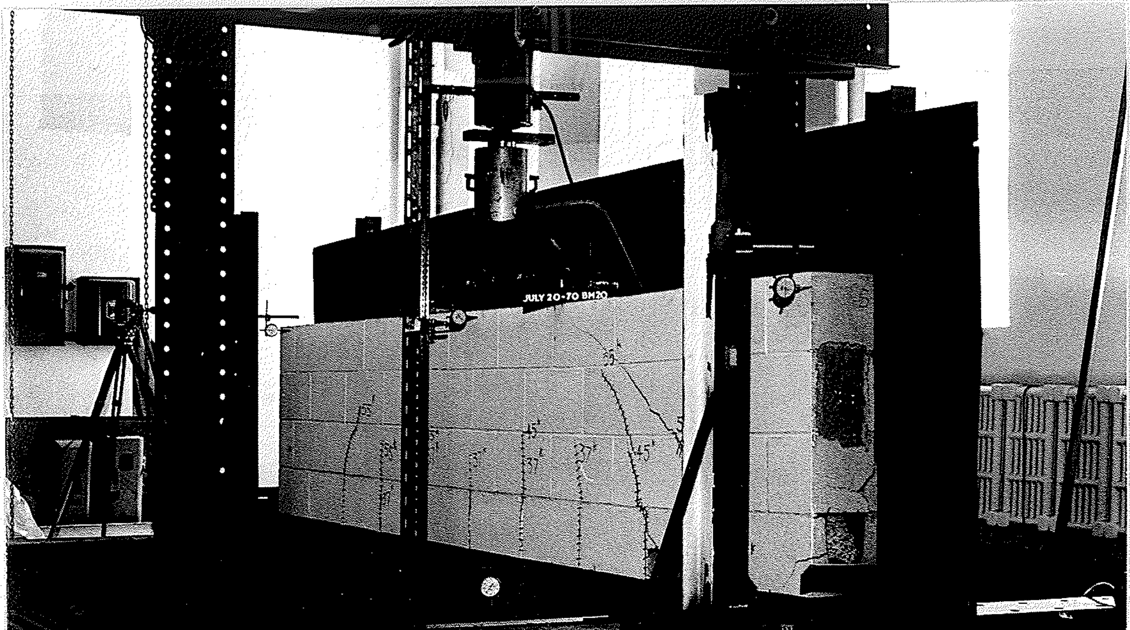

TEST FRAME WITH BEAM IN POSITION

FIGURE 17

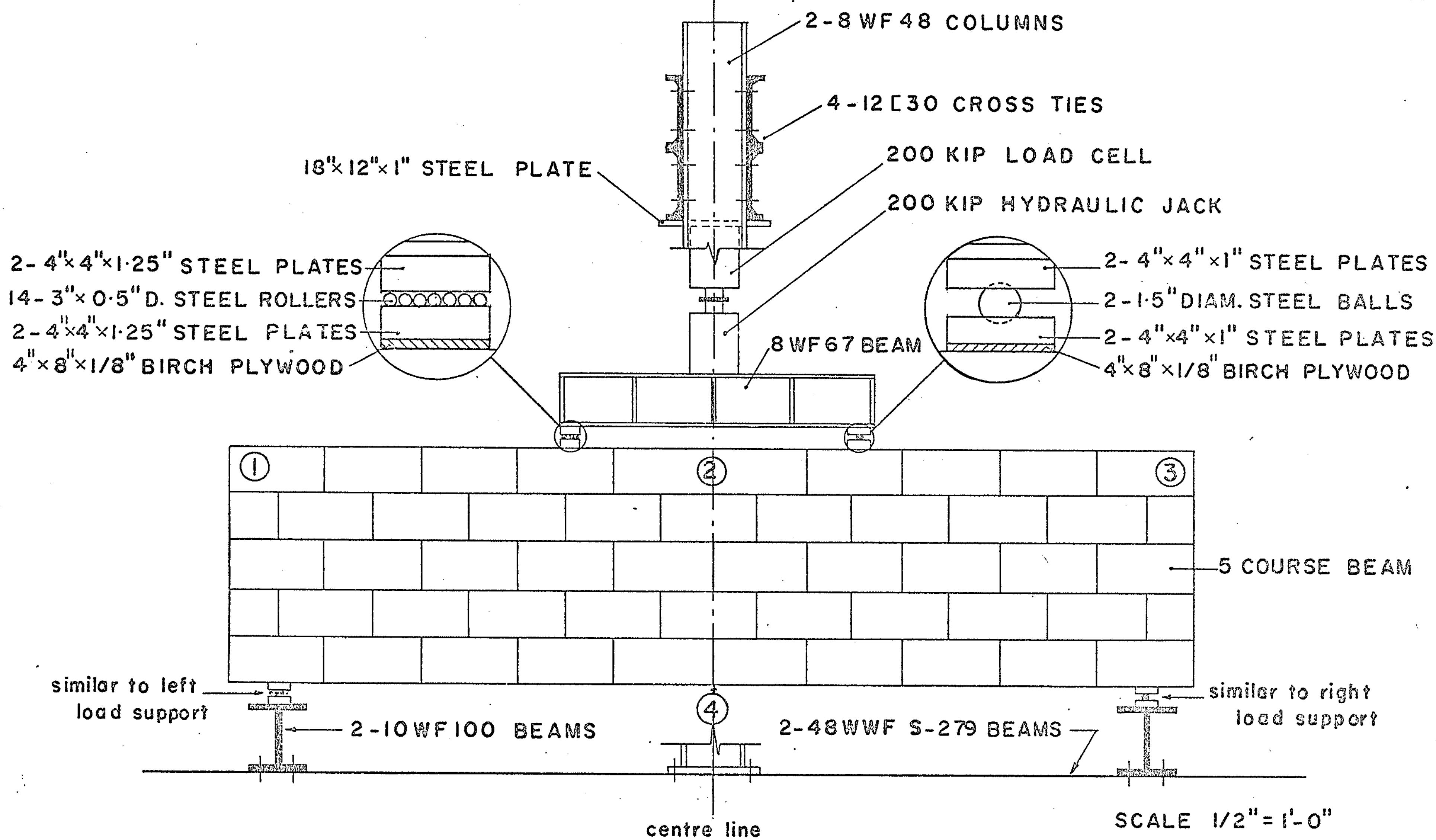

figure 18: beam test frame details

The test procedure was quite simple to perform once the beams were centred in position and the dial gauges set and zeroed. The load was read through a Wheatstone Bridge connected to the load cell. A reading of 1 microinch per inch was equivalent to 0.2 kips of load. Load was applied in increments of 0.1 kips to 2.5 kips depending on the beam size. Following each load increment the gauges were read and locations of cracking traced with ink indicating also the total load at the time.

(b) Wall Sections:

All sections were tested about two months after the concrete had been poured. The sections were tested in a vertical position in a closed frame system. An axial load was supplied through a 400,000 lb. hydraulic jäck. As the sections were built adjacent to the frame, they were moved into the frame in a vertical position using a self-clamping hook attached to the overhead hoist. Frame details and a photograph with the section in position are shown in Figures 19 and 20.

Aligning the sections in the frame was a simple operation. Two rectangular collars, with inside dimensions equal to the cross sectional dimensions of the wall sections, were vertically aligned and attached to the bottom and top bearing plates. The bottom and top surfaces of each section were capped with plaster to ensure uniform loading.

The section was fitted into the bottom collar.

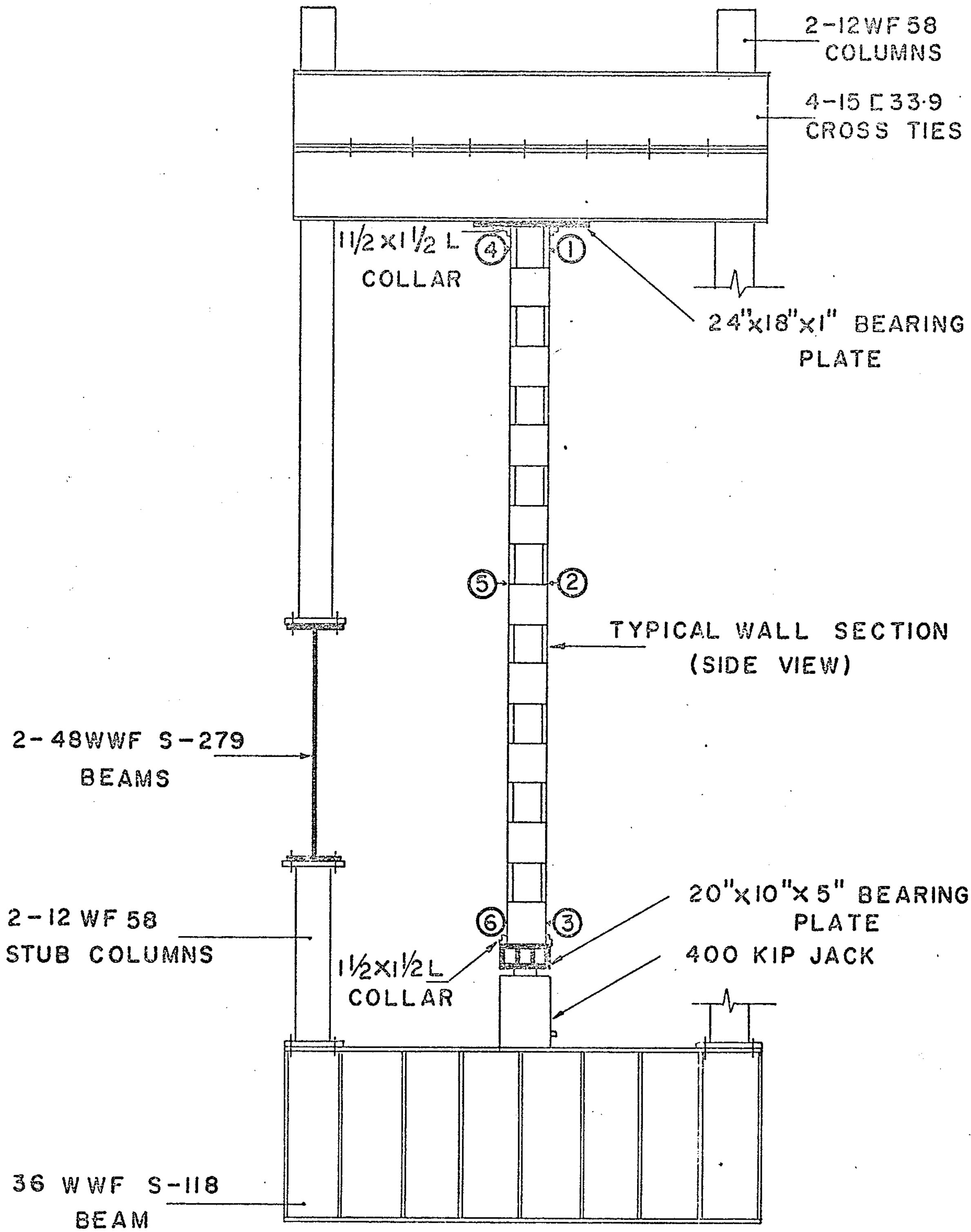

figure 19: wall section frame details

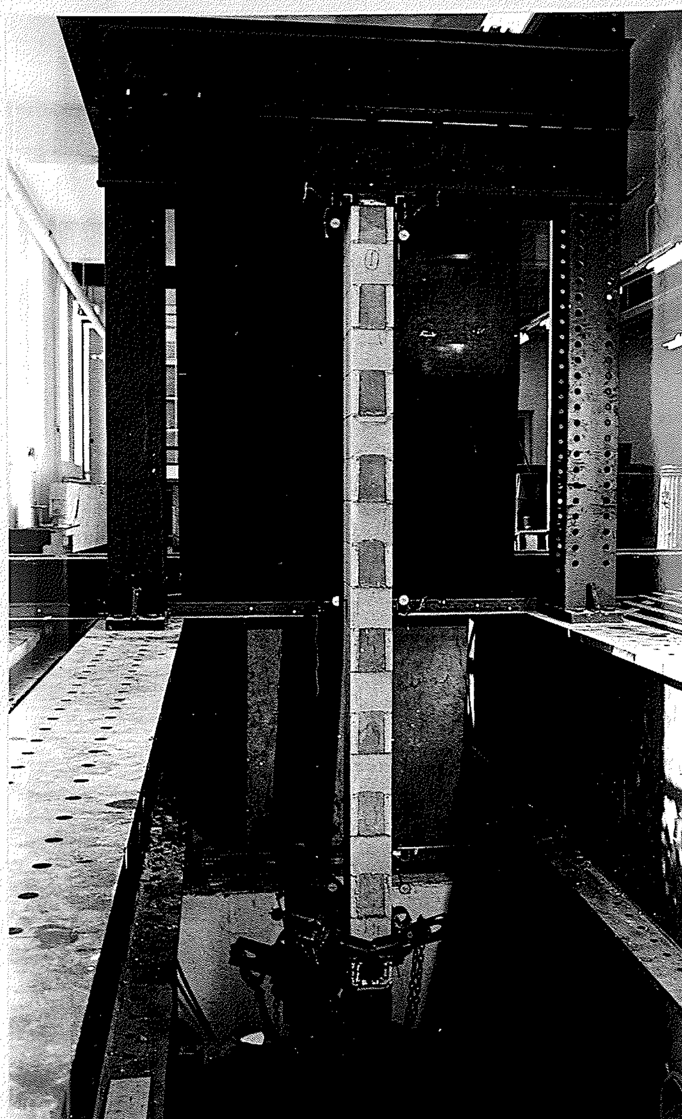

TEST FRAME WITH WALL SECTION IN POSITION

FIGURE 20

The jack was then raised fitting the top of the section into the top collar. The collars aligned the sections vertically and prevented any lateral movement. The load was brought up to 500 p.s.i. and the plaster allowed to set overnight.

Mercer dial gauges, reading to the nearest thousandth of an inch, were set on the right face at the top, centre and bottom. Any lateral deflection would be read by these gauges. Three additional gauges were set in similar positions on the left faces of sections 1 and 2. In using these additional gauges, any expansion of the section due to Poisson's effect or to the separation of the block from the concrete fill, could be measured. The position of the dial gauges are shown by circled numbers 1 to 6 inclusive in Figure 19.

The load was read through a pressure gauge attached to the jack. A gauge pressure of 100 p.s.i. was approximately equivalent to 4 kips. The pressure gauge was calibrated on the 200,000 lb. Riele Testing machine. The calibration curve of pressure against load is shown in Figure 21.

With the gauges set and zeroed, the load was increased in increments of 10 kips. After each load increment, the load was kept constant for a few minutes while the gauges were read and the section inspected for cracks. The gauges were generally removed at a load of 200 kips. The load was then increased to failure.

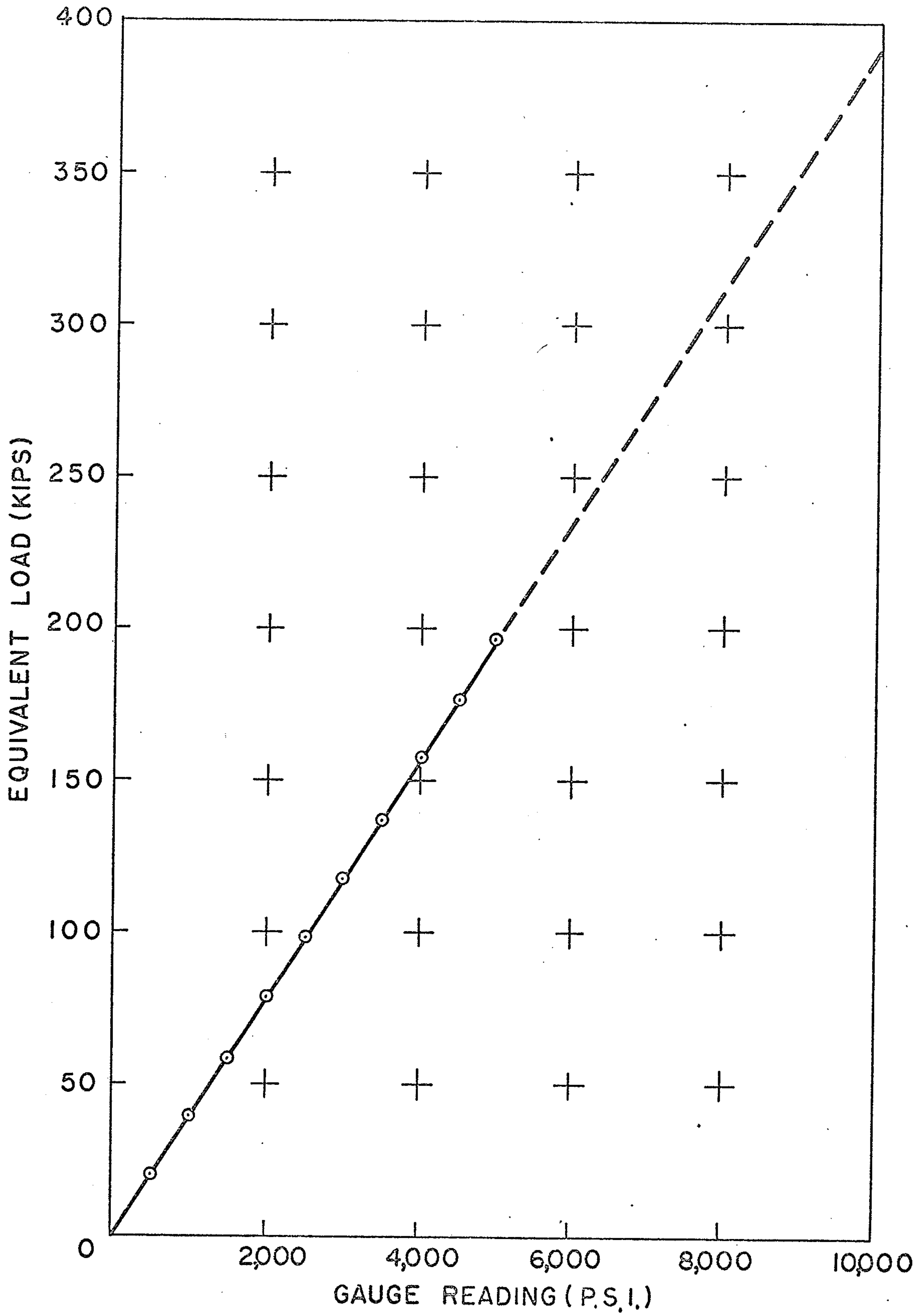

figure 21 : calibration curve for 400 kip jack

TABLE III

SIEVE ANALYSIS OF MORTAR SAND

No. Sieve	Percent Passing
16	96.1
3	71.9
50	26.2
100	6.0
200	1.2

TABLE I

CONCRETE BLOCK COMPRESSION TEST DATA

Type of block	Total Load (kips) (Avg. of 3 units)	Compressive Avg. Gross Area	Strength (psi) Avg. Net Area
H	185	1540	3080
O	223	1850	3700
U	197	1640	3280
Standard	165	1375	2750
Lintel	185	1540	3080

TABLE II

CONCRETE CYLINDER TESTS (Beams)

(6"x12" Cylinders)

Beam No	Test No	Total Load (pounds)	Comp. Stress (p.s.i.)	Avg. f'_c (p.s.i.)	Age (days)
1,2,9	1	60,000	2,120		
	2	63,000	2,220	2,170	22
3,4	1	65,000	2,300		
	2	75,000	2,660	2,480	42
5,6	1	73,000	2,580		
	2	75,000	2,650	2,610	44
7,8	1	67,000	2,380		
	2	70,000	2,480	2,430	41
10	1	64,000	2,260		
	2	65,000	2,300	2,280	24
11 to 24 inclusive	1	68,500	2,420		16
	2	67,000	2,370		16
	3	75,000	2,650		18
	4	79,000	2,790		18
	5	87,000	3,080		19
	6	67,000	2,370		19
	7	81,000	2,860		22
	8	85,000	3,000		22
	9	72,000	2,540		23
	10	71,000	2,500		23
	11	85,000	3,000		23
	12	72,000	2,540		25
	13	68,000	2,400		26
	14	72,000	2,540	2,630	26
25	1	116,000	4,100		
	2	146,000	5,150		
	3	117,000	5,030		
	4	147,000	5,200		
	5	119,000	4,200	4,740	40
26	1	120,000	4,240		
	2	126,000	4,450		
	3	110,000	3,880		
	4	108,000	4,100	4,100	43

TABLE IV

MORTAR CUBE TESTS (Beams)

(4"x4" cubes)

Beam No.	Test No.	Total Load (pounds)	Comp. stress (p.s.i.)	Avg. f'_m (p.s.i.)	Age (days)
1,2,&9	1	16,500	1,060		
	2	16,500	1,060	1,060	30
3,4&5	1	18,300	1,140		
	2	19,000	1,190	1,165	35
5 to 10 incl.	1	21,600	1,350		
	2	20,800	1,300	1,325	36
11 to 14 incl.	1	22,150	1,380		
	2	22,000	1,370		
	3	31,000	1,940	1,560	40
15 and 16	1	27,700	1,760		
	2	27,500	1,740	1,750	36
17 and 18	1	31,700	1,980		
	2	32,500	2,030	2,000	38
19 and 20	1	44,700	2,800		
	2	46,100	2,880	2,840	40
21 & 22	1	48,300	3,020		
	2	52,400	3,280	3,150	36
23	1	48,000	3,000		
	2	46,000	2,870	2,935	38
24	1	49,200	3,070		
	2	52,200	3,260	3,165	34
25	1	39,600	2,470		
	2	38,800	2,420	2,445	44
26	1	44,400	2,770		
	2	43,900	2,800	2,785	44

TABLE V

PHYSICAL PROPERTIES OF THE REINFORCEMENT

Beams Sampled	Type of Bar	Sectional Area (sq.ins.)	Test No.	Yield Point			Ultimate			Average Elong. in 8 inches (per cent)
				Load (pounds)	Stress (p.s.i.)	Avg. Stress (p.s.i.)	Load (pounds)	Stress (p.s.i.)	Avg. Stress (p.s.i.)	
1 to 10 inclusive	#6 (long)	0.441	1	23,400	53,000		37,100	84,000		
			2	23,100	52,400		37,050	83,950		
			3	23,100	52,400		37,200	84,250		
			4	23,400	53,000		37,250	84,300		
			5	23,300	52,800	52,700	37,000	83,950	84,200	21
11 to 24 inclusive	#3 (Vert.)	0.11	1	5,900	53,600		8,200	74,600		
			2	5,900	53,600		8,300	75,400		
			3	5,800	52,700		8,250	74,500		
			4	5,800	52,700	53,150	8,370	76,000	75,200	22
11,12,14 15,16&17	#6 (long.)	0.441	1	22,600	51,200		33,360	75,800		
			2	21,980	49,980	50,090	33,220	75,500	75,650	23
13 to 22 inclusive	#8 (long.)	0.79	1	37,830	48,250		59,110	75,000		
			2	38,100	48,500	48,375	58,840	74,500	74,750	24
18 to 24 inclusive	#9 (long.)	1.00	1	53,600	53,600		79,790	79,790		
			2	53,390	53,390	53,500	79,860	79,860	79,825	24
25 and 26	#4 (Vert.)	0.20	1	9,200	46,00		14,900	74,500		
			2	9,400	47,000		15,100	75,500		
			3	9,350	46,750	46,580	14,900	74,500	74,830	22
25 & 26	#9 (long.)		1	48,600	48,600		75,270	75,270		
			2	47,900	47,900		75,280	75,270		
			3	47,700	47,700	48,070	75,120	75,120	75,220	26

TABLE VI

REINFORCING BAR SCHEDULE

TYPE 1 (bottom steel)

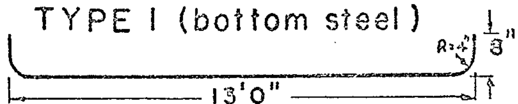

TYPE 2 (stirrups)

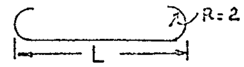

BEAM No.	REINFORCEMENT TYPE	L (INS)	SIZE OF BAR	NUMBER OF BARS
1, 2	1	—	6	1
3 to 10	1	—	6	2
11, 12	1	—	9	1
	1	—	6	1
13	1	—	8	1
14, 15	1	—	8	2
	1	—	6	2
	2	19	3	12
16, 17	1	—	8	1
	1	—	6	1
	2	19	3	12
18	1	—	9	1
	1	—	8	1
19, 20	1	—	9	1
	1	—	8	1
	2	27	3	12
21, 22	1	—	9	2
	1	—	8	2
	2	27	3	12
23, 24	1	—	9	2
	2	35	3	12
25	1	—	9	2
	2	27	4	12
26	1	—	9	2
	2	39	4	8
	2	18	4	2

TABLE VII

CONCRETE CYLINDER TESTS (6"x12" Cylinders)
MORTAR CUBE TESTS (4"x4" cubes)

(Wall Section)

CONCRETE						MORTAR			
Section No.	Test No.	Total Load (pounds)	Comp. Stress (p.s.i.)	Avg. f'c (p.s.i.)	Age (days)	Total Load (pounds)	Comp. Stress (p.s.i)	Avg. f'c (p.s.i.)	Age (days)
1	1	140,000	4,950			28,000	1,750		
	2	142,000	5,000	4,975	70	30,000	1,860	1,825	80
2	1	128,000	4,520			31,500	1,940		
	2	136,000	4,800	4,660	70	29,700	1,855	1,900	
3	1	121,000	4,270			28,000	1,750		
	2	110,000	3,880	4,075	70	30,000	1,860	1,805	80
4	1	128,000	4,520			33,400	2,090		
	2	140,000	4,950	4,735	70	32,600	2,040	2,065	80
5	1	119,000	4,200			35,100	2,190		
	2	126,000	4,450	4,325	70	32,600	2,040	2,115	90
6	1	136,000	4,800			35,100	2,190		
	2	126,000	4,420	4,625	70	32,600	2,040	2,115	90

III. TEST RESULTS

(a) Beams:

The test results are summarized with the help of the tables, curves and photographs. These are found in the Appendix under Tables X to XXXI inclusive and Figures 35 to 81 inclusive. Detailed description of the behavior as well as comparative results of the tests with analysis are also given.

General Modes of Failure

There were three modes of failure: flexural, shear and a combination of both. For all beams, vertical tension cracks initially formed in the bottom central portion of the beams and quickly proceeded up.

Failure by flexure usually resulted in beams with minimum steel percentages. Failure occurred by the development of tension cracks across the beam followed by yielding of the longitudinal steel. At this point, large deflection increments were recorded with little increase in load. This was arrested as the steel entered the strain hardened region increasing its tensile capacity. Ultimate failure occurred by crushing of the concrete in the compression zone. At this point, the load capacity was reduced by about 50% of the maximum load. This is similar to reported behavior for reinforced concrete beams.

Failure by shear occurred in beams with high percentages of longitudinal steel and little or no web reinforcement. Diagonal tension cracks usually developed at mid-depth, midway between the load and beam supports. These cracks, initially at about 45° with the horizontal, developed with increased load in the directions of the load and beam supports. The angle of the crack was somewhat reduced as it entered the compression zone.

For shallow beams with no web reinforcement,failure occurred as a result of longitudinal splitting in the compression zone in addition to splitting along the top layer of longitudinal reinforcement near the end of the beam. Failure was sudden with the critical crack forming at approximately 80% of the maximum load. Although the beams carried some additional load after the formation of the critical crack, the deterioration was rapid. On failure the only force preventing the end of the beam from completely breaking away was the dowel action of the longitudinal steel.

For deeper beams with web reinforcement, the load capacity was greatly increased past the first appearance of diagonal tension cracks. On failure, the web reinforcement remained anchored to both sides of the crack giving the beam some load capacity. A photograph of the interior of the beam after a diagonal tension failure is shown in Figure 22.

A good comparison of shear and flexural failures can be seen in beams 12 and 13 whose only variable was the percentage of longitudinal steel. Beam 12 contained 1.64% and Beam 13 contained 0.83%. Load deflection curves and photographs for the two beams can be compared in Figures 23, 24 and 25. The slope of the curve in Beam 12 remained fairly constant up to failure, indicating elastic behavior. For beam 13, the slope decreased from a relatively low load becoming horizontal at failure.

In all tests there was no sign of slippage between the steel and concrete indicating no bond failures between these materials. Good bond also existed between the concrete block and fill. This point is illustrated in Figure 22. In no case did the block separate from the fill before the ultimate load was reached.

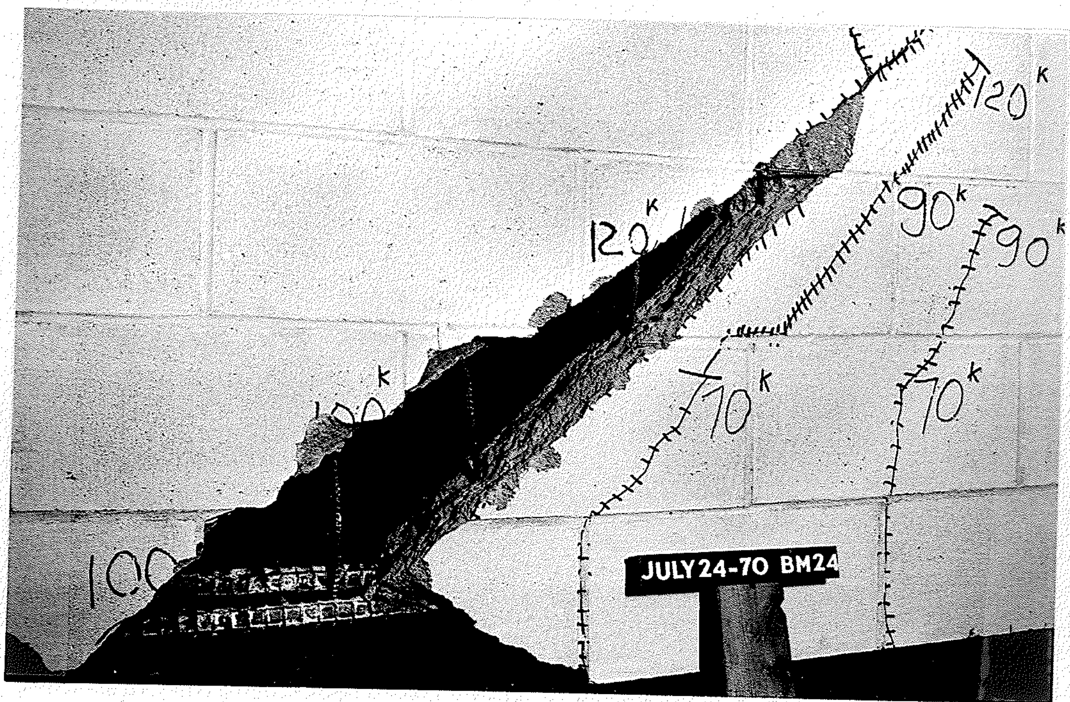

INTERIOR OF BEAM AFTER DIAGONAL TENSION FAILURE SHOWING BOND BETWEEN CONCRETE BLOCK AND FILL

FIGURE 22

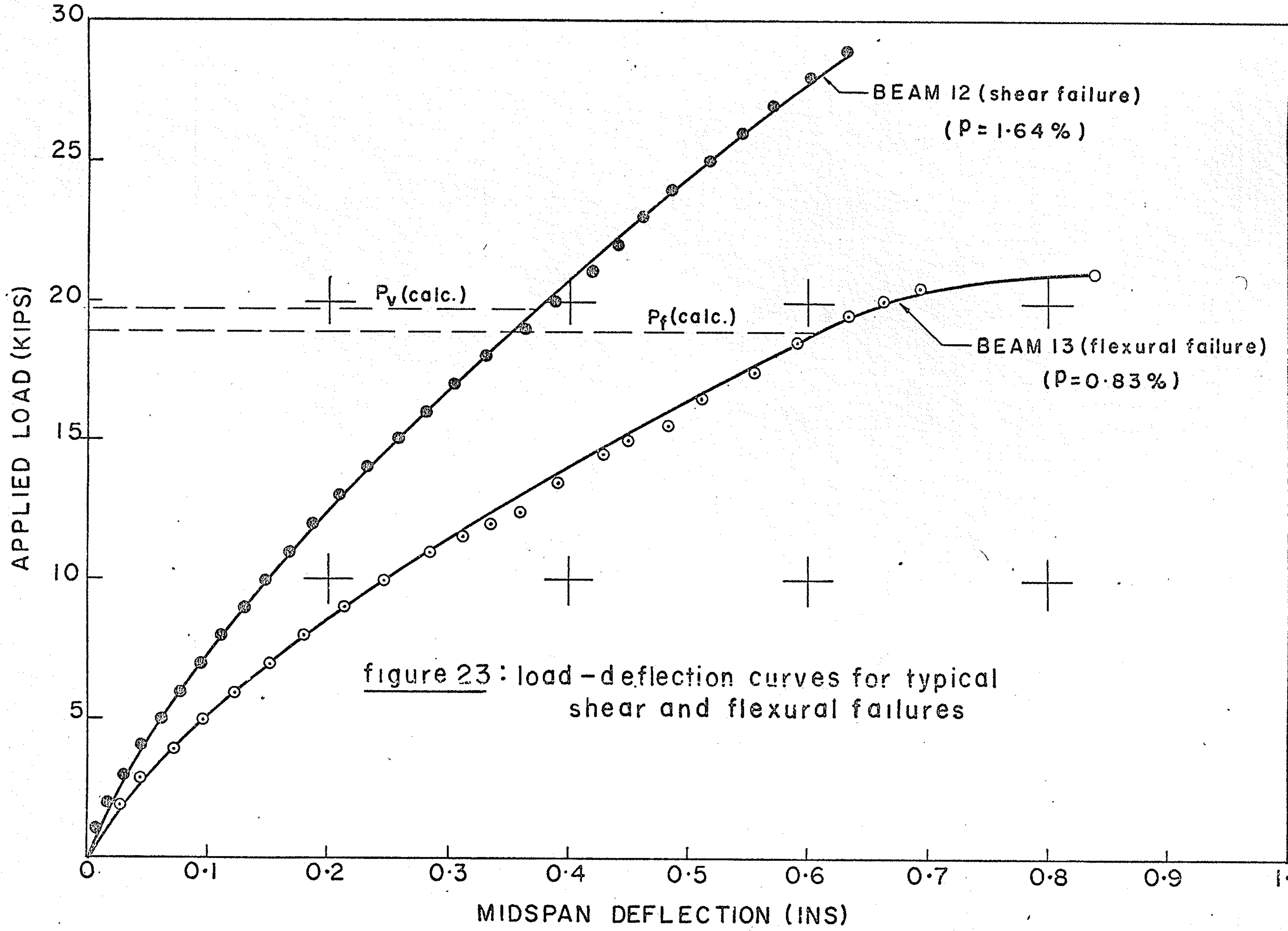

figure 23 : load – deflection curves for typical shear and flexural failures

50

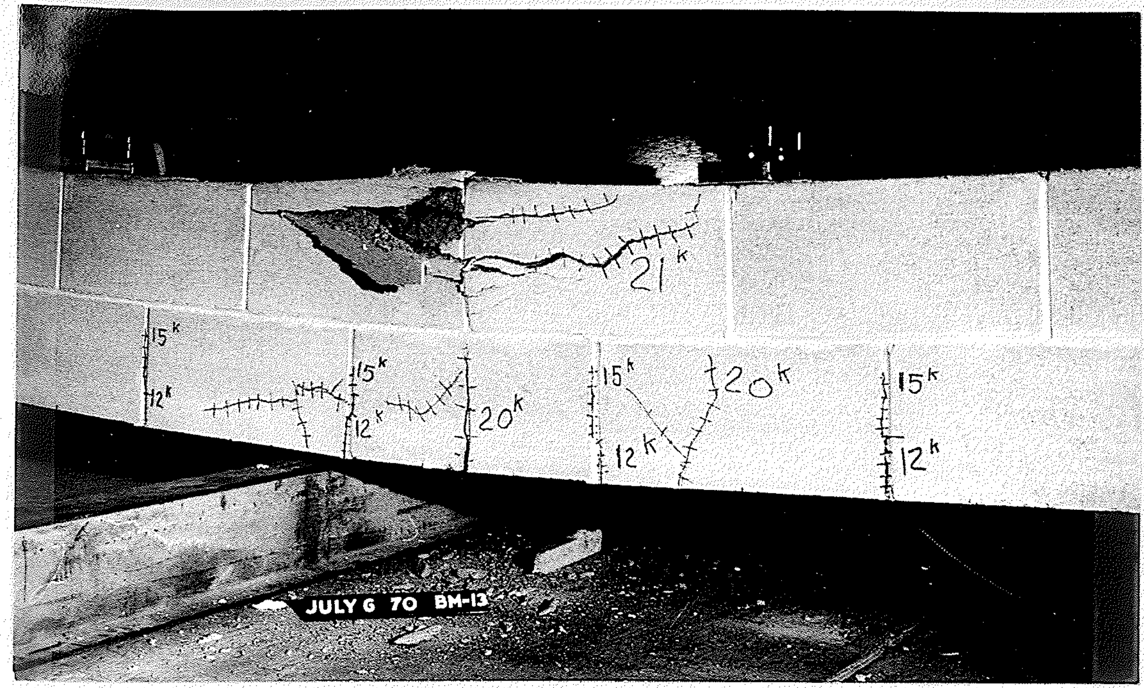

TYPICAL BEAM FLEXURAL FAILURE

FIGURE 24

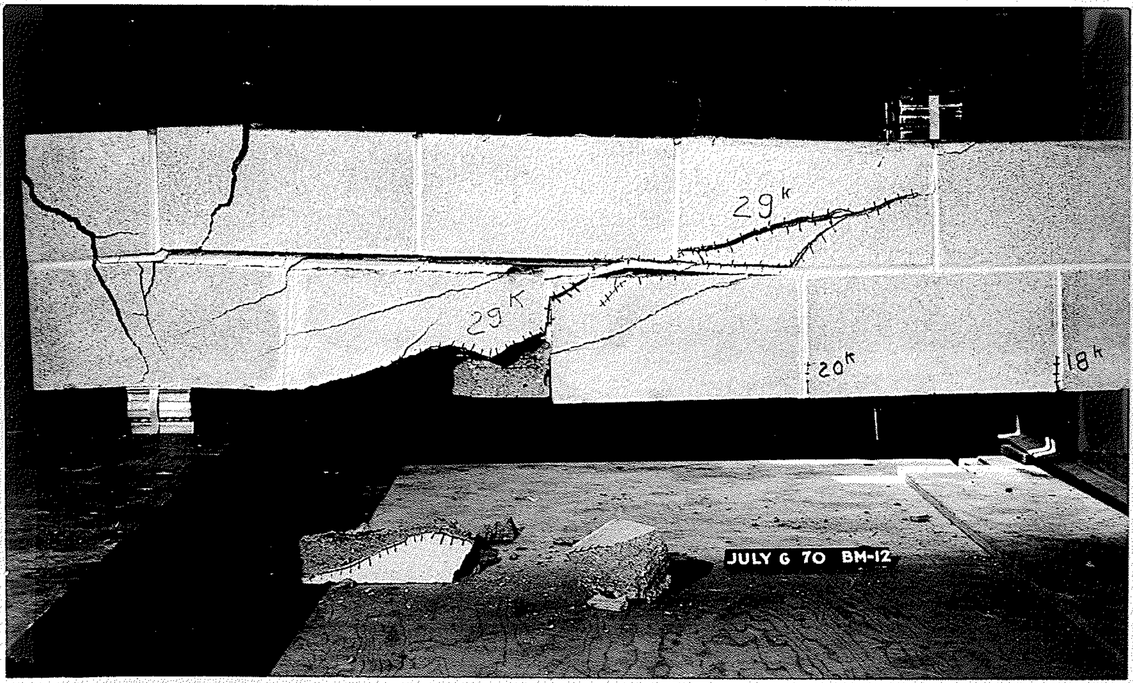

TYPICAL BEAM SHEAR FAILURE

FIGURE 25

Design and Analysis

The beams were designed and analysed by ultimate strength design in accordance with "ACI Standard Building Code for Reinforced Concrete, (ACI 318-63)".

In considering the beam section, the concrete fill was assumed to cover the complete section. This meant that the three materials, concrete fill, mortar and concrete block would be considered to be one material with the same strength as the concrete fill. This is illustrated in Figure 26.

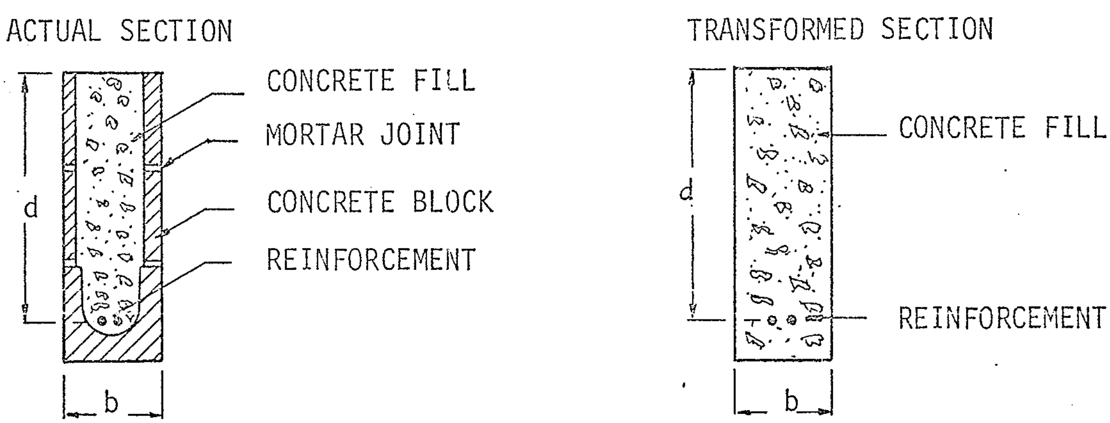

FIGURE 26: TRANSFORMED BEAM SECTION

- Percentages of Longitudinal Reinforcements:

The minimum percentage was governed by :-

$$p \geq \frac{200}{f_y} \quad \text{--------------------} \quad (1)$$

The maximum percentage was governed by:-

$$p \leq 0.75 \left[\frac{0.85\ K_1 f'c}{f_y} \cdot \frac{87,000}{87,000 + f_y} \right] \text{---} \quad (2)$$

where p = percentage of longitudinal steel (As/bd)

b = breadth of beam

d = depth from compression face to centroid of longitudinal reinforcement.

As = area of longitudinal reinforcement

K_1 = constant (0.85)

$f'c$ = ultimate compressive unit strength of concrete fill

f_y = unit stress of steel at yield point

- Ultimate Flexural Capacity:

The ultimate flexural capacity was found by combining equations (3), (4) and (5)

$$P_f = \frac{M_u}{2} \quad \text{---------------------} \ (3)$$

$$M_u = \frac{A_s f_y}{12} (d - \frac{a}{2}) \quad \text{---------} \ (4)$$

$$a = \frac{A_s f_y}{0.85 f'cb} \quad \text{---------------} \ (5)$$

Thus

$$P_f = \frac{A_s f_y}{24} \left[d - \frac{A_s f_y}{1.7 f'cb} \right] \text{---} (6)$$

where P_f = load at ultimate flexural capacity

M_u = Moment at ultimate flexural capacity

- Ultimate Shear Capacity

The ultimate strength in shear was found by the following equations.

<u>Shear Capacity of Concrete</u> :

$$V_c = bd \ \ 1.9 \ \ f'c + \frac{2500 \ p \ Vd}{M} \quad \text{---} \ (7)$$

$$\frac{M}{V} = \frac{M_{max} - d}{V} \quad \text{------------} \ (8)$$

or

$$\frac{M}{V} = (\frac{M_{max}}{V} - \frac{a'}{2}) \quad \text{---------------} \ (9)$$

where $\frac{M}{V}$ used in largest of Eqns. (8) or (9)

and M_{max} = maximum moment in shear span considered

V = external shear in the shear span considered

a' = length of the region of constant shear

V_c = ultimate shear capacity of concrete section.

Shear Capacity of Web Reinforcement:

$$V_w = bd\,(Kr\,f_v) \quad \text{----------------} \quad (10)$$

$$r = \frac{A_v}{b\,s\,\sin\alpha}$$

where $K = (\sin\alpha + \cos\alpha)\,\sin\alpha$

r = percentage of web reinforcement

A_v cross-sectional area of web reinforcement

α = angle between inclined web reinforcement and axis of beam.

b = width of beam

s = horizontal spacing of web reinforcement.

V_w = ultimate shear capacity of web reinforcement

$$P_v = 2(V_c + V_w) \quad \text{-----------------} \quad (12)$$

where P_v = load at ultimate shear capacity of beam.

Note: The relation of load to shear and moment is obtained from the loading diagram (Figure 15)

Allowable Midspan Deflection:

The maximum allowable deflection caused by short time loads is:

$$\Delta(\max) = \frac{L}{360}$$

where L = clear span.

for L = 12 ft.

Δ (max) = 0.4 inches.

Individual Behavior

Beams #1 and #2 :

Beam properties were single course with 8" high lintel blocks; 1.13% longitudinal steel; Concrete strength of 2170 p.s.i.

Both beams behaved elastically up to failure. Initial tension cracks started at about 1.5 kips. Beam #1 failed at 4.1 kips by yielding of the longitudinal steel with a deflection of 1.185 in. The P (test) /P (calc.) ratio was 1.0. Beam #2 failed in a similar manner at 3.5 kips with deflection of 1.02 in. The P(test)/P_f(calc.) ratio was 0.85.

Beam details, load-midspan deflection curves and photographs at failure are shown in Figures 35 to 37 inclusive. Test data is listed in Table X. (See pages 91 to 93).

Beams #3 and #4:

Beam properties were two courses using the H-block in upper course; 0.93% longitudinal steel; concrete strength of 2280 p.s.i.

Load-Deflection characteristics were similar in both beams. The slope was essentially constant up to about 8 kips where the first tension cracks appeared. With the slope reduced somewhat, elastic behavior continued up to about 19 kips, where it was evident that the steel was yielding. By this time, tension cracks had developed and widened across each beam. The beams continued to take loads with large increases in deflection. Ultimate failure was by crushing of concrete in the compression zone.

Beam #3 failed at 23.0 kips with a midspan deflection of 0.95 in. and a P(test) /P_v(calc.) ratio of 1.23. Beam #4 failed at 22.0 kips with a midspan deflection of 0.90 in. and a P (test) /P_v (calc.) ratio of 1.18.

Beam details, load-span deflection curves, and photographs at failure are shown in Figures 38 to 40. Test data is listed in Table XI. (See Pages 94 to 96).

Beam #5 and #6:

Beam properties were two curves using the U-block in upper course; 0.93% longitudinal steel; concrete strength of 2615 p.s.i. Load-deflection characteristics were similar to beams #3 and #4. The first tension cracks appeared at about 8 kips. This is denoted with a change in slope of the load-midspan deflection curve.

Tension cracks continued to develop.and widen across the beam. However, at about 16 kips the slope of these cracks near the beam supports became inclines, thus forming diagonal tension cracks. The load was increased to failure causing large deflection increments. Both failures were sudden and were caused by the opening of diagonal tension cracks near the beam supports. Failure caused the end portion of the beams to separate. Beam #5 failed at 23 kips with a mid-span deflection of 0.9 in. and a P(test) /P_v(calc.) ratio of 1.155. Beam #6 failed at 22.0 kips with a mid-span deflection of 0.75 in. and a P(test) /P_v (calc.) ratio of 1.105. Beam details, load-midspan deflections and photographs of failure are shown in Figures 41 to 43 inclusive. Test data is listed in Table XII. (See Pages 97 to 99).

Beams #7 and #8:

Beam properties were two courses using the standard 2 core block in upper course; 0.93% longitudinal steel; concrete strength of 2430 p.s.i.

Beams #7 and #8 displayed similar test behavior to the previous two-course beams up to about 20 kips. At this time, a diagonal tension crack formed near the right beam support of beam #7. This crack widened under increased load causing a sudden failure with the beam breaking away at the right load support. Beam #7 failed at 21.5 kips with a mid-span deflection of 0.75 in. and a P(test) /P_v(calc.) ratio of 1.125. Beam #8 failed solely by yielding of the longitudinal steel followed by crushing of the concrete in the compression zone. Failure occurred at 23 kips with a mid-span deflection of 0.85 in. and a P(test) /P_V(calc.) ratio of 1.195.

Beam details, load-span deflections and photographs of failure are shown in Figures 44 to 46 inclusive. Test data is listed in Table XIII (See Pages 100 to 102).

Beam #9 and #10:

Beam properties were two courses using the O-block in upper course; 0.93% longitudinal steel; concrete strengths of 2170 p.s.i. and 2280 p.s.i. respectively.

Beam #9 behaved elastically through the loading range. Tension cracks developed and widened up to yielding of the longitudinal steel at about 19 kips. Ultimate failure was caused by crushing of the concrete in the compression zone. Failure occurred at 20.0 kips with a deflection of 0.7 in. and a P(test) /P_V(calc.) ratio of 1.095. Beam #10 showed similar behavior to the previous two-course beams up to about 15 kips. At this point, a tension crack, midway between the left load and beam supports, became somewhat inclined forming a diagonal tension crack. The beam continued to take increased load. The longitudinal steel yielding at about 18 kips causing larger mid-span deflections. Meanwhile, the diagonal tension crack developed towards the load and beam supports. Failure was sudden as this crack opened causing the left section of the beam to separate. Failure occurred at 21.5 kips with a midspan deflection of 0.95 in. and a P(test) /P_V (calc.) ratio of 1.15.

Beam details, load-midspan deflection curves and photographs at failure are shown in Figures 47 to 49. Test data are listed in Table XIV (See Pages 103 to 105).

Beams #11 and #12:

Beam properties were two courses using the H-block in upper course; 1.64% longitudinal steel; concrete strength of 2630 p.s.i.

From the load-span deflection curves, it was evident that the beams deflected little up to about 7 kips. At this point, initial cracking occurred, the steel became stressed and the beams behaved elastically up to failure. The only cracking evident before failure were tension cracks starting at the bottom of the beam and developing up to the level of the longitudinal steel. Both failures were sudden. Diagonal tension cracks had developed and opened within a load increment of 1 kip. Failure caused the beams to split along the horizontal mortar joint between their load and beam supports. However, the concrete fill split along the top layer of longitudinal steel about two in. below the mortar joint. Beam #11 failed at 28 kips with a midspan deflection of 0.690 in. and a P(test) /P_v(calc.) ratio of 1.44. Beam #12 failed at 29 kips with a midspan deflection of 0.630 in. and a P(test)/P_v(calc.) ratio of 1.44.

Beam details, load-midspan deflection curves and photographs at failure are shown in Figures 50 and 52. Test data is listed in Table XV. (See Pages 106 to 108).

Beam #13:

Beam properties were two courses using the H-block in upper course; 0.83% longitudinal steel; concrete strength of 2630 p.s.i.

With initial cracking occurring at about 6 kips, the beam behaved elastically up to yielding of the longitudinal steel at 18 kips. Meanwhile, tension cracks became visible up to the level of the steel, at about 12 kips.

These cracks continued up to the middle of the beam where they stopped at the neutral axis of the beam. After the steel yielded, large deflections resulted with increased load. A flexural failure resulted with crushing of the concrete in the compression zone. Beam #13 failed at 21.0 kips with a deflection of 0.84 in. and a P(test) /P_f (calc.) ratio of 1.17.

Beam details, a load-midpsan deflection curve and a photograph of failure are shown in Figures 51 and 53. Test data is listed in Table XX. (See Pages 107 and 123).

Beam #14 and #15:

Beam properties were 3 courses using the H-block in upper courses; 1.65% longitudinal steel; 0.18% vertical steel; concrete strength of 2630 p.s.i.

Both beams behaved similarly throughout the tests. The beams deflected a small amount up to about 25 kips. At this point initial cracking must have occurred as the slope of the load-deflection curve was reduced. Tension cracks were observed at about 35 kips up to the level of the longitudinal steel. These cracks continued to develop and widen across the beams. At about 50 kips the first diagonal tension cracks appeared midway between the load and end bearing supports. With increased load, these cracks developed in the directions of the load and end bearing supports. However, the tension cracks were arrested at about a 10 in. depth.

The beams failed suddenly by diagonal tension cracks opening from the level of the longitudinal steel up into the compression zone. The concrete split along the top layer of longitudinal steel. In beam #15, a secondary failure developed with shearing off of the outer shell at the end 8 in. of the beam. This is illustrated in Figure 58.

Beam #14 failed at 80 kips with a deflection of 0.690 in. and a P(test) /P_f (calc.) ratio of 1.21. Beam #15 failed at 69 kips with a deflection of 0.513 in. and a P(test)/P_f(calc.) ratio of 1.045.

Beam details, load-midspan deflection curves and photographs are shown in Figures 54 to 58 inclusive. Test data is listed in Tables XVI and XVII. (See Page 110 to 115).

Beams #16 and #17:

Beam properties were 3 courses using the H-block in upper courses; 0.805% longitudinal steel; 0.18% vertical steel; concrete strength of 2630 p.s.i.

From the load-deflection curve, it was evident that initial cracking occurred at about 15 kips. From there on the slope of the curve was slightly reduced and the beams behaved elastically up to the yielding of the longitudinal steel. Tension cracks were visible at 25 kips up to the level of the longitudinal steel. Unlike the two previous beams, these cracks developed up into the middle course with increased load. At 40 kips, diagonal tension cracks had formed midway between the load and end bearing supports. The longitudinal steel yielded at about 45 kips resulting with larger deflections up to failure. Meanwhile both tension and diagonal tension cracks were continuing to develop across the beams.

Failure was sudden and was caused by diagonal tension cracks opening through the depth of the beams. However, by this time, the tension cracks had progressed up to the compression zone, the beams were deflecting considerably with little increase in load, indicating a tension failure as well. Beam #16 failed at 61 kips with a midspan deflection of 0.9 in. and a P(test)/P_v(calc.) ratio of 1.32. Beam #17 failed at 65 kips with a midspan deflection of 1.08 in. and a P(test)/P_v(calc.) ratio of 1.40.

Beam details, load-midspan deflection curves and photographs at failure are shown in Figures 59 to 63 inclusive. Test data is listed in tables XVIII and XIX. (See Pages 116 to 120).

Beam #18:

Beam properties were 3 courses using the H-block in upper courses; 1.14% longitudinal steel; concrete strength of 2630 p.s.i.

From the load-deflection curve, it is evident that initial cracking occurred at about 15 kips. From this point on, the slope of the curve remained constant until failure. There were no signs of cracking until 40 kips. At this point, tension cracks had appeared up to the level of the longitudinal steel. In addition, a diagonal tension crack had developed through the depth of the beam within a load increment of 1 kip.

Failure occurred suddenly with the diagonal tension crack opening and splitting the concrete at the longitudinal steel. The entire right end portion broke away from the rest of the beam. The beam failed at 41 kips with a deflection of 0.312 in. and a P(test)-/P_v(calc.) ratio of 1.105.

Beam details, the load-midspan deflection curve and a photograph at failure are shown in Figures 64 and 65. Test data is listed in Table XX. (See Pages 121 to 123).

Beams #19 and #20:

Beam properties were four courses using the H-block in upper courses; 0.855% longitudinal steel; 0.18% vertical steel; concrete strength of 2630 p.s.i.

Both beams behaved elastically up to about 30 kips. At this point, the slope of the load-deflection curve was slightly reduced indicating initial cracking. Tension cracks were first visible in both beams at 35 to 40 kips, at the level of the longitudinal steel.

Initial diagonal tension cracks appeared in Beam #19 at about 50 kips. These cracks developed along the horizontal and vertical mortar joints, contrary to the previous diagonal tension cracks. Meanwhile, the tension cracks had developed up into the second course causing larger deflections for each load increment. Several other diagonal tension cracks developed in similar manner. Beam #19 failed suddenly with the opening of a diagonal tension crack over the left beam support.

Failure occurred at 57 kips with a deflection of 0.36 in. and a $P(test)/P_v(calc.)$ ratio of 0.626.

On initial cracking, Beam #20 showed elastic behavior up to 65 kips. Meanwhile, the tension cracks had developed to mid-depth and diagonal tension cracks had formed near the right beam support. At 65 kips, these cracks began to widen considerably causing large deflections, and resulting in a sudden failure at 69 kips. The deflection at failure was 0.322 in. with a $P(test)/P_v(calc.)$ ratio of 0.76.

Beam details, load mid-span deflection curves and photographs at failure are shown in Figures 66 to 68 inclusive. Test data is listed in Tables XXI and XXII. (See Pages 124 to 127).

Beams #21 and #22:

Beam properties were four courses using the H-block in upper courses; 1.71% longitudinal steel; 0.18% vertical steel; concrete strength of 2630 p.s.i.

The beams behaved elastically up to about 50 kips with little deflection. For example, the midspan deflections at 50 kips were 0.148 and 0.140 in. From the load-midspan deflection curves, it was evident that cracking occurred at this point. However, the first visible signs of cracking appeared at 65 kips with tension cracks developing at mid-span up to the level of the longitudinal steel.

At 75 kips, tension cracks had developed across the beam but they did not increase any higher than the first course. In addition, diagonal tension cracks had appeared midway between the load and beam supports in both beams. With increased load, these cracks increased towards the load and beam supports. Failure occurred suddenly by diagonal tension cracks opening through the depth of both beams. However, splitting of the concrete along the longitudinal steel did not occur as in previous failures.

Beam #21 failed at 111 kips with a midspan deflection of 0.44 in. and a $P(test)/P_V(calc.)$ ratio of 1.088. Beam #22 failed at 104 kips with a midspan deflection of 0.40 kips and a $P(test)/P_V(calc.)$ ratio of 1.02.

Beam details, load-midspan deflection curves and photographs are shown in Figures 69 to 73 inclusive. Test data is listed in Tables XXIII to XXV inclusive. (See Pages 128 to 135).

Beams #23 and #24:

Beam properties were five courses using the H-block in upper courses; 0.72% longitudinal steel; 0.18% vertical steel; concrete strength of 2630 p.s.i.

The slope of the load-midspan deflection curve was constant up to 40 kips indicating elastic behavior in this range. At this point the slope was reduced and again remained constant until just prior to failure. At 50 kips, initial tension cracks appeared at midspan up to the level of the longitudinal steel. At 70 kips, tension cracks had widened and developed across the beam. In addition, they had spread into the second course and had become inclined in areas between the load and beam supports.

Initial diagonal tension cracks formed at 80 kips in areas between the load and beam supports. From this load to failure, similar diagonal tension cracks appeared parallel to the original ones. In addition, the original cracks were expanding towards the load and beam supports. However, the tension cracks did not expand above the second course.

Failure occurred suddenly in both beams by the opening of diagonal tension cracks from the compression zone down to the longitudinal steel. Beam #23 failed at 142 kips with a midspan deflection of 0.49 in. and a P(test)/P_v(calc.) ratio of 1.13. Beam #24 failed at 150 kips with a midspan deflection of 0.48 in. and a P(test)P_v(calc.) ratio of 1.20.

Beam details, load-midspan deflection curves and photographs at failure are shown in Figures 74 to 78 inclusive. Test data is listed in Tables XXVI to XXVIII inclusive. (See Pages 136 to 142).

Beam #25

Beam properties were: four courses using the H-block in upper courses; 0.955% longitudinal steel; 0.328% vertical steel; concrete strength of 4740 p.s.i.

Behavior was essentially elastic for the first 25 kips of applied load. At this point a small change in slope occurred in the load-midspan deflection curve, indicating initial cracking. At 30 kips, initial tension cracks appeared up to the level of the longitudinal steel. These cracks widened and developed across the beam with increased load. At 60 kips, tension cracks had expanded up to the third course, and cracks near the load supports were becoming somewhat inclined.

Diagonal tension cracks appeared at 70 kips midway between the load and beam supports. These cracks developed with increased loads but not to the extent of previous diagonal tension cracks. The tension steel appeared to yield at about 110 kips. At this point, the load was held constant for 10 minutes. The load was then slowly increased to failure.

The beam failed by yielding of the longitudinal steel followed by large deflections and finally crushing of the concrete in the compression zone. On crushing of the concrete, the load dropped to 100 kips and remained steady, indicating a ductile failure.

Beam #25 failed at 133 kips with a midspan deflection of 1.3 in. and a $P(\text{test})/P_f(\text{calc.})$ ratio of 1.29. The beam rebound was 0.5 in. on removing the load.

Beam details, load midspan deflection curve and photographs at failure are shown in Figures 79, 80 and 82. Test data is listed in Table XXIX and XXXI. (See Pages 143 to 148).

Beam #26:

Beam properties were four courses using the H-block in upper courses; 0.95% longitudinal steel; 0.24% web reinforcement inclined at 45° to longitudinal axis; concrete strength of 4100 p.s.i.

The loading behavior and mode of failure were similar to Beam #25. This is not surprising since the only physical difference in the two beams was the concrete strength and web reinforcement. Again, the failure was ductile with the beam capacity reducing to 80 kips after failure.

Beam#26 failed at 128 kips with a midspan deflection of 1.4 in. and a P(test)/P_f(calc.) ratio of 1.22. A rebound of 0.49 in. was recorded on removing the load.

Beam details, load-midspan deflection curve and photographs at failure are shown in Figures 79, 81 and 83. Test data is listed in Tables XXX and XXXI. (See Pages 143 to 148).

(b) Wall Sections:

The test results are summarized with the help of tables, curves and photographs. These are found in the appendix under Tables XXXII to XXXVII inclusive and Figures 84 to 92 inclusive.

Gauges 1,2 and 3 situated on the right face of the section, indicate a lateral displacement to the left by a negative reading. On the other hand, gauges 4,5 and 6 situated on the left face, indicate a displacement to the right by a negative reading, and a displacement to the left by a positive reading. Thus by taking the algebraic sum of the two gauge readings at any level, the lateral expansion of the section can be determined. This is illustrated in Figure 27.

Mode of Failure

The failure pattern was similar for all six sections and resulted by crushing of top two to six courses of the sections. In addition, four of the sections split vertically from the top through the

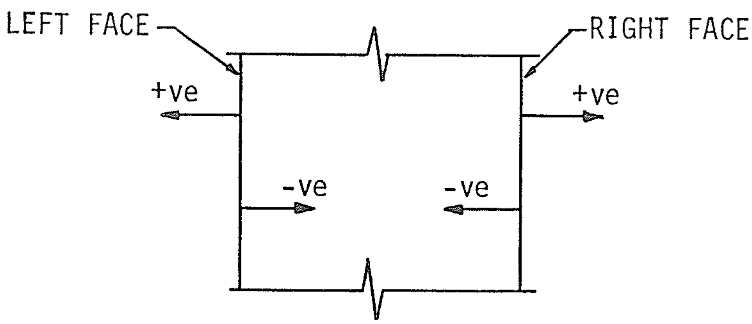

FIGURE 27: WALL SECTION GAUGE DISPLACEMENTS

mortar joints to almost mid-depth.

Failure occurred suddenly by spalling of concrete block and fill near the top of the section. In some cases the complete top was destroyed causing the section to fall sideways in the frame. Figures 28 and 29 show photographs of a section during failure. Pieces of concrete block and fill can be seen in the air.

The identical failure mode was not surprising since all section properties and dimensions were similar except for the methods of consolidation of the concrete. Due to the crushing type of failure, lateral deflections were small, less than 1/10 of an inch.

Analysis

The sections were analysed by ultimate strength design in accordance with "ACI Standard Building Code for Reinforced Concrete, (ACI 318-63) Section 2202."

As in the beams, the concrete fill was assumed to cover the complete section. This is illustrated in Figure 30.

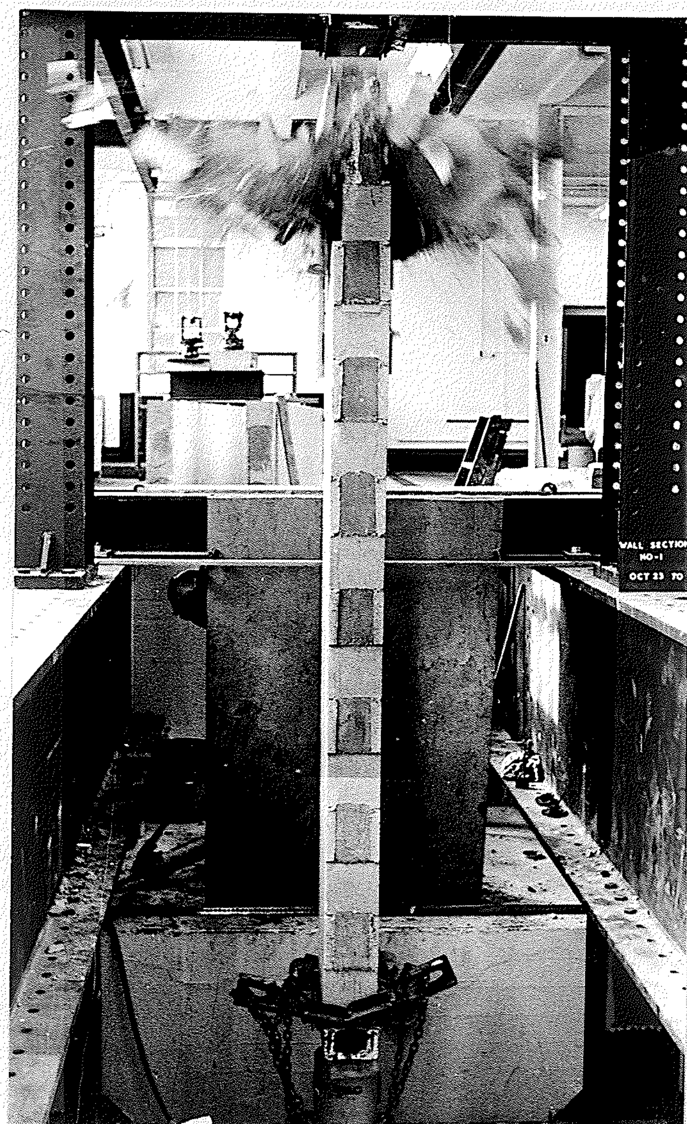

OVER-ALL VIEW OF WALL SECTION DURING FAILURE SHOWING

CONCRETE IN AIR - FIGURE 28

68

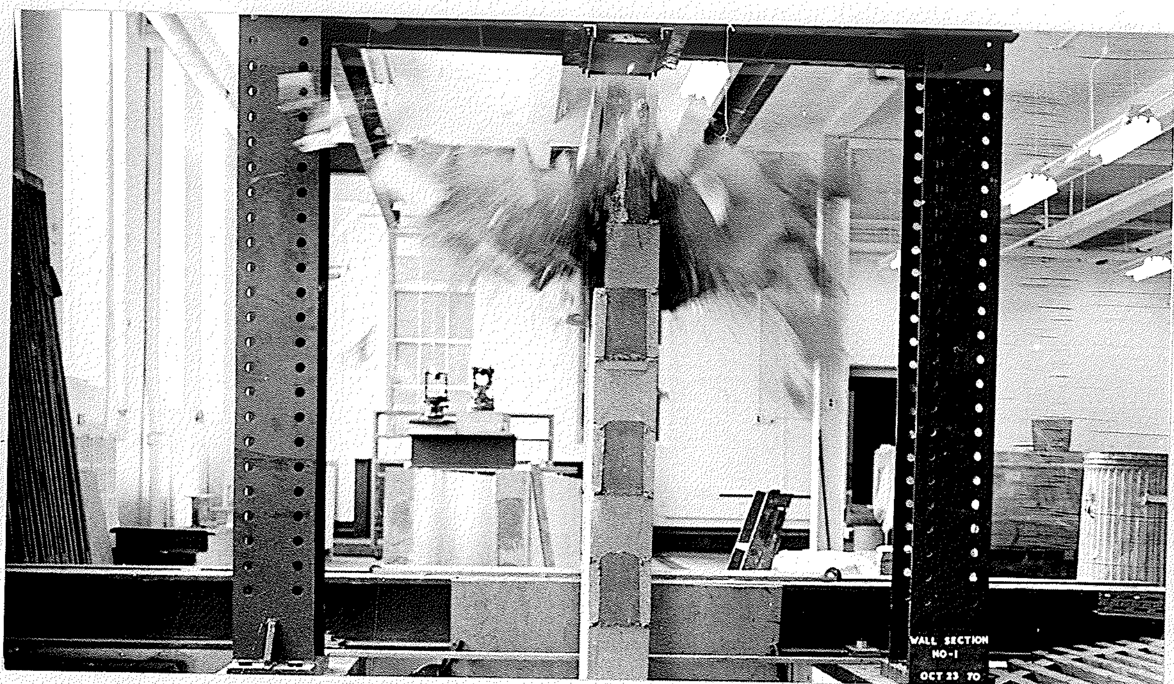

TOP PORTION OF WALL SECTION DURING FAILURE SHOWING

COMPLETE DESTRUCTION - FIGURE 29

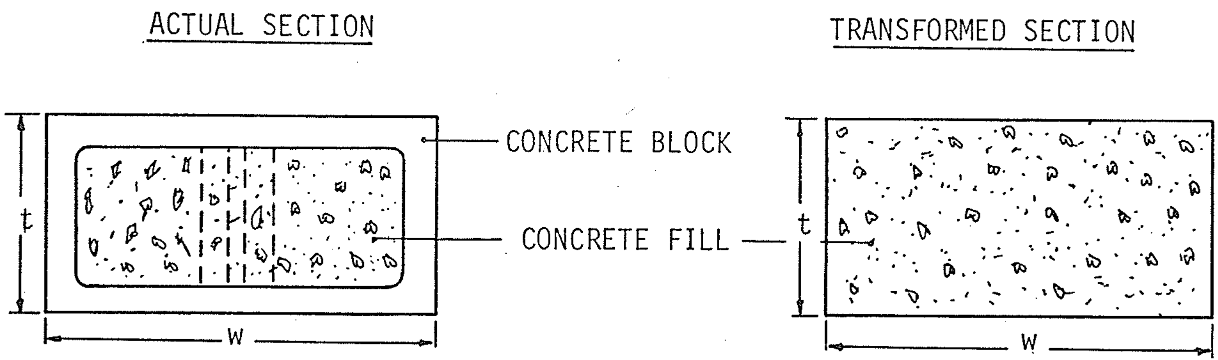

FIGURE 30: TRANSFORMED WALL SECTION

- The ultimate stress was found from the equation :-

$$f_c = 0.427\ f'_c \left[1 - \left(\frac{h}{40t}\right)^3\right] \qquad \text{-----------} \quad (1)$$

where f'_c = concrete cylinder strength

h = height of wall section

t = overall thickness of wall section.

- The ultimate load was found from the equation:-

$$P = t.w.f_c$$

where w = overall width of section.

Individual Behavior

Section 1:

The concrete fill was rodded and the cylinder strength at time of test was 4975 p.s.i. The mortar cube strength was 1825 p.s.i.

The section showed no cracks during the loading period. The gauges were removed at 197.5 kips with a maximum lateral displacement of 0.047 ins. The load was increased in 4 kip increments until failure at 249 kips. Failure occurred by vertical splitting along the mortar joints of the top three courses. The section fell and was further damaged on hitting the side of the frame. The P(test)/ P(calc.) ratio was 1.1.

Curves showing the lateral displacement and expansion, are given in Figures 84 and 86, a photograph at failure is shown in Figure 87. Test data is listed in Table XXXII. (See Pages 149, 151 to 153).

Section 2:

The concrete fill was rodded and the cylinder strength at time of test was 4660 p.s.i. The mortar cube strength was 1900 p.s.i.

The load was applied in 10 kip increments up to 200 kips. At 100 kips, a vertical crack appeared at the side of the second block from the top of the section. There was no further development of this crack on increasing the load. The gauges were removed at 197 kips with a maximum lateral displacement of 0.080 ins. The section failed at 221 kips with a P(test)/P(calc.) ratio of 1.04. Failure occurred suddenly with the spalling of concrete block and fill in the top four courses. The central core in this area was not destroyed. This kept the section in place.

Curves showing the lateral displacement and expansion are given in Figures 84 and 86. A photograph at failure is shown in Figure 88 and test data is listed in Table XXXIII. (See Pages 154 and 155).

Section 3:

The concrete fill was rodded and the cylinder strength at time of test was 4075 p.s.i. The mortar cube strength was 1805 p.s.i

The load was applied in 10 kip increments up to 200 kips. At this point, the gauges were removed. The maximum lateral displacement at this time being 0.099 inches. The load was then increased in 8 kip increments. There was no visible cracking prior to failure at 228 kips. Failure was caused by crushing of the top three courses. In addition, the section was split along the vertical mortar joints from the top to the middle of the section. The P(test /P(calc.) ratio was 1.22.

Curves of lateral displacement against load and a photograph at failure are shown in Figures 84 and 89. Test data is listed in Table XXXIV. (See Pages 156 and 157).

Section 4:

The concrete fill was vibrated and the cylinder strength at time of test was 4735 p.s.i. The mortar cube strength was 2065 p.s.i.

Load was applied in 10 kip increments throughout the test. Gauges were removed at 260 kips; the maximum lateral displacement at the time being 0.032 ins. Failure occurred suddenly at 292 kips with the crushing of the top three courses and vertical splitting along the mortar joints of the top eight courses. The P(test)/P(calc.) ratio was 1.35. Curves of lateral displacement against load and a photograph at failure are shown in Figures 85 and 90. Test data is listed in Table XXXV. (See Pages 150, 158 and 159).

Section 5:

The concrete fill was vibrated and the cylinder strength at time of test was 4325 p.s.i. The mortar cube strength was 2115 p.s.i.

Load was applied in 10 kip increments throughout the test. The gauges were removed at 236 kips with the maximum lateral displacement being 0.025ins. At this point, a vertical crack had appeared in the top course mortar joint. Similar cracks had also appeared in the bottom four courses. Failure occurred suddenly at 244 kips by spalling of concrete block and fill from the top to a depth of nine courses. The P(test)/P(calc.) ratio was 1.24.

Curves of load against lateral displacement and a photograph at failure are shown in Figures 85 and 91. Test data is listed in Table XXXVI. (See Pages 160 and 161).

Section 6:

The concrete fill was vibrated and cylinder strength at time of test was 4625 p.s.i. The mortar cube strength was 2115 p.s.i.

The load was applied in 10 kip intervals up to 240 kips. At this point, the maximum lateral displacement was 0.058 ins. Upon removing the gauges, the loading was continued in 4 kip increments. At 260 kips, a vertical crack had developed in the bottom course mortar joint. The section failed suddenly at 280 kips with spalling of concrete block and fill from the top three courses. The P(test)/P(calc.) ratio was 1.24.

Curves of load against lateral displacement and a photograph at failure are shown in Figures 85 and 92. Test data is listed in Table XXXVII. (See Pages 162 and 163).

IV. EVALUATION OF TEST RESULTS

(a) Beams

Table VIII presents a summary of properties and results for all 26 beams tested. Included in the summary are the calculated failure loads by Ultimate Strength Analysis for shear and flexure, denoted by P_v and P_f respectively. P_v and P_f are also shown on the load - midspan deflection curves. The P(test)/P(calc.) ratio was calculated for each beam. The P(calc.) value used was the P_v or P_f that governed failure.

The 26 beams tested yield an average P(test)/P(calc.) ratio of 1.14 The 7 beams governed by flexure yielded an average P(test)/P(calc.) ratio of 1.18. The remaining 19 beams were governed by shear, 8 beams, with web reinforcement, yielded an average P(test)/P(calc.) ratio of 1.207.

The results of the beams without web reinforcement can be compared to results of reinforced concrete beams tested by Moody, Elstner, Hognestad and Viest[14]. Their analysis and properties were similar to the author's. The P(test)/P(calc.) ratio was 1.076 for 45 beams tested. This compares to a P(test)/P(calc.) ratio of 1.207 for 11 beams tested by the author.

The results of the beams with web reinforcement can be compared to results of 94 beams tested by Clark[3], Guralnick[6], Moretto[15], Thurston[21], Bresler and Scordelin[2]. These tests yielded an average P(test)/P_v(calc.) ratio of 1.368 compared to a 1.01 for 11 beams tested by the author. However, it must be pointed out that the percentage of longitudinal steel in these beams was generally three times larger than the author's. This would account for the increase in capacity.

The mid-span deflections at ultimate load are listed in Table VIII

TABLE VIII

SUMMARY OF BEAM PROPERTIES AND RESULTS

BEAM PROPERTIES												BEAM RESULTS						
			Longitudinal Steel					Web Steel		Concrete and Mortar								
Beam No.	No. of Courses	Type of block	b (ins.)	d (ins.)	As (in.^{2})	p %	fy (p.s.i.)	r %	f_v (p.s.i.)	f'_c (p.s.i.)	f'_m (p.s.i.)	P_v(calc.) (kips)	P_f(calc.) (kips)	P(test) (kips)	P(test)/P(calc.)	Maximum Defln. (ins.)	Load at allow.Def (kips)	Mode of Failure
1	1	L	7.625	5.1	0.44	1.13	52,700	-	-	2170	1060	7.1	4.15	4.1	1.0	1.185	1.6	Flexure
2	1	L	7.625	5.1	0.44	1.13	52,700	-	-	2170	1060	7.1	4.15	3.5	0.85	1.020	1.6	flexure
3	2	H	7.625	12.4	0.88	0.93	52,700	-	-	2280	1165	18.65	20.88	23.0	1.23	0.950	15.0	flexure
4	2	H	7.625	12.4	0.88	0.93	52,700	-	-	2280	1165	18.65	20.88	22.0	1.18	0.900	15.0	flexure
5	2	U	7.625	12.4	0.88	0.93	52,700	-	-	2615	1325	19.8	21.25	23.0	1.155	0.900	14.5	shear
6	2	U	7.625	12.4	0.88	0.93	52,700	-	-	2615	1325	19.8	21.25	22.0	1.105	0.750	14.5	shear
7	2	S	7.625	12.4	0.88	0.93	52,700	-	-	2430	1325	19.2	21.3	21.5	1.125	0.750	14.0	shear
8	2	S	7.625	12.4	0.88	0.93	52,700	-	-	2430	1325	19.2	21.3	23.0	1.195	0.850	15.5	flexure
9	2	O	7.625	12.4	0.88	0.93	52,700	-	-	2170	1325	18.25	20.8	20.0	1.095	0.700	13.5	flexure
10	2	O	7.625	12.4	0.88	0.93	52,700	-	-	2280	1325	18.7	20.9	21.5	1.15	0.950	13.5	shear
11	2	H	7.625	11.5	1.44	1.64	52,600	-	-	2630	1560	19.4	29.2	28.0	1.44	0.690	19.0	shear
12	2	H	7.625	11.5	1.44	1.64	52,600	-	-	2630	1560	19.4	29.2	29.0	1.495	0.630	20.5	shear
13	2	H	7.625	12.5	0.79	0.83	48,350	-	-	2630	1560	20.0	17.9	21.0	1.17	0.840	14.0	flexure
14	3	H	7.625	19.5	2.46	1.65	49,500	0.18	53,150	2630	1560	66.0	81.0	80.0	1.21	0.690	57.5	shear
15	3	H	7.625	19.5	2.46	1.65	49,500	0.18	53,150	2630	1750	66.0	81.0	69.0	1.045	0.513	59.0	shear
16	3	H	7.625	20	1.23	0.81	49,500	0.18	53,150	2630	1750	63.0	46.3	61.0	1.32	0.900	61.0	flexure
17	3	H	7.625	20	1.23	0.81	49,500	0.18	53,150	2630	2000	63.0	46.3	65.0	1.40	1.080	47.0	flexure
18	3	H	7.625	20.5	1.79	1.14	51,200	-	-	2630	2000	37.1	68.0	41.0	1.105	0.312	-	shear
19	4	H	7.625	27.5	1.79	0.86	51,200	0.18	53,150	2630	2840	91.0	95.0	57.0	0.626	0.360	-	shear
20	4	H	7.625	27.5	1.79	0.86	51,200	0.18	53,150	2630	2840	91.0	95.0	69.0	0.76	0.322	-	shear
21	4	H	7.625	27.5	3.58	1.71	51,200	0.18	53,150	2630	3150	102	169	111.0	1.088	0.440	106.0	shear
22	4	H	7.625	27.5	3.58	1.71	51,200	0.18	53,150	2630	3150	102	169	104.0	1.02	0.400	104.0	shear
23	5	H	7.625	36.5	2.0	0.72	53,800	0.18	53,150	2630	2935	125.5	149.5	142.0	1.13	0.490	126.0	shear
24	5	H	7.625	36.5	2.0	0.72	53,800	0.18	53,150	2630	3165	125.5	149.5	150.0	1.20	0.480	132.0	shear
25	4	H	7.625	27.5	2.0	0.96	48,070	0.33	46,580	4740	2445	130.0	104.0	133.0	1.29	1.500	104.0	flexure
26	4	H	7.625	27.5	2.0	0.96	48,070	0.24	46,580	4100	2785	111.0	103.0	128.0	1.22	1.500	100.2	flexure

together with the load at which the maximum allowable (L/30) of 0.4 in. was reached. In addition, the allowable deflection is shown on all load-midspan deflection curves.

With the exception of Beams #1 and #2, all beams reached their maximum allowable deflection at loads greater than 65% of ultimate load. Assuming a working load of 50% of ultimate, it can be said that the deflections were not critical. However, tension cracks were visible up to the level of the longitudinal steel from loads of 40% of ultimate. These cracks were not structurally important as the concrete below the neutral axis was assumed to crack in any case. It was found that the deflection decreased by about 40% when the percentage of longitudinal steel was doubled.

Beams #3 to #10 inclusive all exceeded their computed shear and flexural capacities. Since the only variable in these beams was the shape of the block in the second course, the performance of the individual type block can be evaluated.

The ultimate load varied from 20 kips to 23 kips, thus the performance cannot be evaluated on this basis. However, the H-block was chosen for the continuation of the test program on other merits, which were as follows:

(1) With a single web in the centre, the H-block was balanced and could be easily held and laid.

(2) The vertical joints were offset from the web, preventing a vertical mortar joint from crossing one face to the other. This formed a moisture controlled joint and prevented the mortar joints from crossing the compression zone. (See Figure 31).

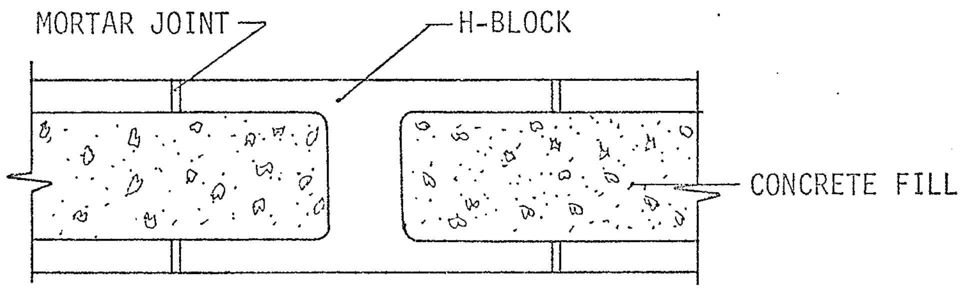

FIGURE 31: BEAM COMPRESSION FACE SHOWING H-BLOCK

(3) Horizontal continuity and placement of concrete was best achieved.

Three beams failed at loads below their theoretical capacity. Beam #2 failed at 3.5 kips while its theoretical flexural capacity was 4.15 kips.

Beams #19 and #20, with similar dimensions and properties, both failed at loads below their theoretical capacity. The governing criteria in this case was shear with a theoretical capacity of 91 kips whereas Beams #19 and #20 failed at 57 and 69 kips respectively.

Their are several reasons why these beams failed below their theoretical capacity, which became evident when the beams were broken apart and inspected. The concrete was not well placed around the longitudinal steel in the end zone. The reason for this was insufficient vibration. (In fact, the concrete was delivered at a fast rate with only one vibrator on the job.) This resulted in poor anchorage of both the longitudinal and vertical steel, thereby reducing their shear capacity.

The bond had been broken between the vertical face of the blocks' webs and the concrete fill. This resulted in a failure crack greater than 45 degrees to the horizontal, thereby crossing fewer vertical stirrups than calculated in design. It is the author's opinion that the vertical stirrups were ineffective in these beams. In this case, the $P(test)/P_v(calc.)$ ratio for beams 19 and 20 would have been 1.11 and 1.35 respectively

The compressive strength of the mortar was always less than the compressive strength of the concrete block or fill. However, crushing failures always developed in the concrete block or fill and never in the mortar. This agrees with the tests conducted by Hilsdorf[8], which proves that mortar in a joint can sustain a higher compressive stress than when subjected to a cube test. This is explained by the bond and friction developed at the block and mortar interface which confines the mortar. Thus an internal state of stress develops which causes triaxial compression in the mortar. It is only because of this triaxial state of compression that a mortar joint can be subjected to external stresses which exceed the uniaxial compressive stress of the mortar.

As may be expected, vertical cracks always started at mortar joints in the bottom course. However, in the one and two course beams, similar cracks also appeared at the centre of the blocks. The presence of the vertical joints may have caused initial cracking at an earlier load, but in no way did they influence the ultimate capacity of the beams.

Diagonal tension cracks generally started midway between the load and end bearing supports. Their slope was about 45 degrees to the longitudinal axis. It was found that when they crossed a vertical or horizontal mortar joint, the direction of the cracks was not usually changed by the presence of the mortar joints. Thus it can be concluded that the presence of the mortar joints did not constitute weak joints for the development of diagonal tension cracks.

The overall performance and results of the 26 beams tested agreed very closely with numerous previous tests on reinforced concrete beams. It was noted that beams without web reinforcement sustained greater loads than those forming initial diagonal tension cracks. Since no force can be transmitted across the crack, a redistribution of internal forces takes place. The shear force is then carried partly by the dowel action in the longitudinal reinforcement, but mainly by the concrete in the uncracked compression zone.

Initial diagonal tension cracks were formed at an earlier percentage of ultimate load in beams with web reinforcement. This agrees with previous results by others that the vertical steel does not become stressed until after the formation of diagonal tension cracks. The vertical steel may have yielded at failure, but in no case was their ultimate tensile capacity reached.

(b) Wall Sections:

Table IX presents a summary of properties and results for the six sections tested. Included in the summary are the calculated stresses and loads by ultimate strength analysis denoted by fc(calc.) and P(calc.). The actual compressive stresses and loads at failure are denoted by fc(test) and P(test).

The average P(test)/P(calc.) ratios were 1.12 for the rodded sections and 1.30 for the vibrated sections. The average cylinder strengths were 4570 p.s.i. for the rodded sections and 4561 p.s.i. for

TABLE IX

SUMMARY OF WALL SECTION PROPERTIES AND RESULTS

Wall Section Properties							Wall Section Results					
Wall Sect. No.	Type of Consolidation	t (ins)	w (ins)	h (ins)	f'_m (psi)	f'_c (psi)	f_c(calc) (psi)	f_c (test) (psi)	P(calc) (kips)	P(test) (kips)	P(test) / P(calc.)	$\frac{f_c\text{ (test)}}{f'_c}$
1	rodded	7 5/8	15 5/8	144	1825	4975	1900	2084	227	249	1.1	0.420
2	rodded	7 5/8	15 5/8	144	1900	4660	1785	1842	212	221	1.04	0.396
3	rodded	7 5/8	15 5/8	144	1805	4075	1560	1900	186	228	1.22	0.466
4	vibrated	7 5/8	15 5/8	144	2065	4735	1810	2430	216	292	1.35	0.513
5	vibrated	7 5/8	15 5/8	144	2115	4325	1650	2030	197	244	1.24	0.470
6	vibrated	7 5/8	15 5/8	144	2115	4625	1770	2330	211	280	1.32	0.502

the vibrated sections. With the cylinder strengths virtually the same, it is seen that the vibrated sections yielded ultimate loads 16% higher than the rodded sections. The average fc (test) was 1940 p.s.i. for the rodded sections and 2260 p.s.i. for the vibrated sections. Comparing with the cylinder strengths, the average fc (test)/f'c was 0.425 for the rodded sections and 0.491 for the vibrated sections.

These results can be compared to 12 concrete walls, tested by Richart[23] and analysed in similar manner to the author's. The average P(test)/P(calc.) ratio was 1.8. However for walls with cylinder strengths in the 4000 p.s.i. range, the P(test)/P(calc.) ratio was reduced to 1.4. This ratio compares with the author's of 1.3 for vibrated wall sections. The fact that the compressive strength of walls does not increase proportionately with the cylinder strength has been proven by other investigators. Several series of tests reported by Seddon[24] indicate up to a 20% increase in compressive strength with the addition of reinforcement. It should be noted that Richart's tests contained reinforcement. The mode of failure in the tests reported by Seddon was again similar to the author's, namely local crushing of concrete below the bearing plate and vertical splitting of the wall.

Although the mortar was the weakest of the three materials, there is no evidence to indicate that failure was caused by crushing of the mortar joint.

The similar failure pattern found in the six sections can be accounted for in several ways:

(1) The concrete in the bottom of the section could be of a higher strength than at the top. This concrete would be subjected to the impact loads and weight of a twelve foot

column of concrete. This in turn could result in better consolidation and hence a higher strength concrete at the bottom.

(2) The top course contained two split blocks, while the bottom course contained a single block. Since the mortar joint was not grouted solid, but only buttered at the ends, the effective bearing area was reduced. (See Figure 32)

(3) The end bearing plates could have transferred the loads from the frame and jack in different positions. This could introduce local stresses in excess of the average stress in

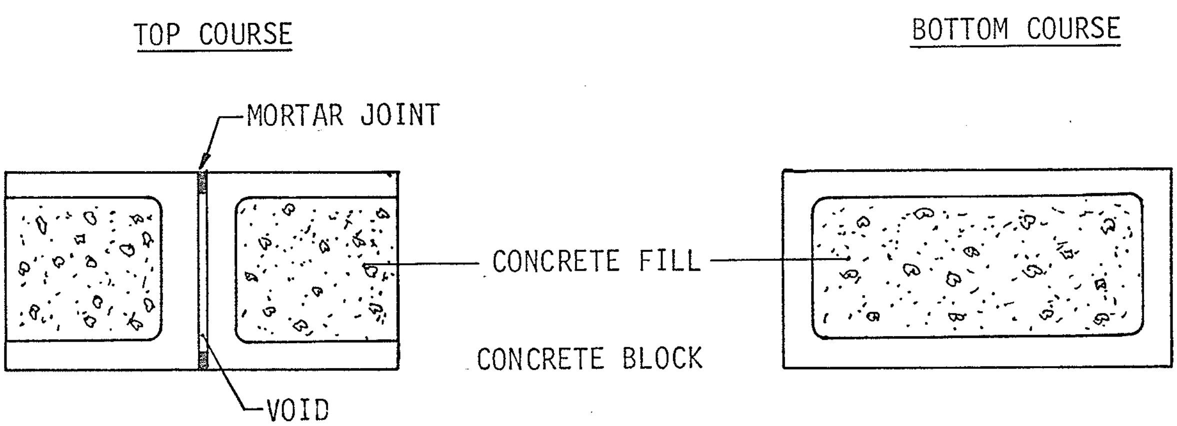

FIGURE 32: WALL SECTION BEARING AREAS

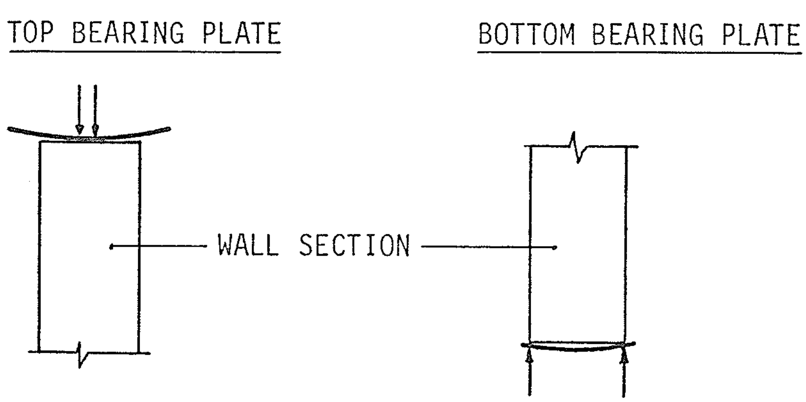

FIGURE 33: WALL SECTION BEARING EFFECTS

SIDE VIEW

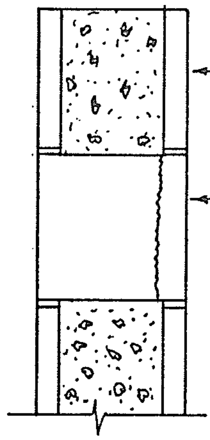

FIGURE 34: CRACKED ZONE OF WALL SECTION

the section. The top bearing plate was more rigid at the centre while the bottom bearing plate was more rigid along the outer edges. This would result in the bearing plate causing the section to bulge at the top and to be confined at the bottom. (See Figure 33).

There is additional evidence to indicate that the bearing plates were in fact causing such end conditions. For sections 1 and 2, gauges were installed on opposite faces to measure any lateral expansion. These results are plotted in Figure 86. They indicate a consistent expansion of the sections near the top, in the order of 0.015 in. to 0.022 in. for a 200 kip load.

At the middle and bottom of the sections, there is a scatter of readings on either side of the axis of zero expansion. However, the readings at the bottom indicate a small contraction of both sections.

Poisson's effect could have caused a maximum expansion of about 0.002 in. for the loads reached. Thus the relatively large expansion only at the top of the sections would indicate an end effect caused by the bearing plate. This expansion now leads to the question of block separation prior to failure. In section 2, a vertical crack appeared in the side of the second block from the top, at a load of 100 kips. (See Figure 34).

This would further indicate that the concrete block shell was in fact separating from the inner core of concrete. Since my measured or visual evidence of expansion only occurred near the top of the sections, the separation should be considered a local condition.

Another similarity in the failure mode was the vertical splitting of four of the sections at failure. This split started from the top course and separated the sections along the vertical mortar joints to about mid-depth. There was in fact a plane of weakness along the sections due to the vertical mortar joints. Thus any lateral tension generated in a section would cause it to split along those joints.

The mode of failure and recorded lateral displacements indicated a definite crushing failure in all the sections. However, the lateral displacements did indicate some bending was occurring (See Figures 84 and 85). This bending could have been caused by a small eccentricity in the loading system but in no way contributed to failure.

V CONCLUSIONS

The 26 beams and 6 wall sections tested verified the two assumptions made, namely:

(1) Unity of action exists between the block, concrete fill and the reinforcement in properly built block-formed structural elements.

(2) Each individual component of the construction-blocks, concrete fill, masonry and reinforcement - contributes to the ultimate strength of the composite construction.

Beams governed by shear generally produced sudden or brittle type failures while those governed by flexure produced gradual or ductile failures. However, the deflections for the beams governed by flexure were about 40% greater than those governed by shear, when comparing beams of similar dimensions. These results agree with numerous previous tests conducted on reinforced concrete beams.

The average P(test)/P(calc.) ratios for the beams and wall sections were 1.14 and 1.21 respectively. Thus block-formed structural members can be safely designed by Ultimate Strength Theory based on "ACI Building Code for Reinforced Concrete".

The mortar strengths were about 80% of the concrete strength in the beams and 40% of the concrete strength in the wall sections, however, failure in both beams and wall sections was never caused by crushing of the mortar joint. Therefore, provided the mortar strength is not less than 40% of the concrete strength, the compressive strength of the concrete fill can govern the design.

The horizontal mortar joints of the beams all contained joint reinforcement, thus no evaluation can be made on the advantage of such reinforcement. However, as this reinforcement crossed all diagonal tension cracks, some benefit would have resulted. On the other hand, the wall sections did not contain any joint reinforcement so neither can any evaluation be made on this basis. However, the presence of joint reinforcement near the top of the sections would have delayed the splitting type failures.

A high slump concrete (about 8") is essential for proper consolidation of the concrete in block-formed walls. It was evident that water was absorbed by the block from during filling. This resulted in immediately lowering the w/c ratio thus increasing the concrete strength. In addition, vibrating the concrete fill increases the wall strength by 16% over rodding the fill.

Poor stirrup anchorage was a partial cause for the premature failure of two beams. Therefore, the adequacy of a standard hook at the bottom of the single leg stirrup is questionable.

The function of the concrete block is primarily that of a form, therefore the ASTM specifications on face-shell and web thicknesses can be neglected. These dimensions should be governed by handling stresses and lateral pressures imposed by the concrete fill. However, the compressive strength of the net block area should conform to ASTM specifications.

The H-block is the most suitable for both beam and wall members. The webs could be recessed to carry longitudinal steel where required. The lintel block used in the bottom courses of the beams, with its present shape makes concrete placement difficult around the bottom steel. Both the bottom and face-shell dimensions could be reduced to 1 1/4".

VI RECOMMENDED DESIGN AND CONSTRUCTION PROCEDURES

The design methods should be similar to that of reinforced concrete. With design mortar strengths 50% of the concrete fill, the design can be based on the concrete fill strength for the overall section. The web reinforcement should be designed to carry the total shear in beams.

The construction methods should follow standard construction procedures for both reinforced concrete and masonry construction. In addition, certain procedures should be adopted.

(1) Excess mortar should be removed from the interior of the blocks and from the reinforcement. For a wall, a hole should be provided at the bottom through which this mortar could be removed. For a beam, where a clean-out hole may be impractical, the bottom steel should be raised to provide a receptacle for the mortar. This mortar could remain below the steel without affecting the performance.

(2) The cores should not be filled until 24 hours after mortaring the blocks. However, more time would be needed if conditions retarded the setting of mortar.

(3) The concrete fill should have about an 8" slump with either rodding or vibration as the method of consolidation.

VII SUGGESTED FUTURE RESEARCH

Further research is necessary in both beams and wall sections.

The ductility and shear capacity of beams should be considered. An effective method would involve testing beams of similar overall dimensions but changing the percentages of steel, stirrup spacing, top steel and possibly loading arrangement. Tests on restrained beams are important. Additional beams could be tested with the blocks put together without mortar or with certain courses left unfilled.

Wall sections could be built with varying percentages of reinforcement and tested under axial, eccentric and lateral loading arrangements.

There is little information available on the subject of durability, moisture penetration and resistance to the action of freezing and thawing, in spite of its importance. Research should be performed to determine these qualities and how they may be improved.

BIBLIOGRAPHY.

1. Bradshaw, R.E., Hendry, A.W., "Preliminary Crushing Tests on Storey-Height Cavity Walls", Proceedings of International Conference on Masonry Structural Systems, University of Texas, Austin, Texas, November, 1967.

2. Bresler, A.C.; Scordelin, A.C.; "Tests On Simple Beams With Web Reinforcement", ACI Manual of Concrete Practice, Partz, 1968, p. 426-71.

3. Clark, A.P., "Diagonal Tension in Reinforced Concrete Beams", ACI Journal, Proceedings V. 48, No. 2, Oct. 1951, pp. 145-146.

4. Converse, Frederick J., "Tests on Reinforced Concrete Masonry", Building Standards Monthly, February, 1946.

5. Cox, F.W.; Ennenga, J.L.; "Transverse Strength of Concrete Block Walls," ACI Journal, Proceedings, V. 54, 1958, pp. 951-960.

6. Guralnick, S.A.; "High Strength Deformed Steel Bars for Concrete Reinforcement", ACI Journal, Proceedings V. 57, No. 3, Sept. 1960, pp. 241-282.

7. Hedstrom, R.O.; Load Tests of Patterned Concrete Masonry Walls, ACI Journal, Proceedings V. 57, 1961, pp.1265-1286.

8. Hilsdorf, H.K.; "Investigation Into the Failure Mechanism of Brick Masonry Loaded in Axial Compression", Proceedings of International Conference on Masonry Structural Systems, University of Texas, Austin, Texas, November 1967.

9, Holmes, I.L., "Masonry Buildings" in High Intensity Seismic Zones", Proceedings of International Conference on Masonry Structural Systems, University of Texas, Austin, Texas, November 1967.

10. Kunze, Walter E.; Sbarounis, John A.; Amrhein, James E., "The March 27, 1964, Alaskan Earthquake," Portland Cement Association, 1965.

11. Leba, Theodore, "The Application of Non-reinforced Concrete Masonry Load-Bearing Walls in Multi-story Structures", National Concrete Masonry Association, 1965.

12. Lyse, Inge., "Tests of Reinforced Brick Columns". Journal of the American Ceramic Society, Vol. 16, No. 11, November 1933, pp. 584-597.

13. Mayrose, Herman E., "Tests of Reinforced Concrete Block Masonry Lintels", National Concrete Masonry Association, 1954.

14. Moody, K.G.; Viest, I.M.; Elstner, R.C.; and Hognestad, E., "Shear Strength of Reinforced Concrete Beams - Parts 1 and 2", ACI Journal, Proceedings V. 51: No. 4, December 1954, pp. 317-332; No. 5, January 1955, pp. 417-434.

15. Moretto, O., "An Investigation of the Strength of Welded Stirrups in Reinforced Concrete Beams", ACI Journal, Proceedings Vol. 42, No. 2, November 1945, pp. 141-162.

16. Plummer, Harry C. and Blume, John A., "Reinforced Brick Masonry and Lateral Force Design", Structural Clay Products Institute, Washington,D.C., 1953.

17. Richart, Frank E., Moorman, Robert B., and Woodworth, Paul M., "Strength and Stability of Concrete Masonry Walls", University of Illinois, Engineering Experiment Station, Bulletin No. 251, 1932.

18. Saemann, Jesse C., "Investigation of the Structural Properties of Reinforced Concrete Masonry", National Concrete Masonry Association, 1955.

19. Schneider, R.R., "Lateral Load Tests on Reinforced Grouted Masonry Shear Walls", University of Southern California, Engineering Centre, Report No. 70-101, 1959, pp. 1-47.

20. Scrivener, J.C., "Static Racking Tests on Concrete Masonry Walls", Proceedings of International Conference on Masonry Structural Systems, University of Texas, Austin, Texas, November 1967.

21. Thurston, C.W., "Tests of Simple Beams With Web Reinforcement", ACI Manual of Concrete Practice, Part 2", 1968.

22. Withey, M., "Tests on Reinforced Brick Masonry Columns". Proceedings, Part II, Technical Papers, American Society for Testing Materials, Vol. 34, 1934, pp. 387-403.

23. Richart, Frank E.; Newmark, Nathan M., "The Strength of Monolithic Concrete Walls", University of Illinois, Engineering Experiment Station, Bulletin No. 251, 1932.

24. Seddon, A. E., "The Strength of Concrete Walls Under Axial and Eccentric Loads", Proceedings of a Symposium on the Strength of Concrete Structures, Cement and Concrete Association, London, May 1956.

APPENDIX

- BEAM DETAILS
- CURVES
- PHOTOGRAPHS
- TABLES

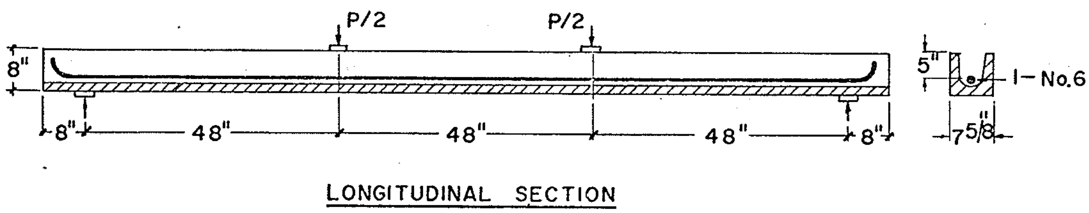

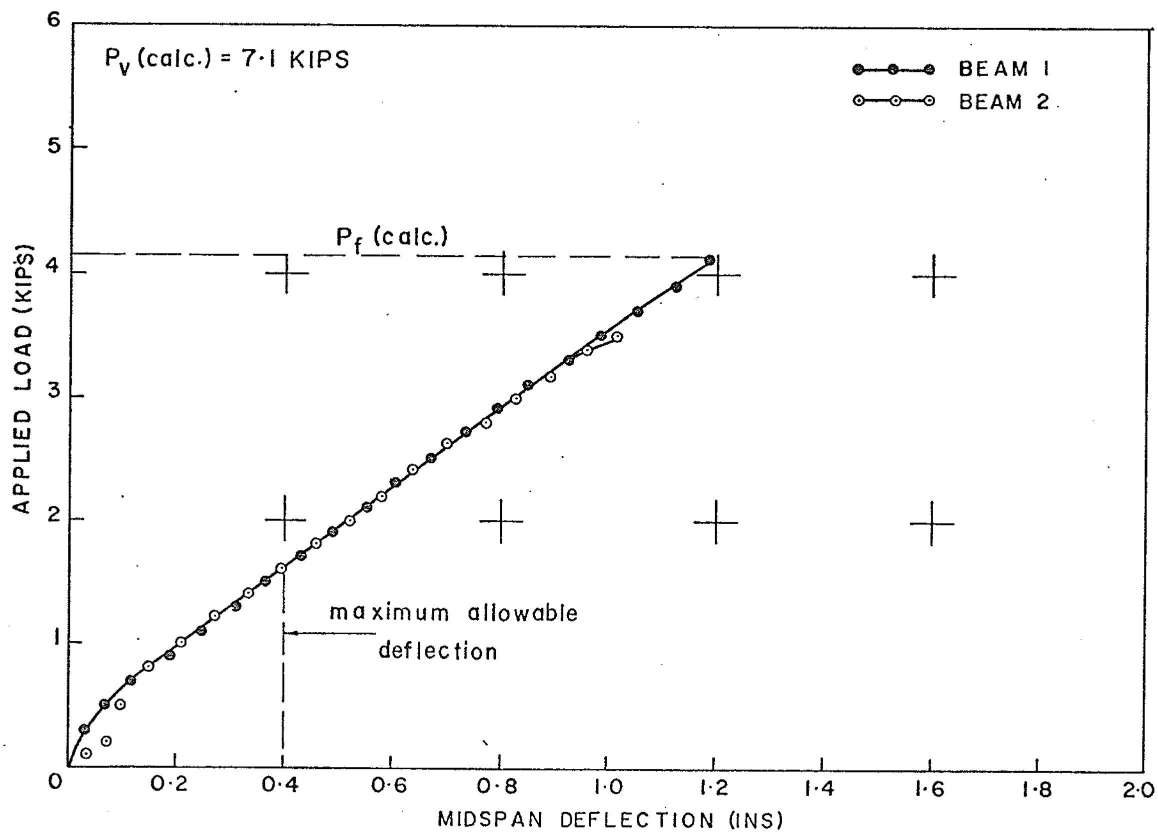

figure 35: details and load—deflection curves for beams 1 and 2

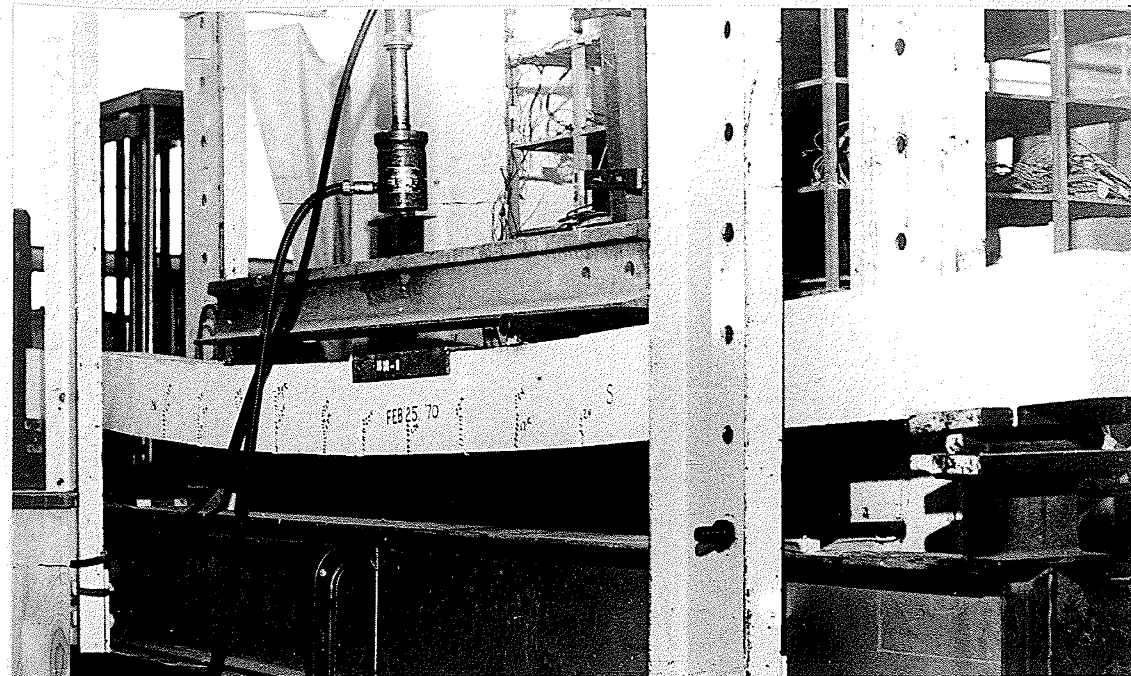

BEAM 1 SHOWING FLEXURAL FAILURE

FIGURE 36

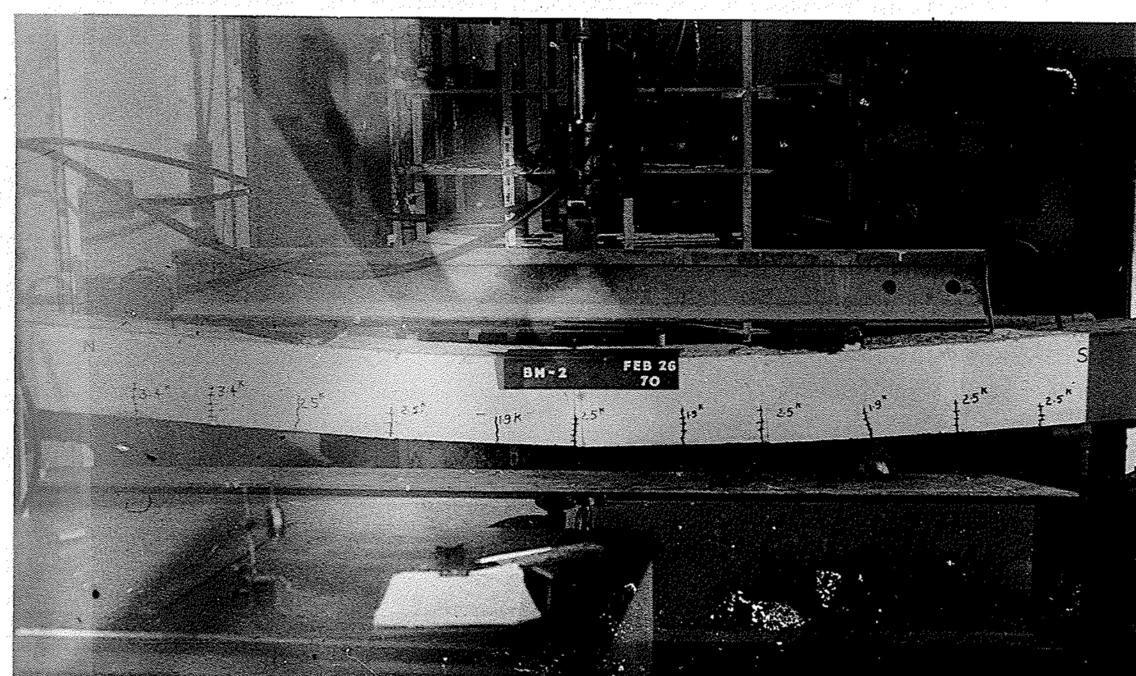

BEAM 2 SHOWING FLEXURAL FAILURE

FIGURE 37

TABLE X

TEST DATA FOR BEAMS 1 AND 2
LOAD-MIDSPAN DEFLECTION RESULTS

Load (Bm.1) (kips)	Deflection (Bm.1) (inches)	Load (Bm.2) (kips)	Deflection (Bm.2) (inches)
0.0	0.0	0.0	0.0
0.2	0.021	0.1	0.040
0.3	0.031	0.2	0.075
0.4	0.047	0.3	0.085
0.5	0.068	0.4	0.095
0.6	0.090	0.5	0.105
0.7	0.117	0.6	0.115
0.8	0.156	0.7	0.125
0.9	0.188	0.8	0.155
1.0	0.218	0.9	0.185
1.1	0.247	1.0	0.210
1.2	0.278	1.1	0.240
1.3	0.310	1.2	0.270
1.4	0.335	1.3	0.300
1.5	0.365	1.4	0.335
1.6	0.400	1.5	0.370
1.7	0.430	1.6	0.400
1.8	0.460	1.7	0.430
1.9	0.490	1.8	0.460
2.0	0.520	1.9	0.490
2.1	0.550	2.0	0.530
2.2	0.575	2.1	0.555
2.3	0.605	2.2	0.585
2.4	0.635	2.3	0.615
2.5	0.670	2.4	0.640
2.6	0.705	2.5	0.675
2.7	0.735	2.7	0.720
2.8	0.765	2.7	0.750
2.9	0.795	2.8	0.780
3.0	0.825	2.9	0.810
3.1	0.850	3.0	0.840
3.3	0.925	3.1	0.870
3.5	0.985	3.2	0.910
3.7	1.055	3.3	0.940
3.9	1.125	3.4	0.975
4.1	1.185	3.5	1.020

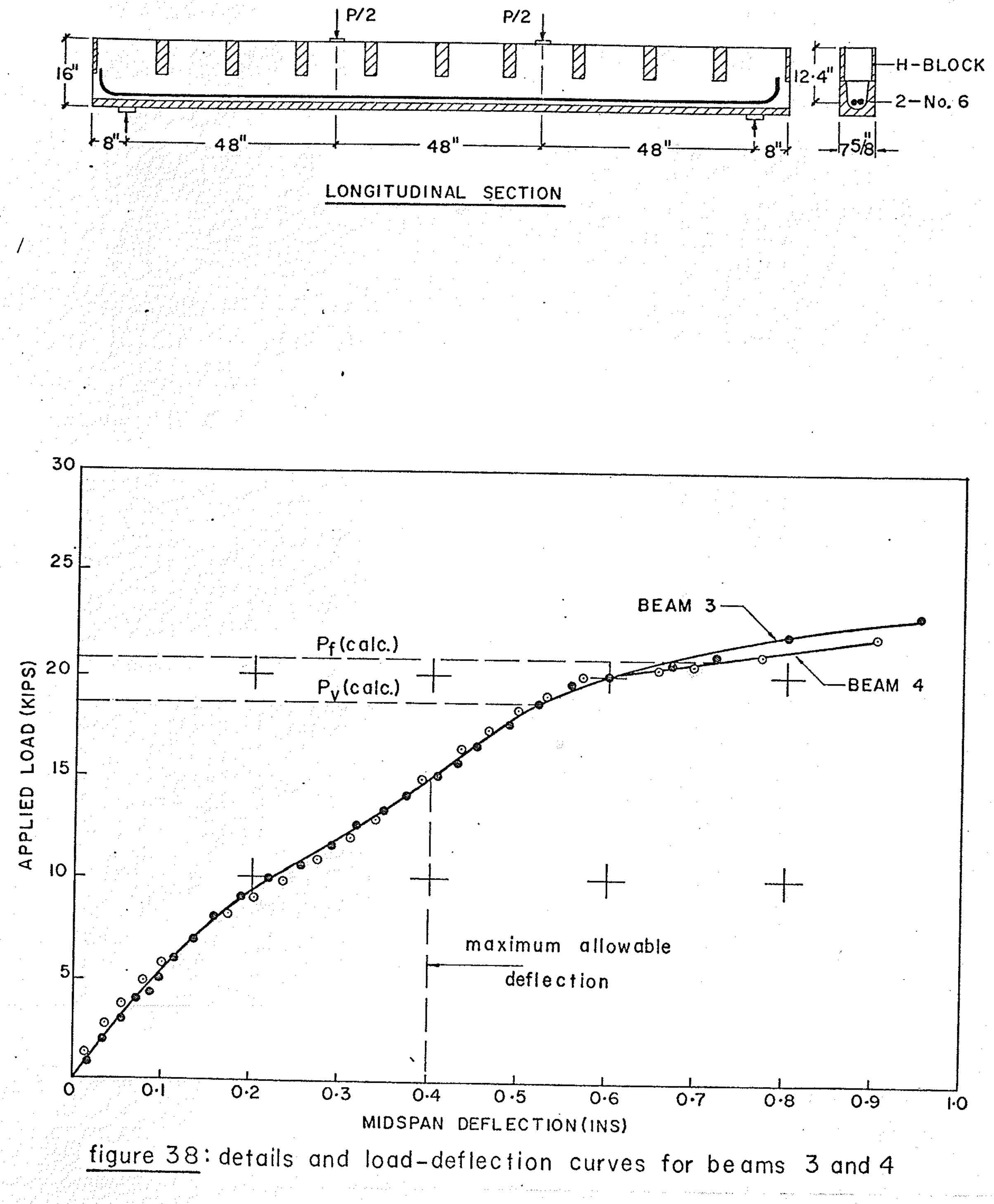

figure 38: details and load-deflection curves for beams 3 and 4

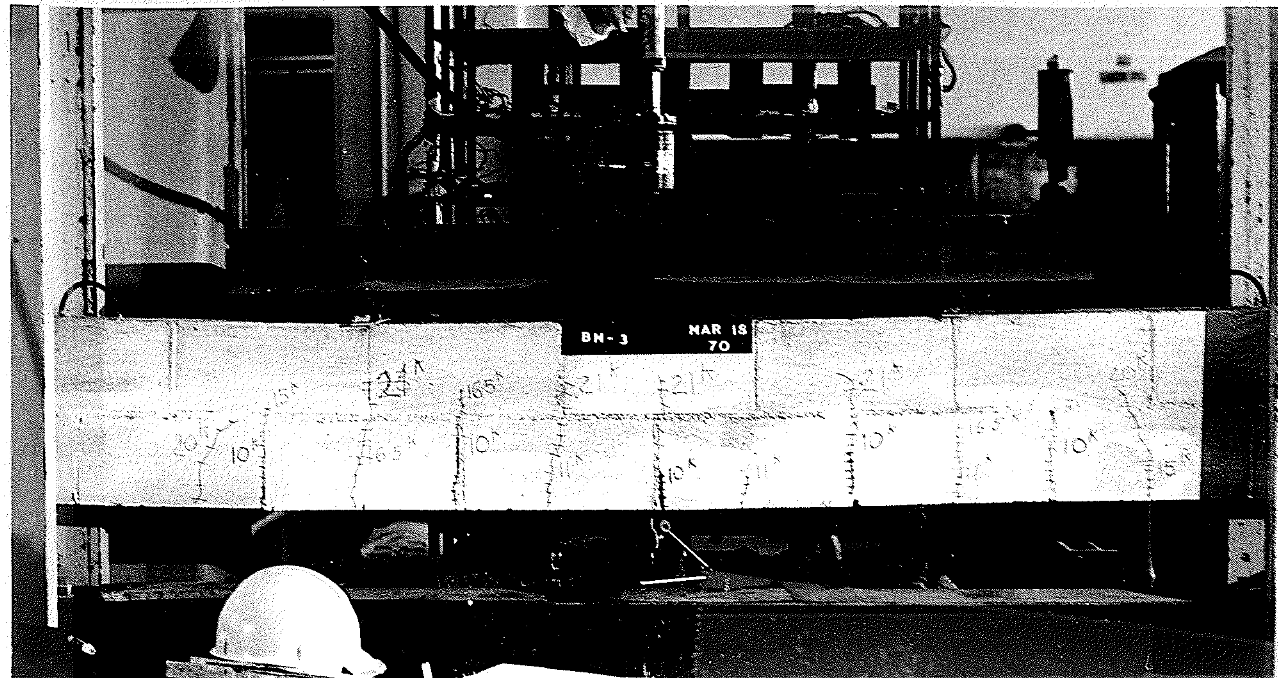

BEAM 3 SHOWING FLEXURAL FAILURE
FIGURE 39

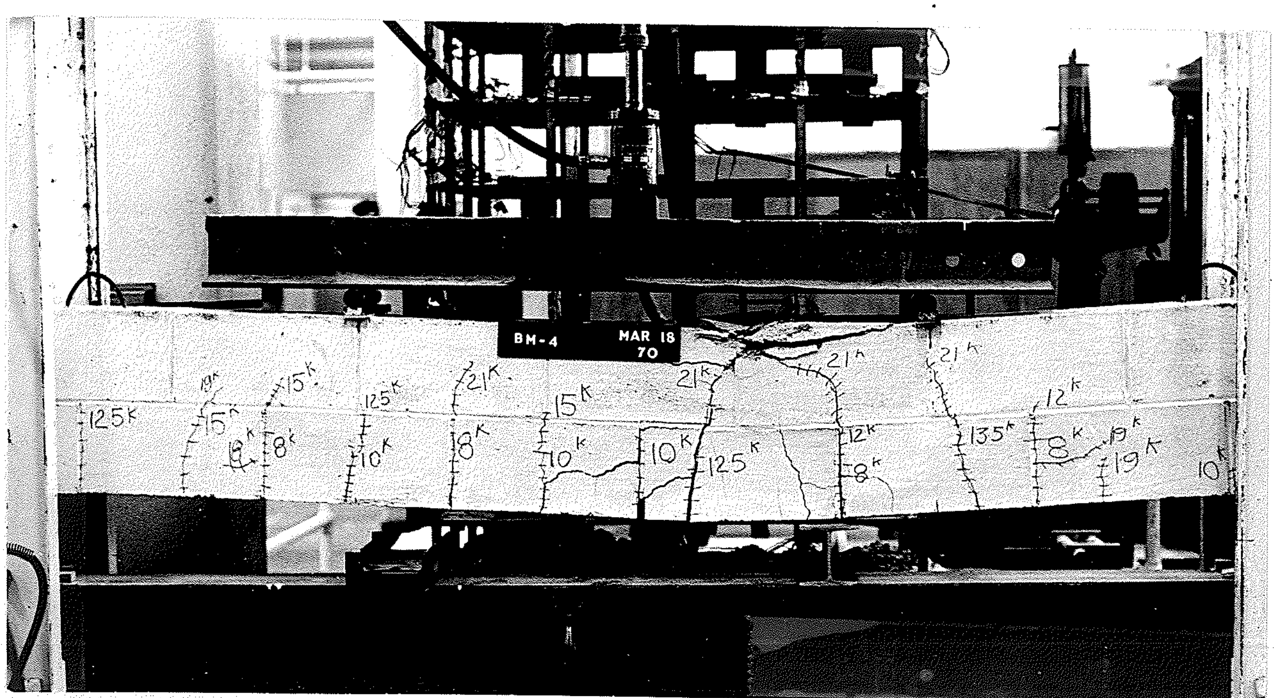

BEAM 4 SHOWING FLEXURAL FAILURE
FIGURE 40

TABLE XI

TEST DATA FOR BEAMS 3 AND 4
LOAD-MIDSPAN DEFLECTION RESULTS

Load (Bm.3) (kips)	Deflection (Bm.3) (inches)	Load (Bm.4) (kips)	Deflection (Bm.4) (inches)
0.0	0.0	0.0	0.0
0.5	0.007	0.5	0.002
1.0	0.015	1.0	0.005
1.5	0.024	1.5	0.012
2.0	0.033	2.0	0.020
2.5	0.042	2.5	0.029
3.0	0.052	3.0	0.039
3.5	0.060	3.5	0.050
4.0	0.070	4.0	0.060
4.5	0.090	4.5	0.072
5.0	0.095	5.0	0.084
5.5	0.102	5.5	0.095
6.0	0.112	6.0	0.106
6.5	0.122	6.5	0.109
7.0	0.136	7.0	0.134
7.5	0.148	7.5	0.148
8.0	0.158	8.0	0.162
8.5	0.170	8.5	0.180
9.0	0.188	9.0	0.192
9.5	0.204	9.5	0.210
10.0	0.220	10.0	0.234
10.5	0.255	10.5	0.258
11.0	0.268	11.0	0.272
11.5	0.288	11.5	0.288
12.0	0.302	12.0	0.310
12.5	0.316	12.5	0.325
13.0	0.334	13.0	0.340
13.5	0.355	13.5	0.354
14.0	0.370	14.0	0.368
14.5	0.380	14.5	0.388
15.0	0.405	15.0	0.401
15.5	0.430	15.5	0.420
16.0	0.438	16.0	0.433
16.5	0.450	16.5	0.450
17.0	0.474	17.0	0.464
17.5	0.487	17.5	0.480
18.0	0.502	18.0	0.495
18.5	0.520	18.5	0.513
19.0	0.538	19.0	0.530
19.5	0.558	19.5	0.552
20.0	0.600	20.0	0.570
20.5	0.670	20.5	0.670
21.0	0.720	21.0	0.770
22.0	0.800	22.0	0.900
23.0	0.950		

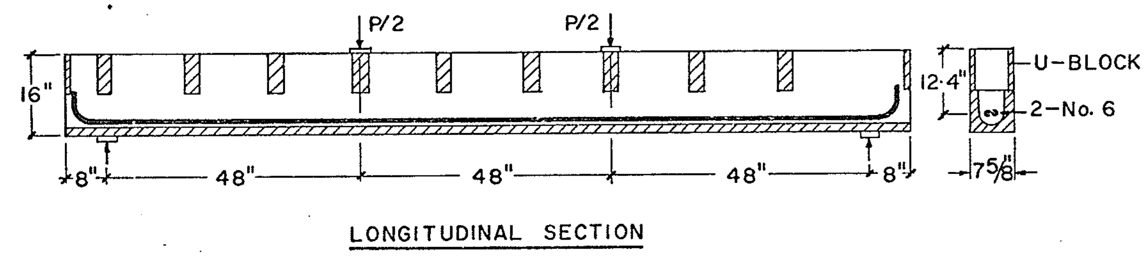

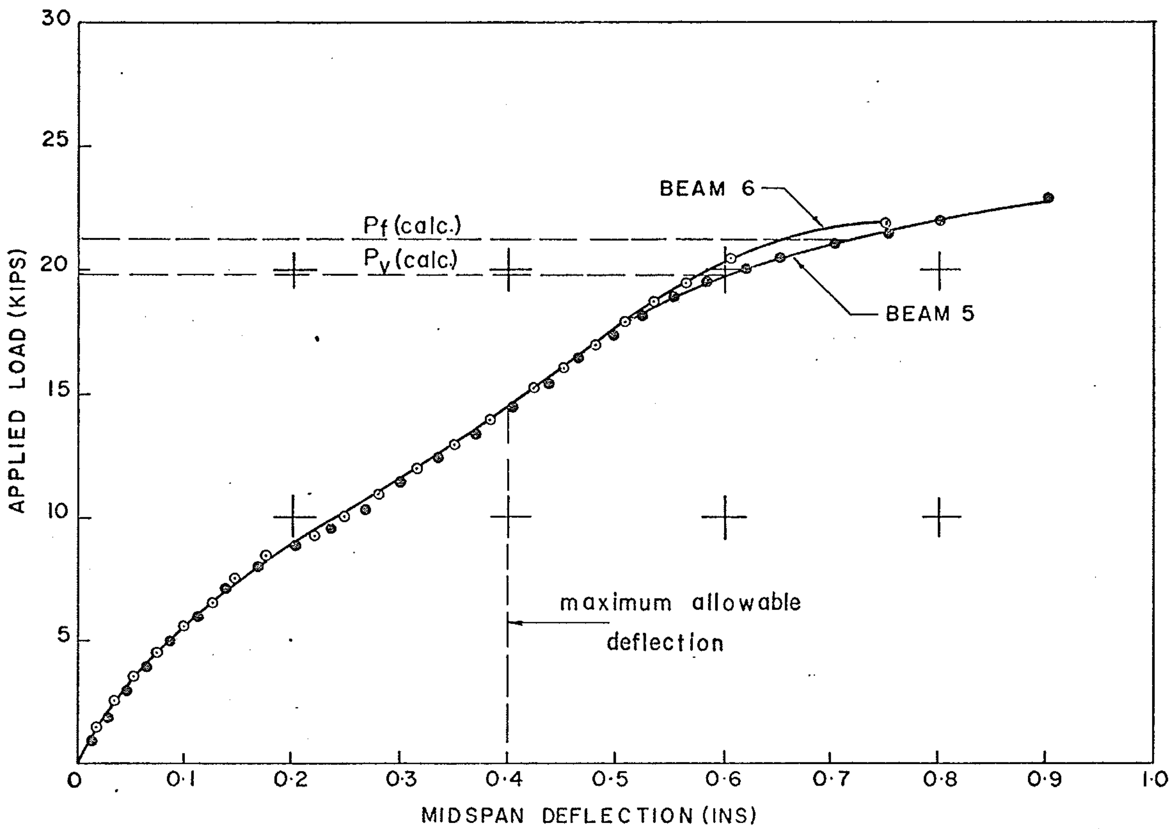

figure 41: details and load-deflection curves for beams 5 and 6

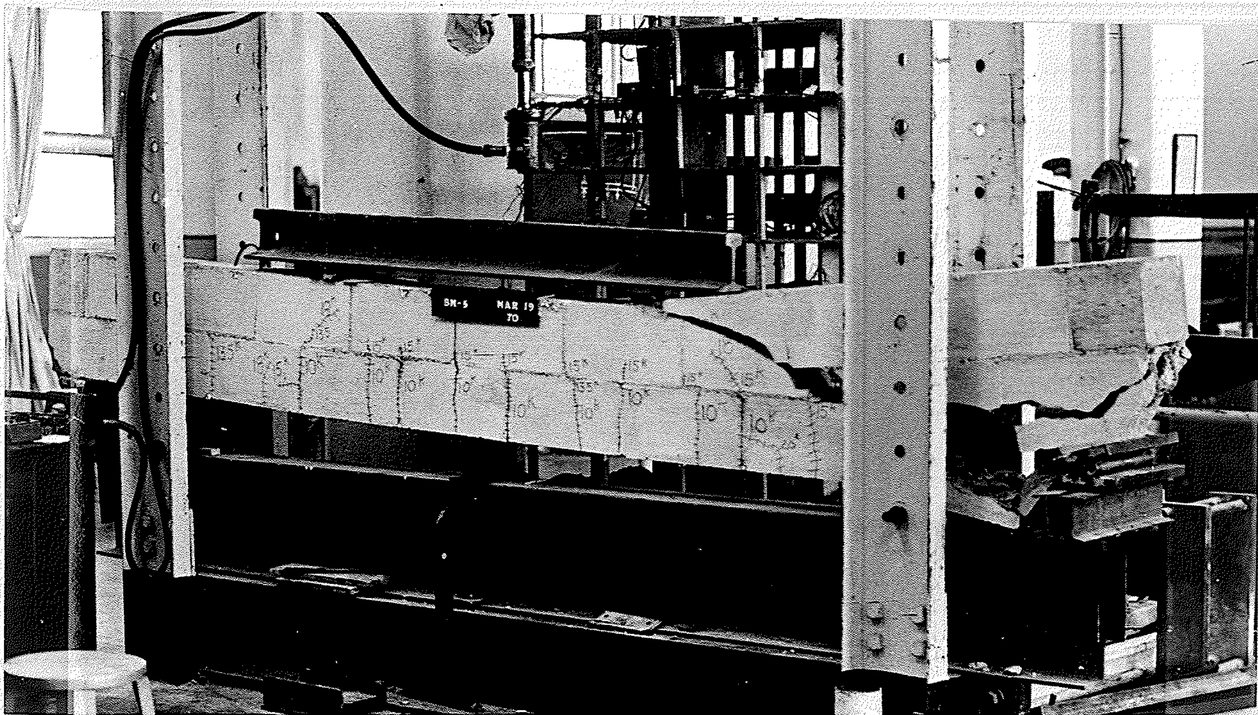

BEAM 5 SHOWING SHEAR FAILURE

FIGURE 42

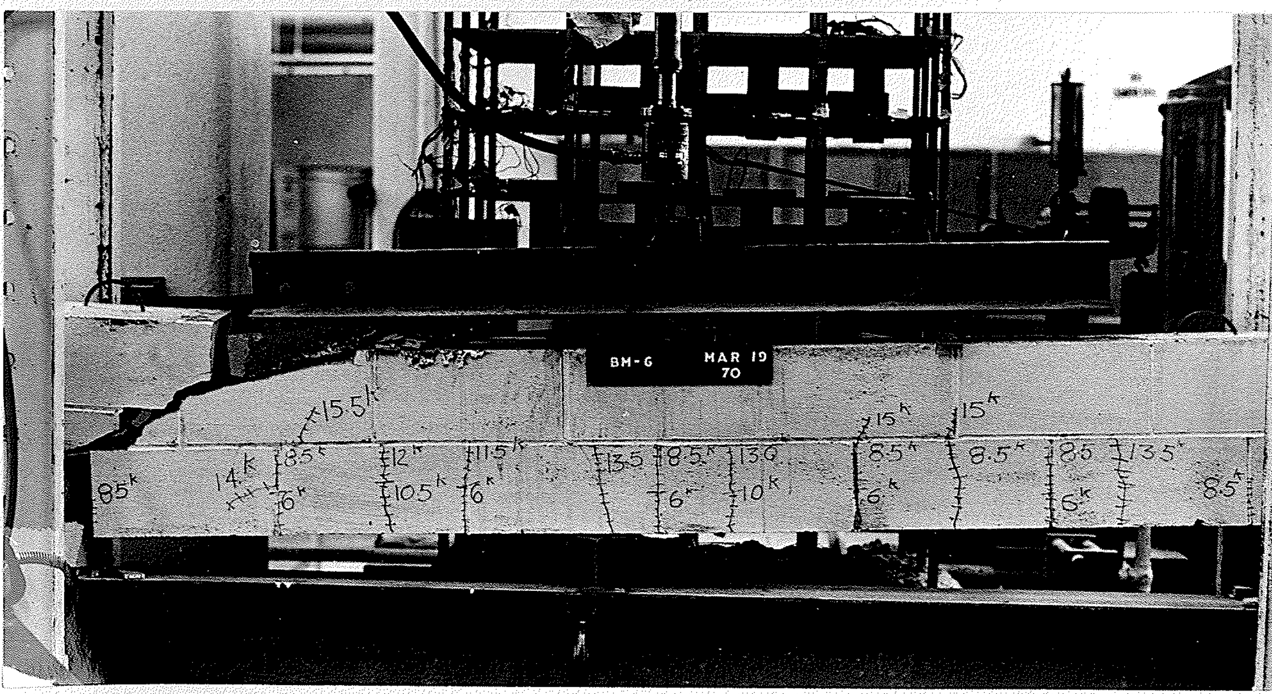

BEAM 6 SHOWING SHEAR FAILURE

FIGURE 43

TABLE XII

TEST DATA FOR BEAMS 5 AND 6
LOAD-MIDSPAN DEFLECTION RESULTS

Load (Bm.5) (kips)	Deflection (Bm.5) (inches)	Load (Bm.6) (kips)	Deflection (Bm.6) (inches)
0.0	0.0	0.0	0.0
0.5	0.007	0.5	0.006
1.0	0.012	1.0	0.011
1.5	0.020	1.5	0.020
2.0	0.028	2.0	0.027
2.5	0.043	2.5	0.036
3.0	0.046	3.0	0.045
3.5	0.055	3.5	0.056
4.0	0.065	4.0	0.065
4.5	0.076	4.5	0.075
5.0	0.086	5.0	0.088
5.5	0.098	5.5	0.100
6.0	0.112	6.0	0.109
6.5	0.120	6.5	0.122
7.0	0.135	7.0	0.132
7.5	0.148	7.5	0.147
8.0	0.160	8.0	0.162
8.5	0.180	8.5	0.176
9.0	0.205	9.0	0.205
9.5	0.232	9.5	0.232
10.0	0.255	10.0	0.250
10.5	0.275	10.5	0.266
11.0	0.285	11.0	0.280
11.5	0.296	11.5	0.296
12.0	0.315	12.0	0.310
12.5	0.333	12.5	0.330
13.0	0.348	13.0	0.348
13.5	0.374	13.5	0.365
14.0	0.390	14.0	0.382
14.5	0.402	14.5	0.402
15.0	0.420	15.0	0.415
15.5	0.440	15.5	0.428
16.0	0.450	16.0	0.446
16.5	0.465	16.5	0.462
17.0	0.485	17.0	0.479
17.5	0.500	17.5	0.496
18.0	0.515	18.0	0.510
18.5	0.540	18.5	0.528
19.0	0.552	19.0	0.545
19.5	0.570	19.5	0.565
20.0	0.590	20.0	0.580
20.5	0.650	20.5	0.605
21.0	0.700	21.0	0.700
22.0	0.800	22.0	0.750
23.0	0.900		

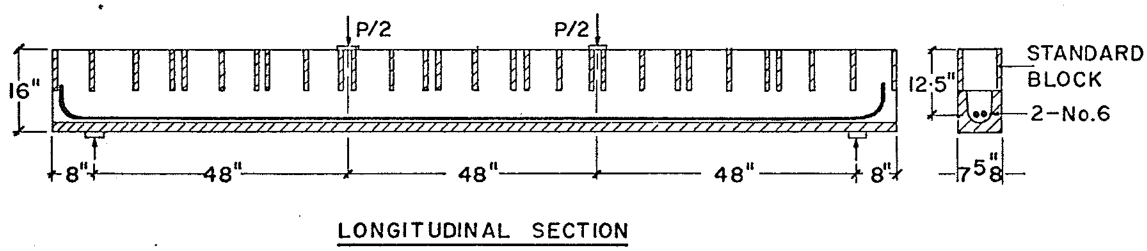

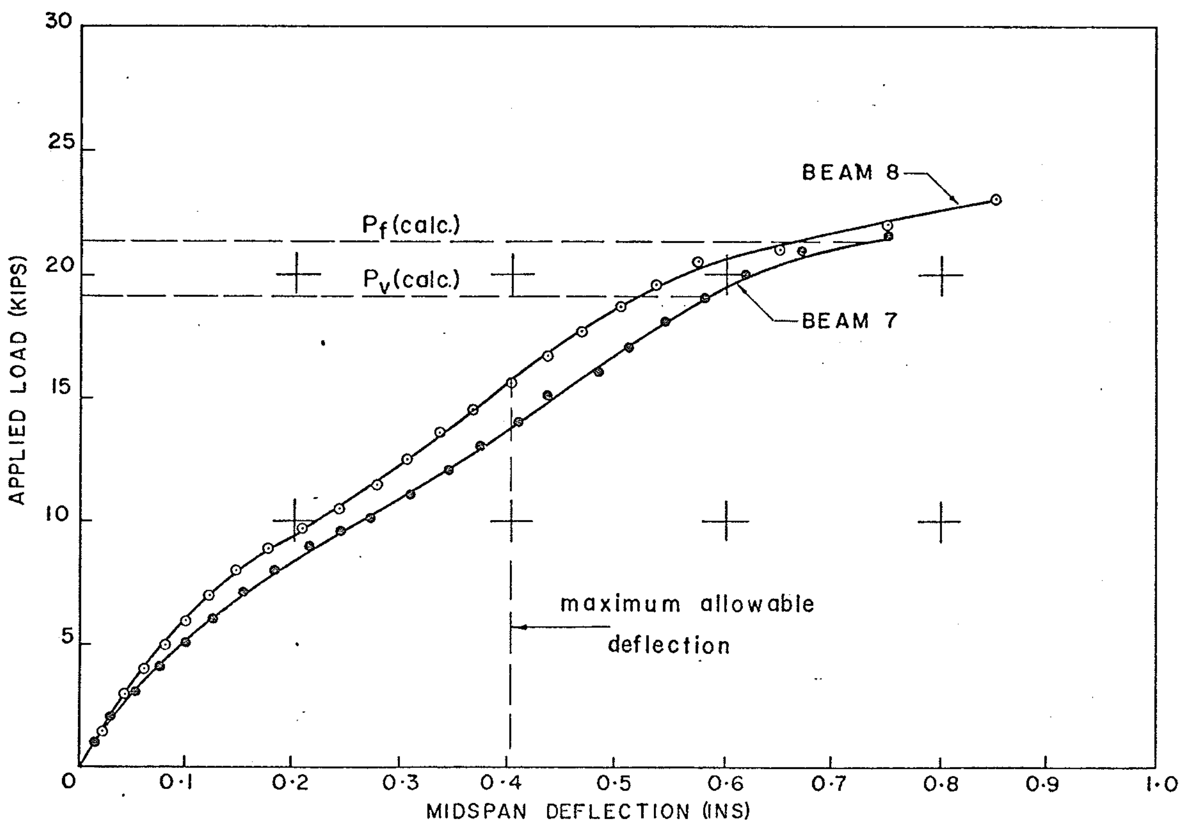

figure 44: details and load-deflection curves for beams 7 and 8

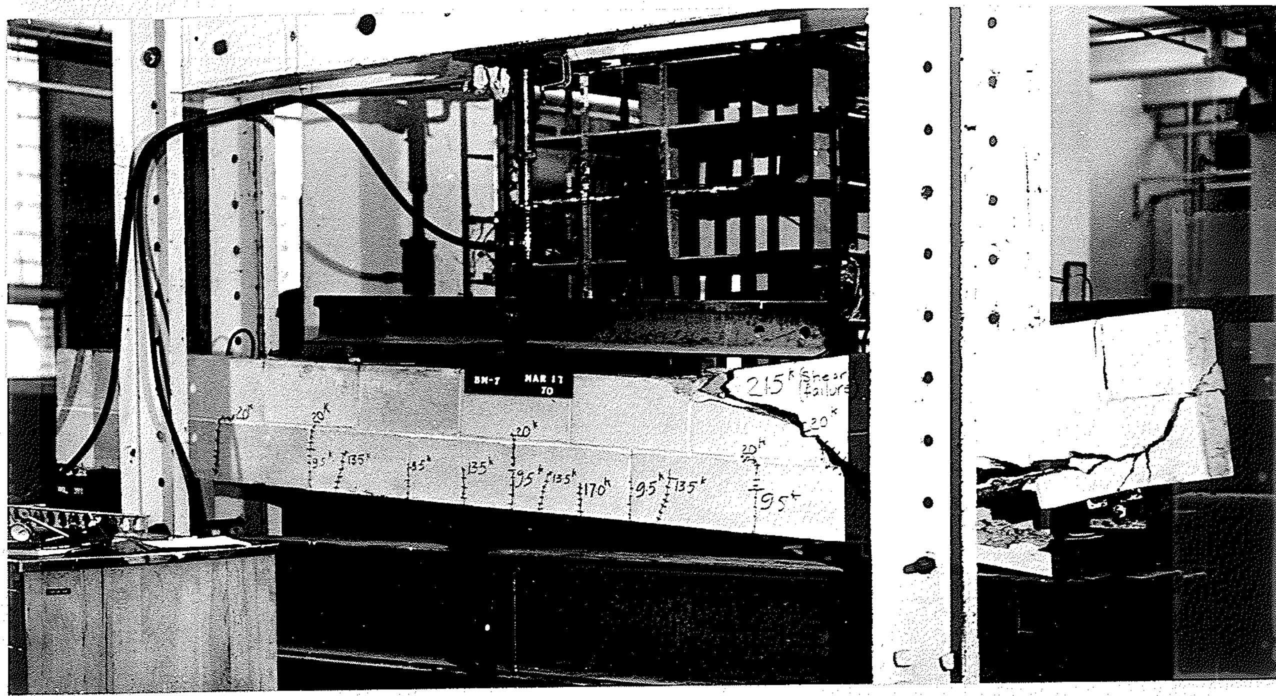

BEAM 7 SHOWING SHEAR FAILURE

FIGURE 45

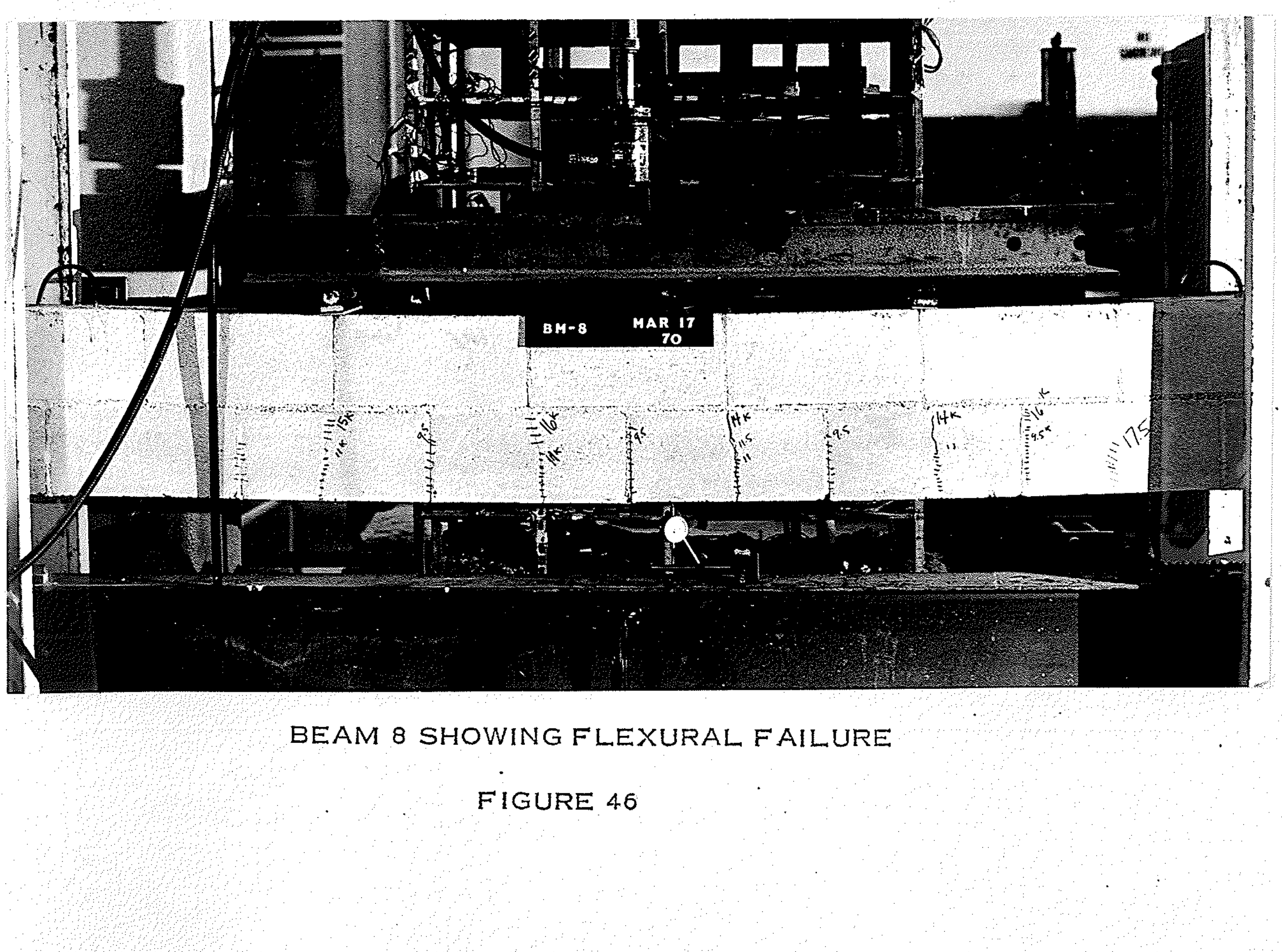

BEAM 8 SHOWING FLEXURAL FAILURE

FIGURE 46

TABLE XIII

TEST DATA FOR BEAMS 7 AND 8
LOAD-MIDSPAN DEFLECTION RESULTS

Load (Bm.7) (Kips)	Deflection (Bm.7) (inches)	Load (Bm.8) (kips)	Deflection (Bm.8) (inches)
0.0	0.0	0.0	0.0
0.5	0.008	0.5	0.007
1.0	0.015	1.0	0.014
1.5	0.023	1.5	0.021
2.0	0.032	2.0	0.028
2.5	0.042	2.5	0.035
3.0	0.052	3.0	0.043
3.5	0.065	3.5	0.051
4.0	0.075	4.0	0.060
4.5	0.085	4.5	0.070
5.0	0.098	5.0	0.080
5.5	0.110	5.5	0.090
6.0	0.125	6.0	0.100
6.5	0.138	6.5	0.110
7.0	0.152	7.0	0.120
7.5	0.165	7.5	0.133
8.0	0.180	8.0	0.145
8.5	0.195	8.5	0.160
9.0	0.215	9.0	0.178
9.5	0.236	9.5	0.190
10.0	0.270	10.0	0.222
10.5	0.288	10.5	0.240
11.0	0.308	11.0	0.262
11.5	0.322	11.5	0.276
12.0	0.340	12.0	0.290
12.5	0.355	12.5	0.305
13.0	0.370	13.0	0.320
13.5	0.386	13.5	0.332
14.0	0.408	14.0	0.346
14.5	0.420	14.5	0.363
15.0	0.435	15.0	0.380
15.5	0.458	15.5	0.397
16.0	0.480	16.0	0.412
16.5	0.495	16.5	0.430
17.0	0.510	17.0	0.445
17.5	0.530	17.5	0.460
18.0	0.545	18.0	0.480
18.5	0.562	18.5	0.495
19.0	0.580	19.0	0.515
19.5	0.600	19.5	0.535
20.0	0.618	20.0	0.553
20.5	0.645	20.5	0.575
21.0	0.670	21.0	0.650
21.5	0.750	22.0	0.750
		23.0	0.850

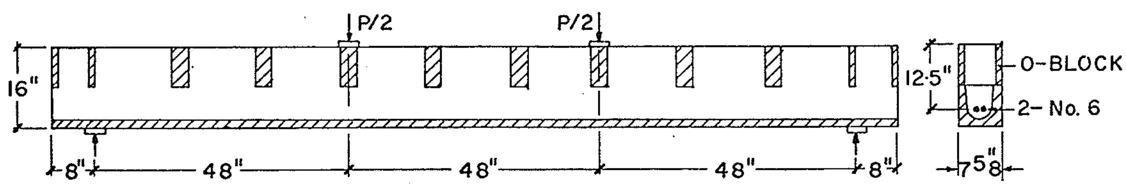

LONGITUDINAL SECTION

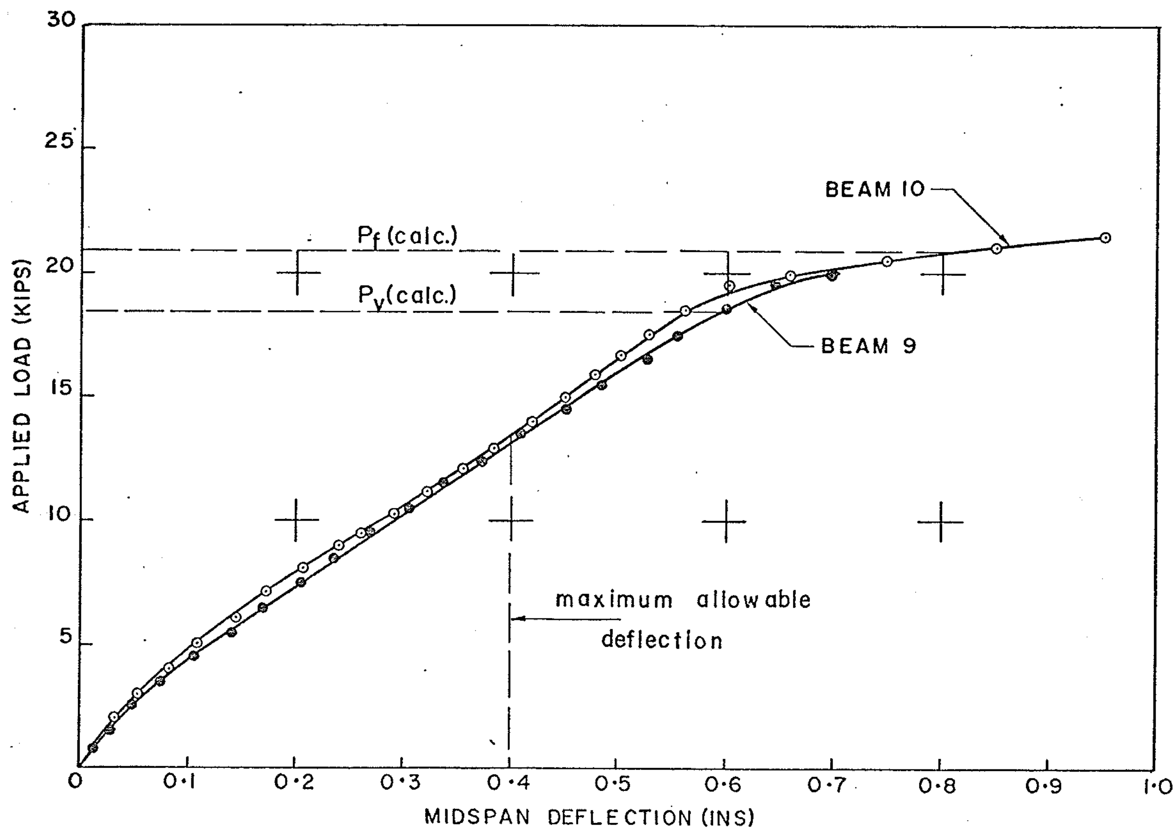

figure 47: details and load-deflection curves for beams 9 and 10

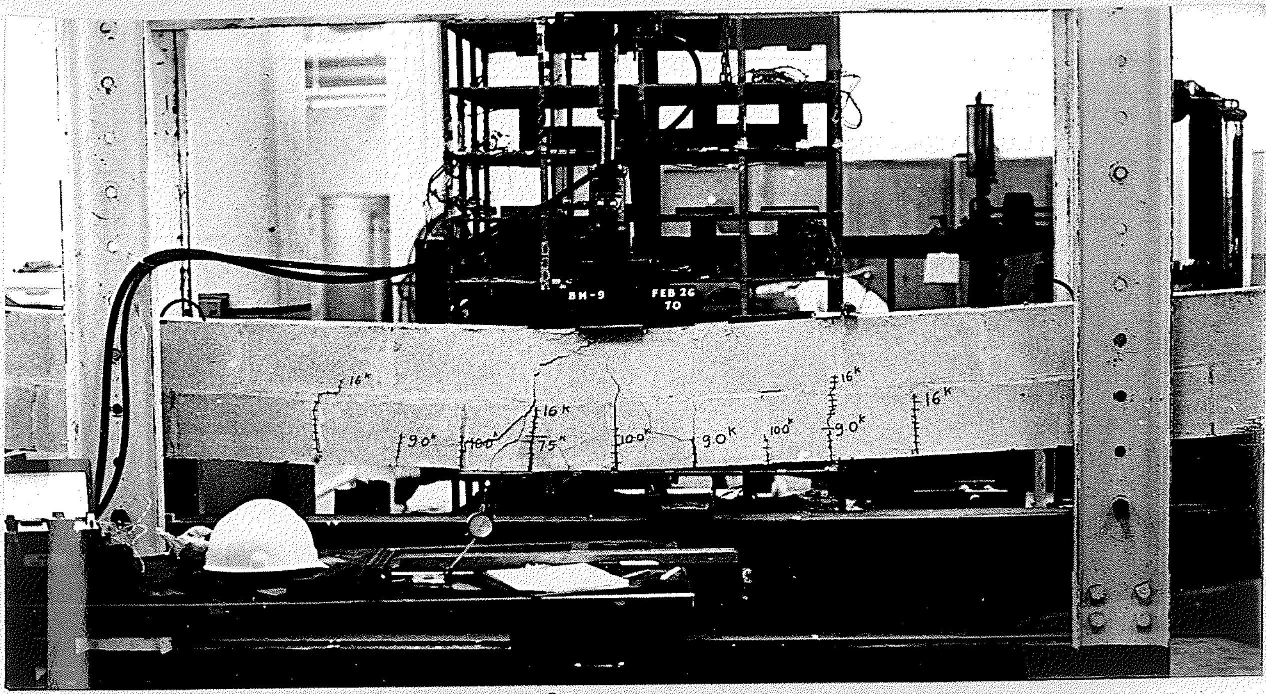

BEAM 9 SHOWING FLEXURAL FAILURE

FIGURE 48

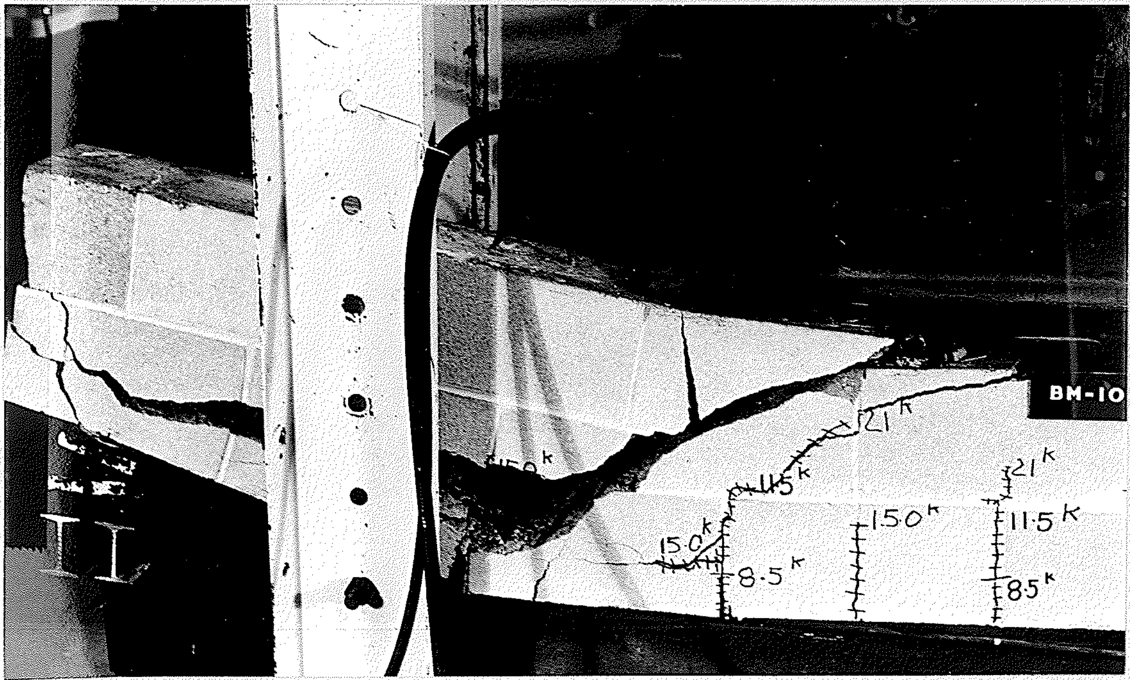

BEAM 10 SHOWING SHEAR FAILURE

FIGURE 49

TABLE XIV

TEST DATA FOR BEAMS 9 AND 10
LOAD-MIDSPAN DEFLECTION RESULTS

Load (Bm.9) (kips)	Deflection (Bm.9) (inches)	Load (Bm.10) (kips)	Deflection (Bm.10) (inches)
0.0	0.0	0.0	0.0
0.5	0.010	0.5	0.007
0.8	0.013	1.0	0.015
1.0	0.018	1.5	0.024
1.3	0.022	2.0	0.034
1.5	0.028	2.5	0.045
1.8	0.033	3.0	0.055
2.0	0.036	3.5	0.067
2.3	0.040	4.0	0.083
2.5	0.048	4.5	0.098
3.0	0.060	5.0	0.110
3.5	0.075	5.5	0.128
4.0	0.090	6.0	0.144
4.5	0.105	6.5	0.158
5.0	0.120	7.0	0.170
5.5	0.140	7.5	0.190
6.0	0.156	8.0	0.208
6.5	0.170	8.5	0.220
7.0	0.190	9.0	0.240
7.5	0.205	9.5	0.262
8.0	0.220	10.0	0.280
8.5	0.235	10.5	0.300
9.0	0.250	11.0	0.318
9.5	0.270	11.5	0.332
10.0	0.285	12.0	0.358
10.5	0.305	12.5	0.370
11.0	0.325	13.0	0.385
11.5	0.338	13.5	0.400
12.0	0.355	14.0	0.412
12.5	0.375	14.5	0.428
13.0	0.390	15.0	0.442
13.5	0.410	15.5	0.463
14.0	0.430	16.0	0.485
14.5	0.450	16.5	0.500
15.0	0.465	17.0	0.512
15.5	0.485	17.5	0.525
16.0	0.500	18.0	0.545
16.5	0.528	18.5	0.560
17.0	0.540	19.0	0.575
17.5	0.555	19.5	0.600
18.0	0.575	20.0	0.660
18.5	0.600	20.5	0.750
19.0	0.620	21.0	0.850
19.5	0.645	21.5	0.950
20.0	0.700	21.5	0.950

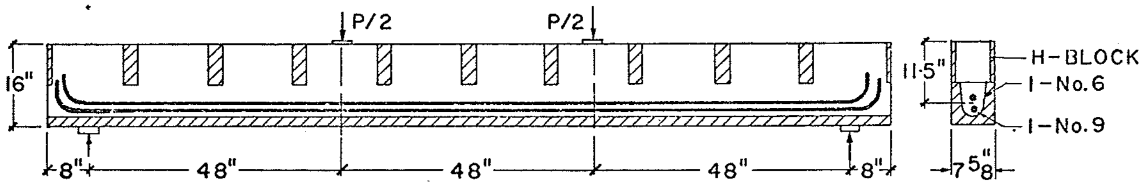

LONGITUDINAL SECTION

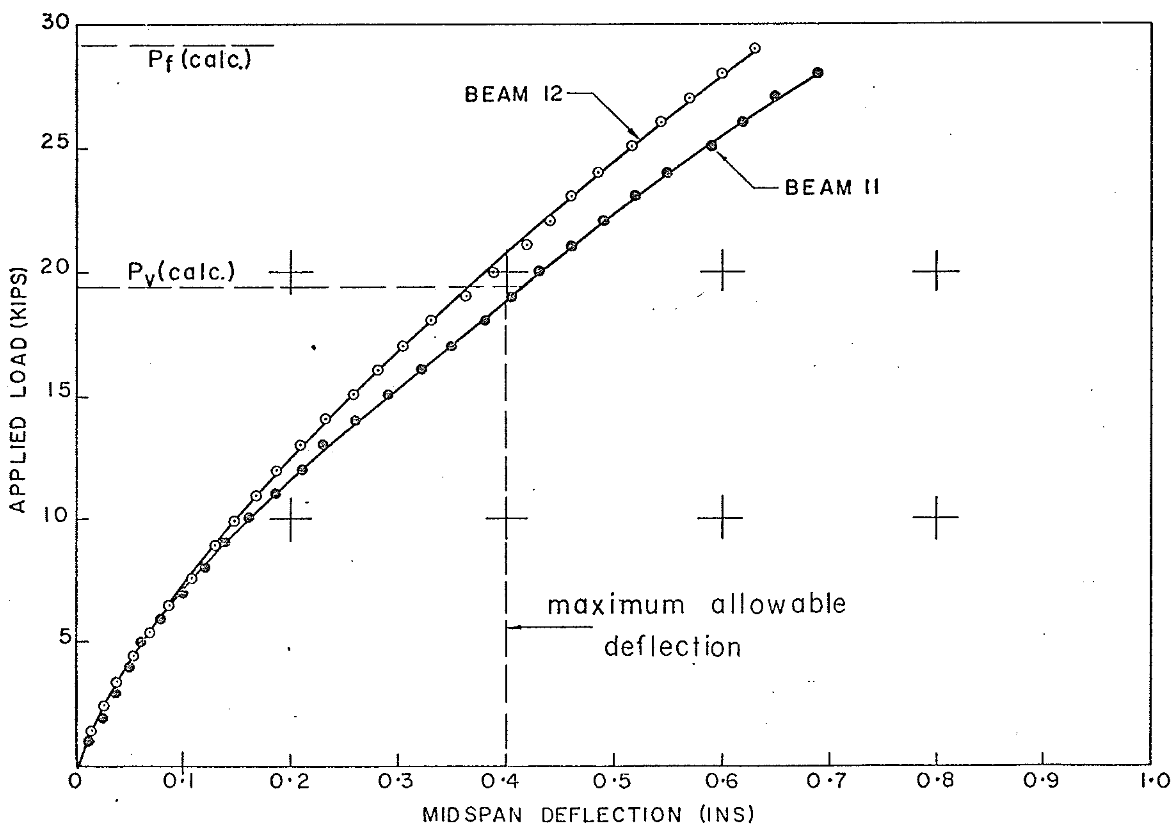

figure 50: load deflection curves and beam details for beams 11 and 12

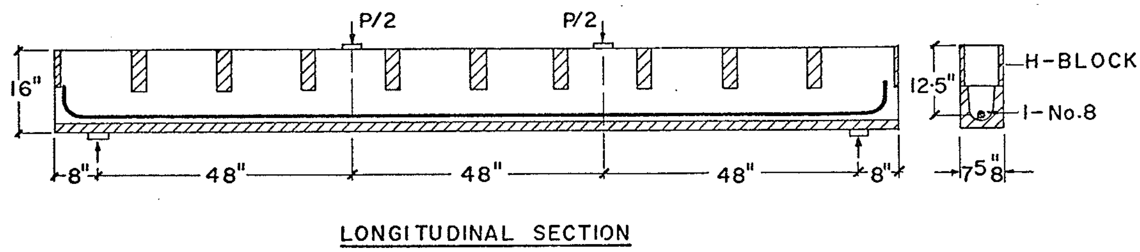

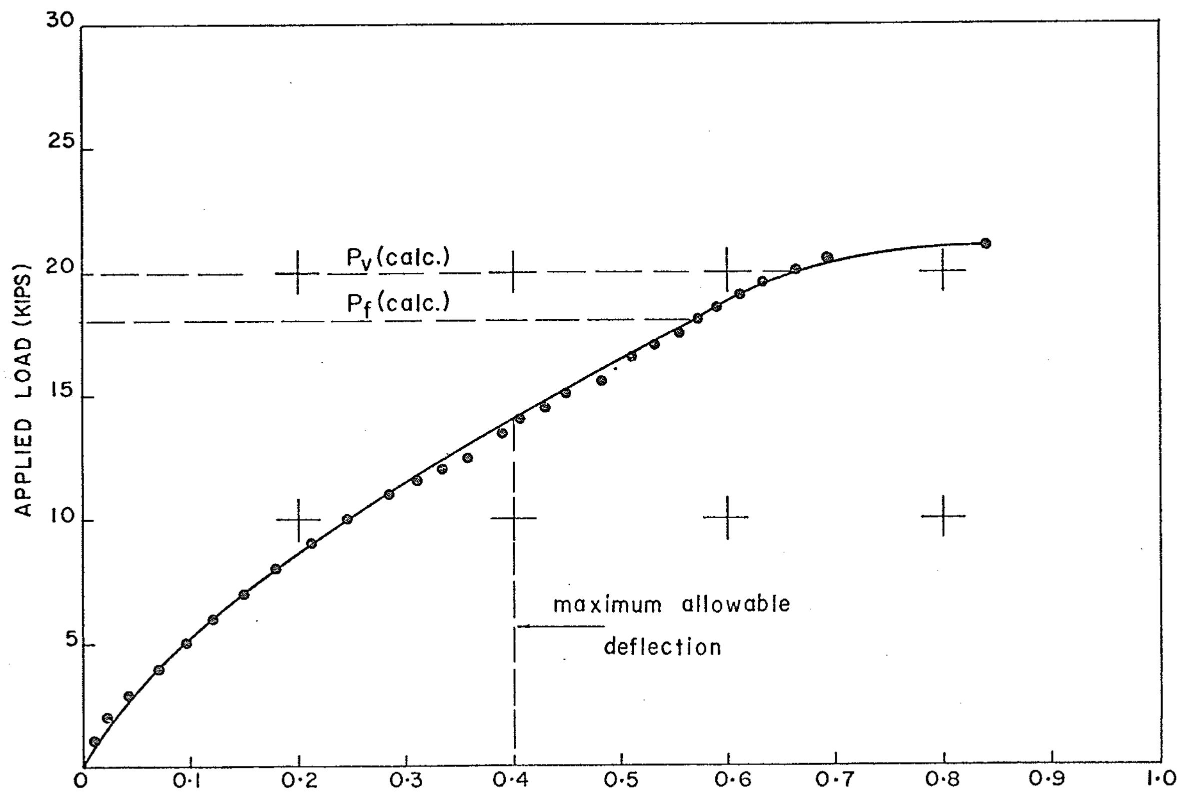

figure 51 details and load-deflection curve for beam 13

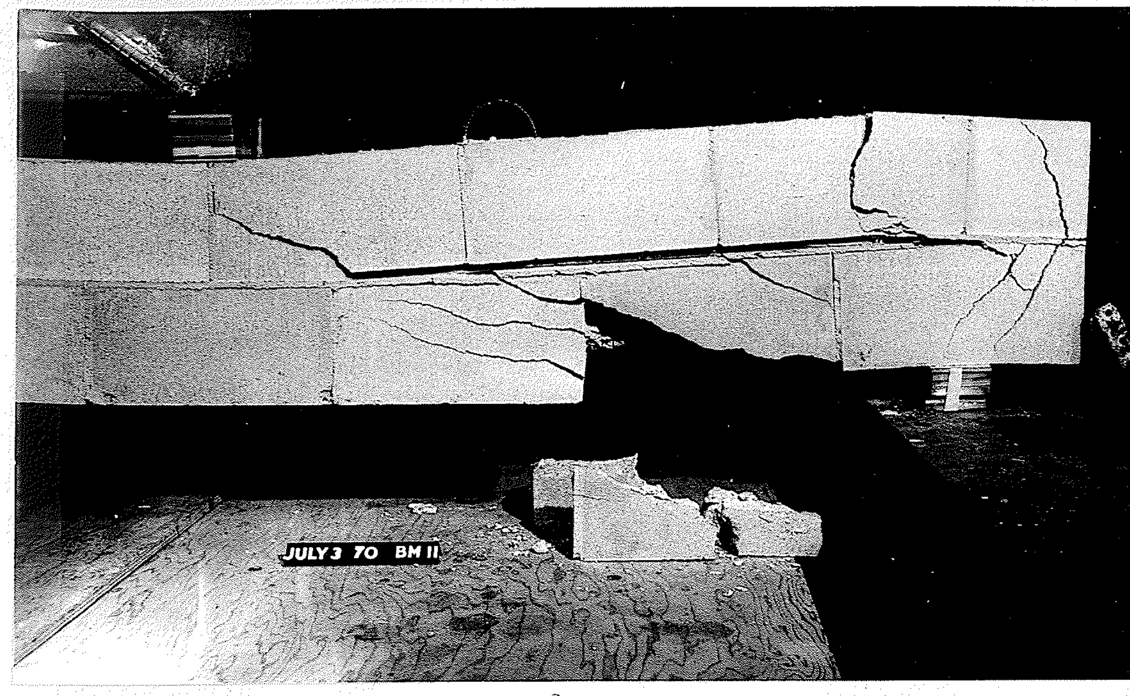

BEAM 11 SHOWING SHEAR FAILURE

FIGURE 52

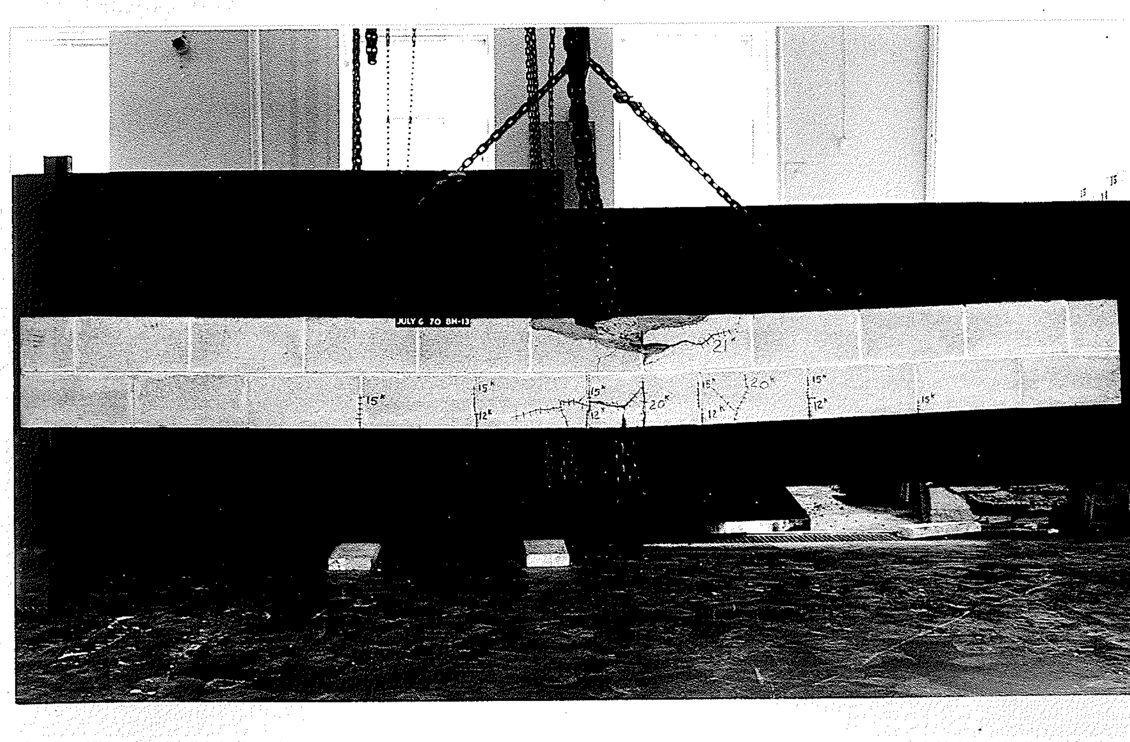

BEAM 13 SHOWING FLEXURAL FAILURE

FIGURE 53

TABLE XV

TEST DATA FOR BEAMS 11 AND 12
LOAD-MIDSPAN DEFLECTION RESULTS

Load (Bm.11) (kips)	Deflection (Bm.11) (inches)	Load (Bm.12) (kips)	Deflection (Bm.12) (inches)
0.0	0.0	0.0	0.0
0.5	0.006	0.5	0.004
1.0	0.012	1.0	0.007
1.5	0.018	1.5	0.012
2.0	0.024	2.0	0.018
2.5	0.030	2.5	0.024
3.0	0.036	3.0	0.031
3.5	0.042	3.5	0.039
4.0	0.049	4.0	0.046
4.5	0.055	4.5	0.054
5.0	0.060	5.0	0.062
6.0	0.080	6.0	0.077
7.0	0.100	7.0	0.094
8.0	0.120	8.0	0.111
9.0	0.140	9.0	0.130
10.0	0.160	10.0	0.148
11.0	0.185	11.0	0.168
12.0	0.210	12.0	0.188
13.0	0.230	13.0	0.208
14.0	0.260	14.0	0.232
15.0	0.290	15.0	0.256
16.0	0.320	16.0	0.280
17.0	0.350	17.0	0.304
18.0	0.380	18.0	0.330
19.0	0.405	19.0	0.362
20.0	0.430	20.0	0.388
21.0	0.460	21.0	0.418
22.0	0.490	22.0	0.440
23.0	0.520	23.0	0.460
24.0	0.550	24.0	0.485
25.0	0.590	25.0	0.518
26.0	0.620	26.0	0.544
27.0	0.650	27.0	0.570
28.0	0.690	28.0	0.600
		29.0	0.630

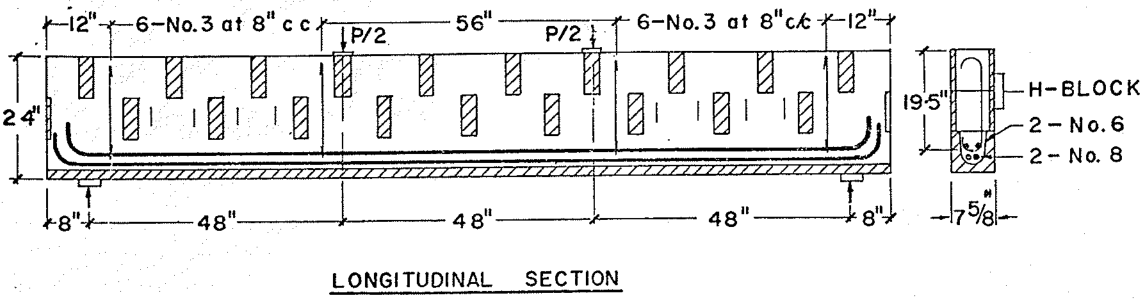

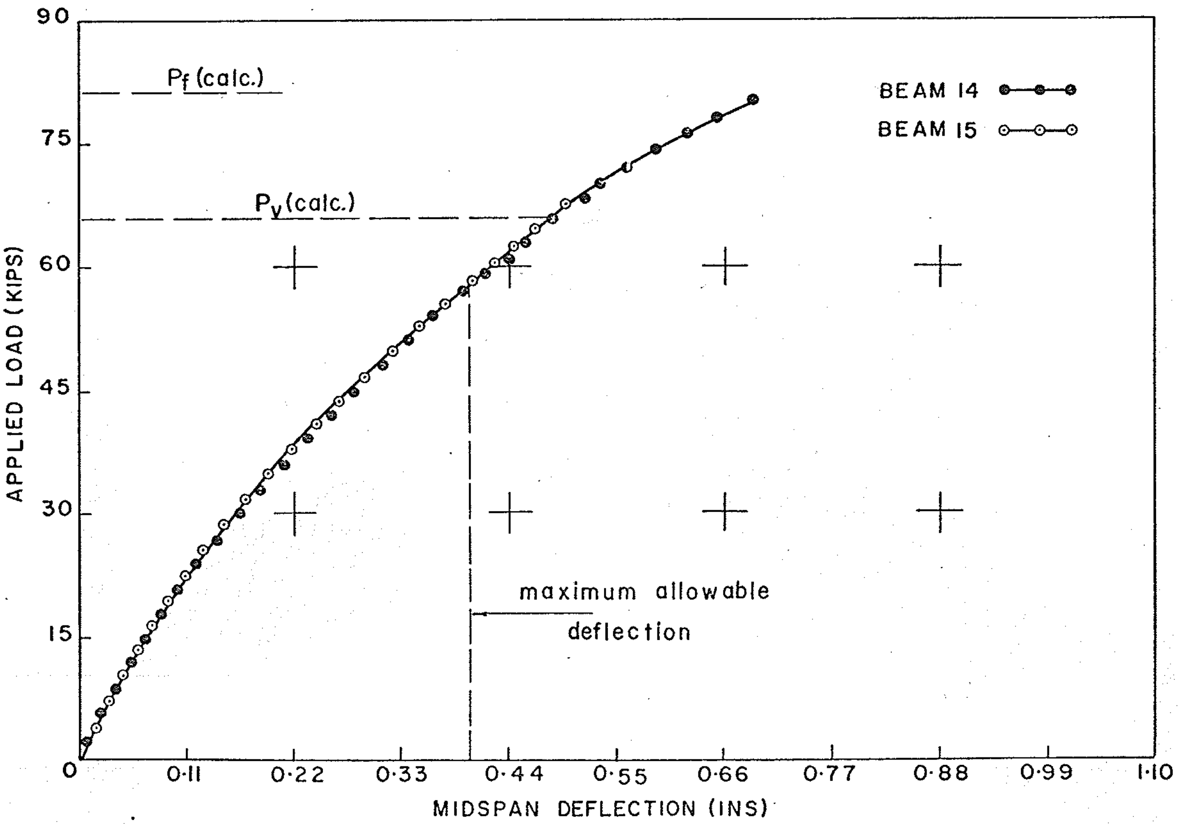

figure 54: details and load-deflection curve for beams 14 and 15

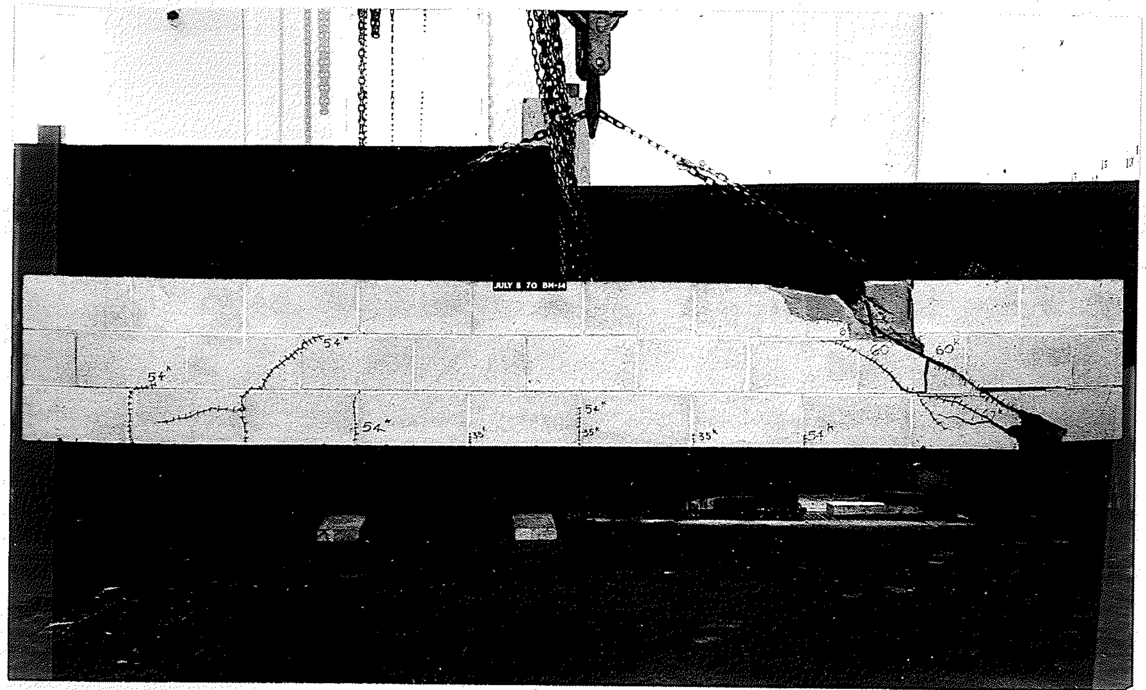

BEAM 14 SHOWING SHEAR FAILURE

FIGURE 55

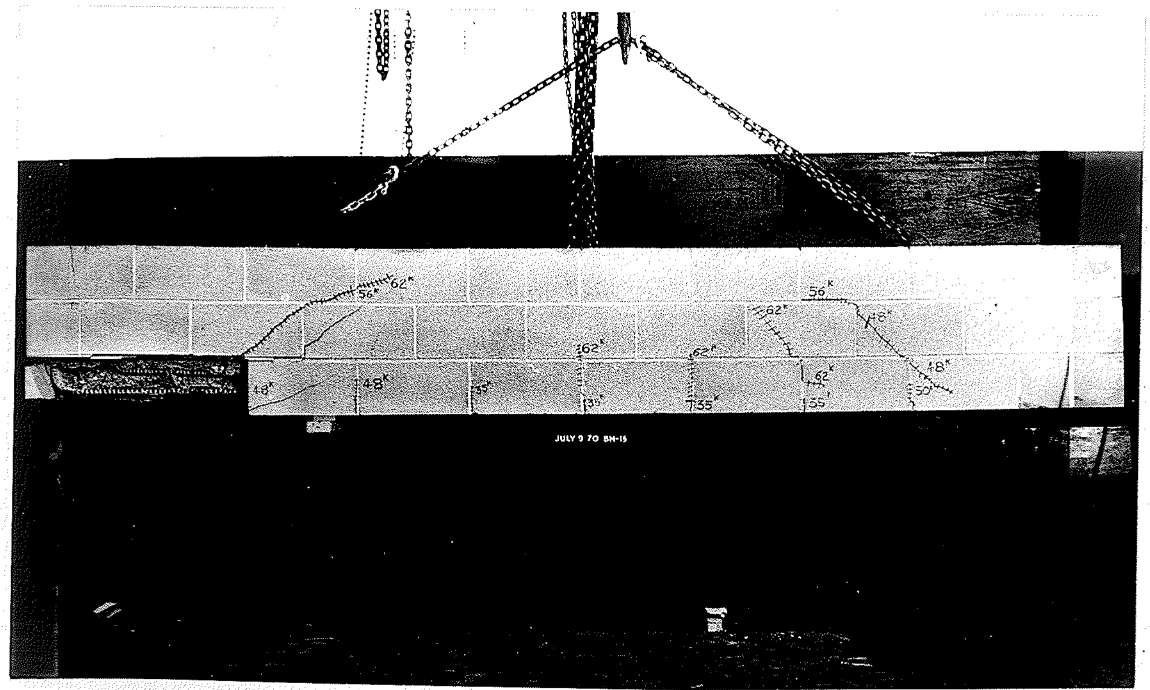

BEAM 15 SHOWING SHEAR FAILURE

FIGURE 56

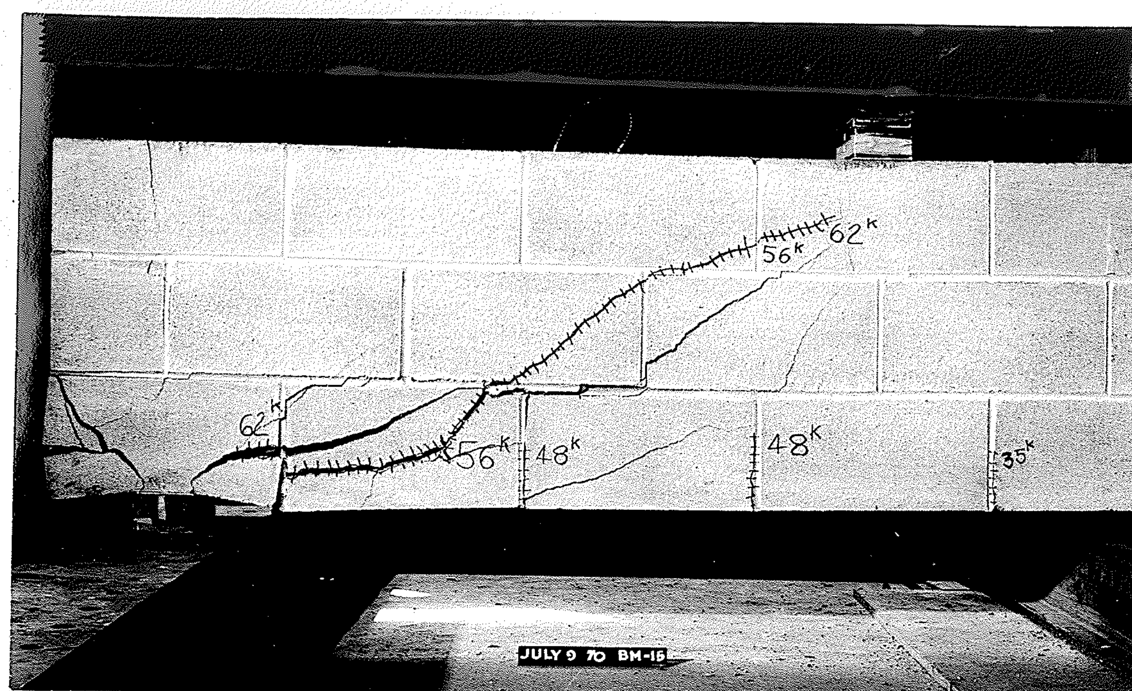

BEAM 15 SHOWING DIAGONAL TENSION CRACK

FIGURE 57

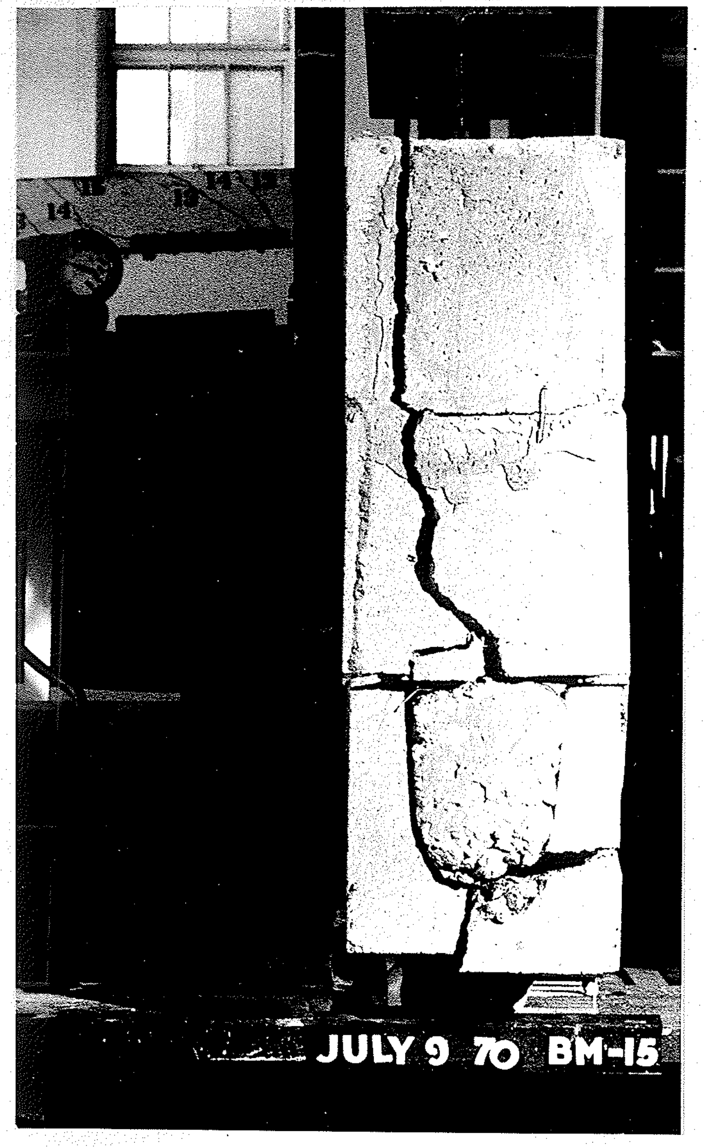

BEAM 15 SHOWING SEPARATION OF END BLOCK

FIGURE 58

TABLE XVI

TEST DATA FOR BEAM 14
LOAD-MIDSPAN DEFLECTION RESULTS

Load (Bm.14) (kips)	Deflection (Bm.14) (inches)	Load (Bm.14) (Kips)	Deflection (Bm.14) (inches)
0.0	0.0	41.0	0.250
1.0	0.005	42.0	0.258
2.0	0.008	43.0	0.264
3.0	0.010	44.0	0.274
4.0	0.014	45.0	0.280
6.0	0.022	46.0	0.290
7.0	0.028	47.0	0.300
8.0	0.032	48.0	0.308
9.0	0.037	49.0	0.318
10.0	0.041	50.0	0.328
11.0	0.046	51.0	0.337
12.0	0.052	52.0	0.345
13.0	0.056	53.0	0.358
14.0	0.060	54.0	0.360
15.0	0.066	55.0	0.384
16.0	0.072	56.0	0.388
17.0	0.076	57.0	0.394
18.0	0.082	58.0	0.410
19.0	0.089	59.0	0.417
20.0	0.094	60.0	0.428
21.0	0.100	61.0	0.442
22.0	0.108	62.0	0.450
23.0	0.114	63.0	0.460
24.0	0.120	64.0	0.466
25.0	0.126	65.0	0.475
26.0	0.135	66.0	0.485
27.0	0.140	67.0	0.495
28.0	0.148	68.0	0.518
29.0	0.155	69.0	0.528
30.0	0.163	70.0	0.536
31.0	0.171	71.0	0.548
32.0	0.178	72.0	0.560
33.0	0.185	73.0	0.575
34.0	0.192	74.0	0.590
35.0	0.200	75.0	0.606
36.0	0.210	76.0	0.622
37.0	0.216	77.0	0.640
38.0	0.225	78.0	0.653
39.0	0.234	79.0	0.670
40.0	0.240	80.0	0.690

TABLE XVII

TEST DATA FOR BEAM 15
LOAD-MIDSPAN DEFLECTION RESULTS

Load (Bm.15) (kips)	Deflection (Bm.15) (inches)	Load (Bm.15) (kips)	Deflection (Bm.15) (inches)
0.0	0.0	35.0	0.194
1.0	0.003	36.0	0.205
2.0	0.006	37.0	0.211
3.0	0.011	38.0	0.218
4.0	0.015	39.0	0.225
5.0	0.019	40.0	0.233
6.0	0.024	41.0	0.241
7.0	0.029	42.0	0.249
8.0	0.033	43.0	0.256
9.0	0.037	44.0	0.264
10.0	0.042	45.0	0.274
11.0	0.047	46.0	0.283
12.0	0.051	47.0	0.291
13.0	0.056	48.0	0.300
14.0	0.060	49.0	0.314
15.0	0.066	50.0	0.321
16.0	0.071	51.0	0.328
17.0	0.076	52.0	0.335
18.0	0.081	53.0	0.343
19.0	0.086	54.0	0.353
20.0	0.092	55.0	0.363
21.0	0.098	56.0	0.371
22.0	0.104	57.0	0.386
23.0	0.109	58.0	0.393
24.0	0.115	59.0	0.400
25.0	0.121	60.0	0.410
26.0	0.127	61.0	0.419
27.0	0.135	62.0	0.430
28.0	0.142	63.0	0.450
29.0	0.150	64.0	0.458
30.0	0.156	65.0	0.468
31.0	0.165	66.0	0.478
32.0	0.172	67.0	0.488
33.0	0.179	68.0	0.500
34.0	0.186	69.0	0.513

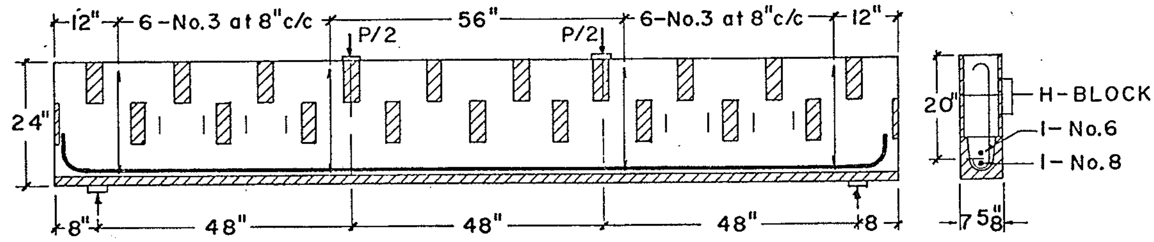

LONGITUDINAL SECTION

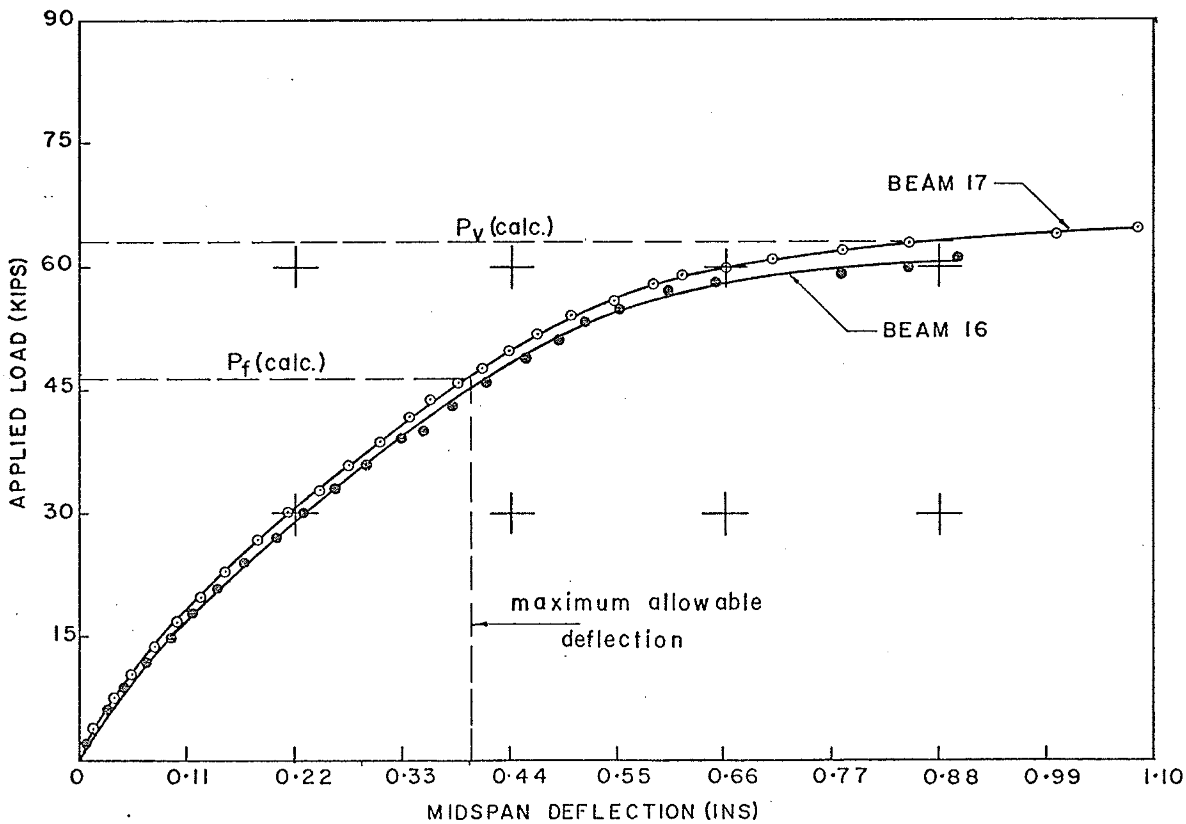

figure 59: details and load deflection curves for beams 16 and 17

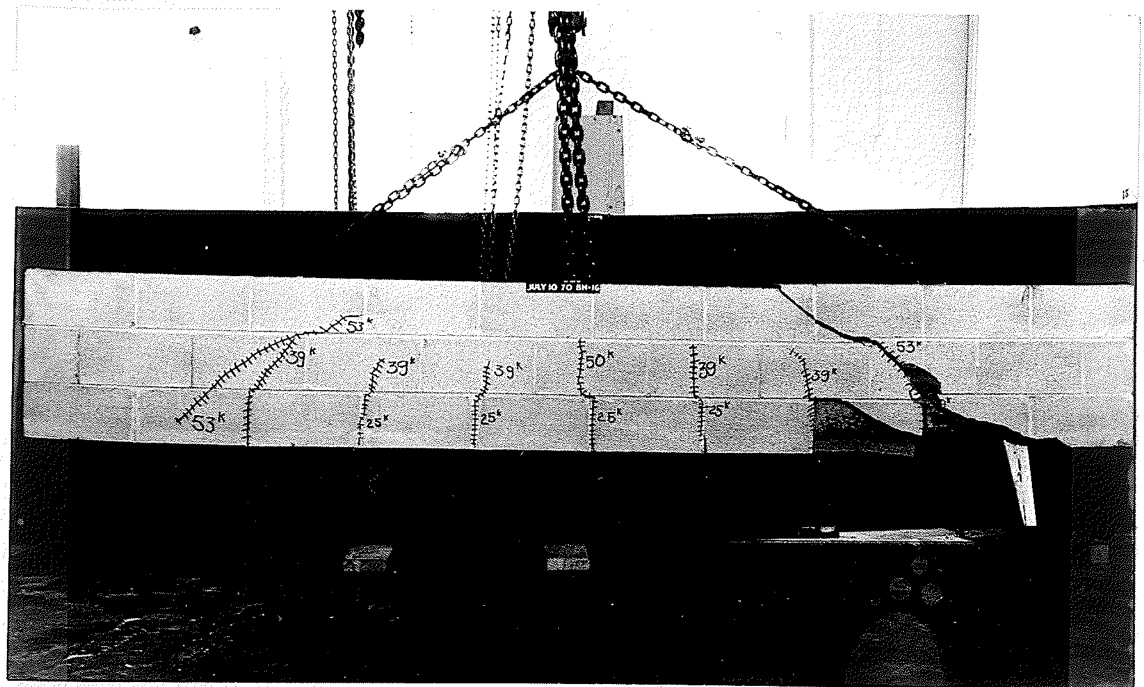

BEAM 16 SHOWING SHEAR FAILURE

FIGURE 60

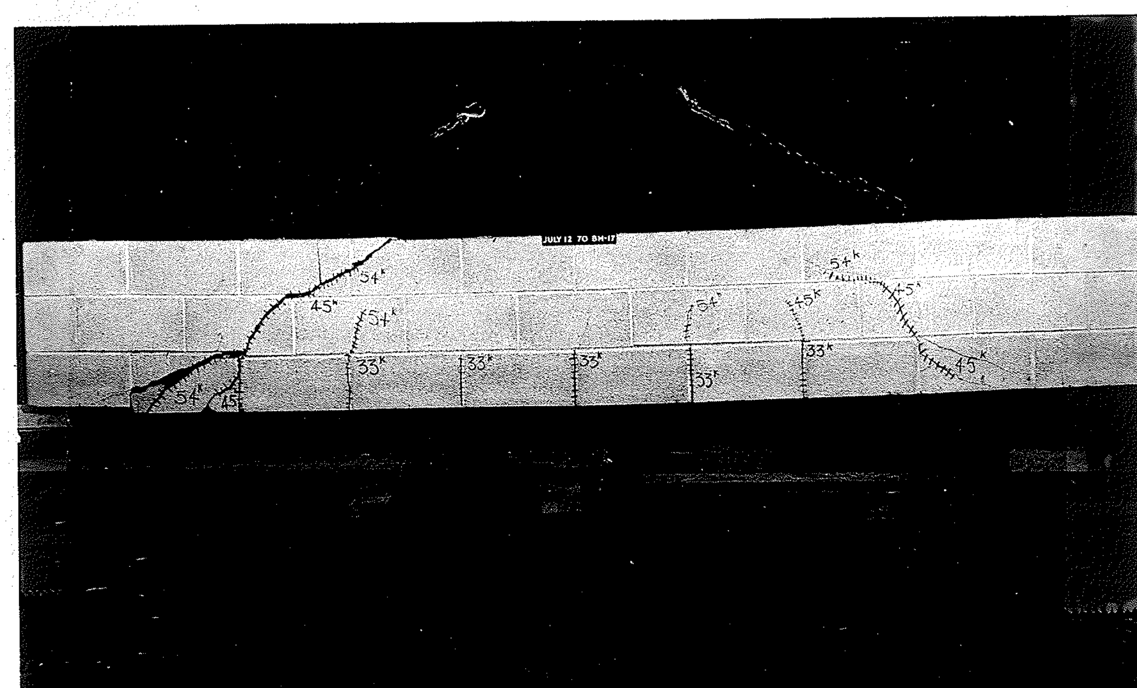

BEAM 17 SHOWING SHEAR FAILURE

FIGURE 61

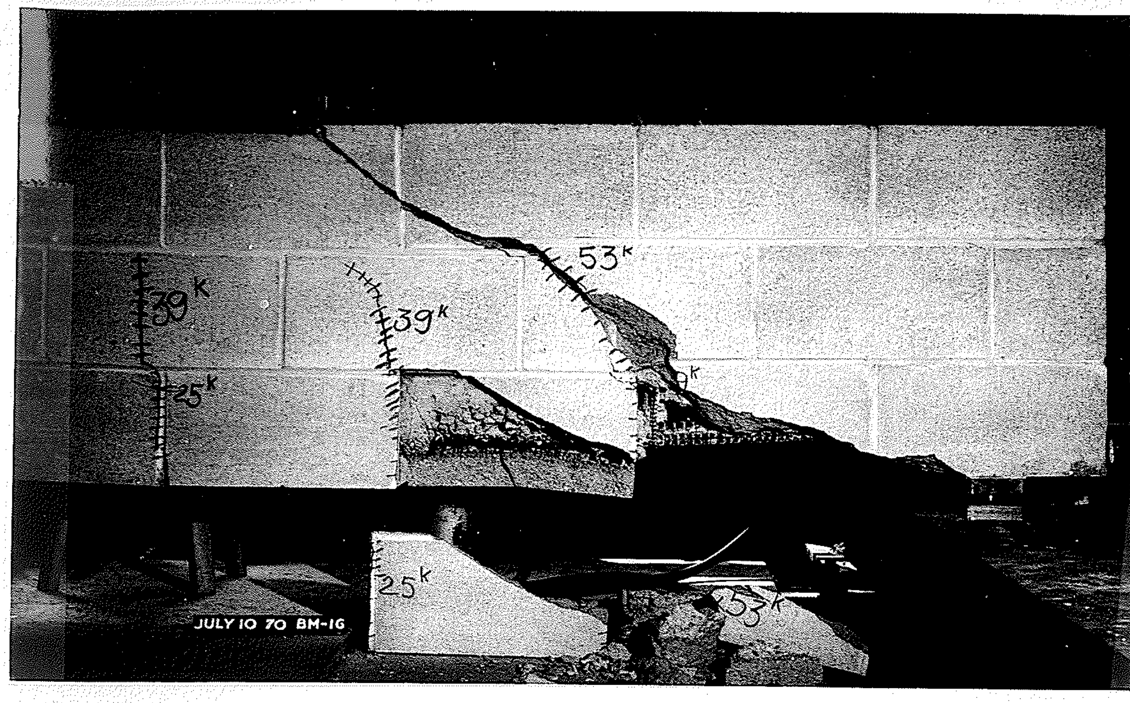

BEAM 16 SHOWING DIAGONAL TENSION CRACK

FIGURE 62

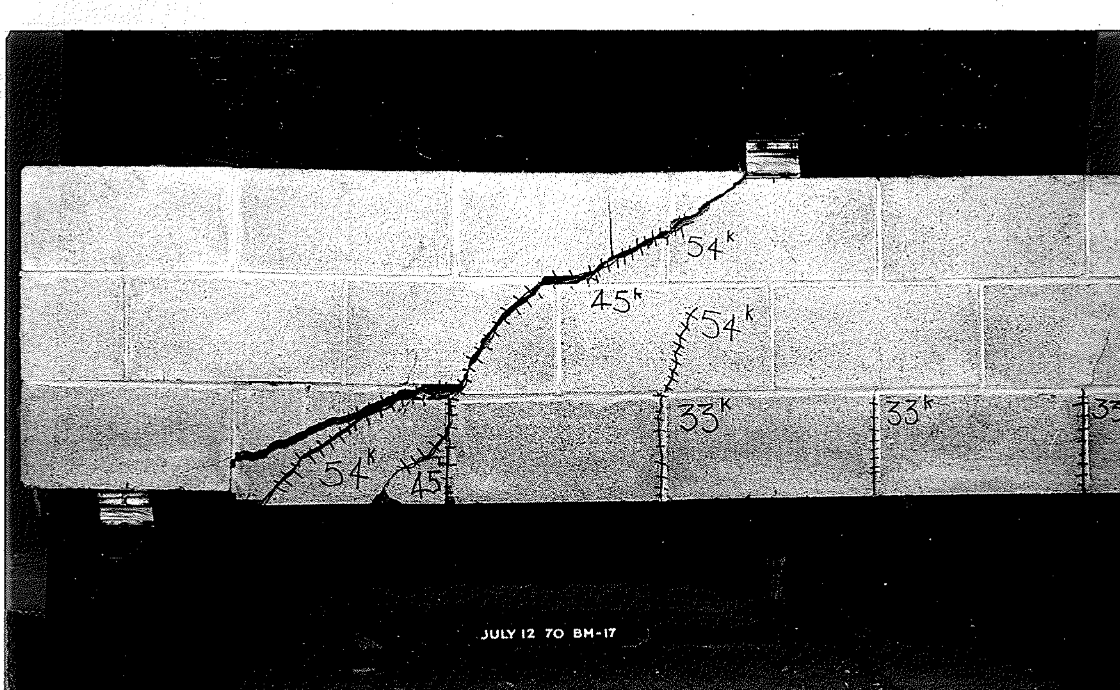

BEAM 17 SHOWING DIAGONAL TENSION CRACK

FIGURE 63

TABLE XVIII

TEST DATA FOR BEAM 16
LOAD-MIDSPAN DEFLECTION RESULTS

Load (Bm.16) (kips)	Deflection (Bm.16) (inches)	Load (Bm.16) (kips)	Deflection (Bm.16) (inches)
0.0	0.0	31.0	0.240
1.0	0.004	32.0	0.250
2.0	0.008	33.0	0.260
3.0	0.012	34.0	0.270
4.0	0.018	35.0	0.281
5.0	0.023	36.0	0.293
6.0	0.029	37.0	0.305
7.0	0.035	38.0	0.318
8.0	0.040	39.0	0.328
9.0	0.047	40.0	0.350
10.0	0.054	41.0	0.358
11.0	0.062	42.0	0.370
12.0	0.070	43.0	0.380
13.0	0.078	44.0	0.390
14.0	0.086	45.0	0.402
15.0	0.094	46.0	0.416
16.0	0.102	47.0	0.430
17.0	0.110	48.0	0.442
18.0	0.116	49.0	0.455
19.0	0.125	50.0	0.468
20.0	0.133	51.0	0.490
21.0	0.142	52.0	0.500
22.0	0.150	53.0	0.515
23.0	0.159	54.0	0.540
24.0	0.169	55.0	0.550
25.0	0.178	56.0	0.568
26.0	0.190	57.0	0.600
27.0	0.200	58.0	0.650
28.0	0.210	59.0	0.780
29.0	0.218	60.0	0.850
30.0	0.228	61.0	0.900

TABLE XIX

TEST DATA FOR BEAM 17
LOAD-MIDSPAN DEFLECTION RESULTS

Load (Bm.17) (kips)	Deflection (Bm.17) (inches)	Load (Bm.17) (kips)	Deflection (Bm.17) (inches)
0.0	0.0	33.0	0.244
1.0	0.004	34.0	0.256
2.0	0.008	35.0	0.264
3.0	0.012	36.0	0.273
4.0	0.016	37.0	0.282
5.0	0.021	38.0	0.292
6.0	0.026	39.0	0.303
7.0	0.032	40.0	0.317
8.0	0.037	41.0	0.325
9.0	0.042	42.0	0.335
10.0	0.050	43.0	0.346
11.0	0.055	44.0	0.357
12.0	0.062	45.0	0.368
13.0	0.070	46.0	0.387
14.0	0.077	47.0	0.396
15.0	0.084	48.0	0.408
16.0	0.092	49.0	0.420
17.0	0.100	50.0	0.438
18.0	0.107	51.0	0.454
19.0	0.114	52.0	0.468
20.0	0.122	53.0	0.482
21.0	0.130	54.0	0.500
22.0	0.138	55.0	0.530
23.0	0.150	56.0	0.545
24.0	0.155	57.0	0.562
25.0	0.163	58.0	0.583
26.0	0.172	59.0	0.615
27.0	0.180	60.0	0.655
28.0	0.189	61.0	0.710
29.0	0.199	62.0	0.780
30.0	0.210	63.0	0.850
31.0	0.221	64.0	1.000
32.0	0.231	65.0	1.080

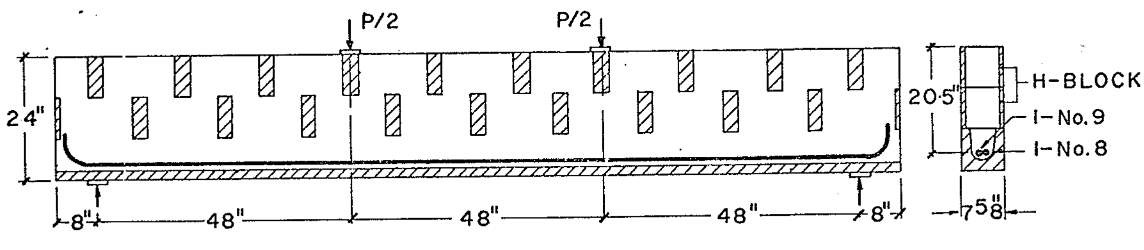

LONGITUDINAL SECTION

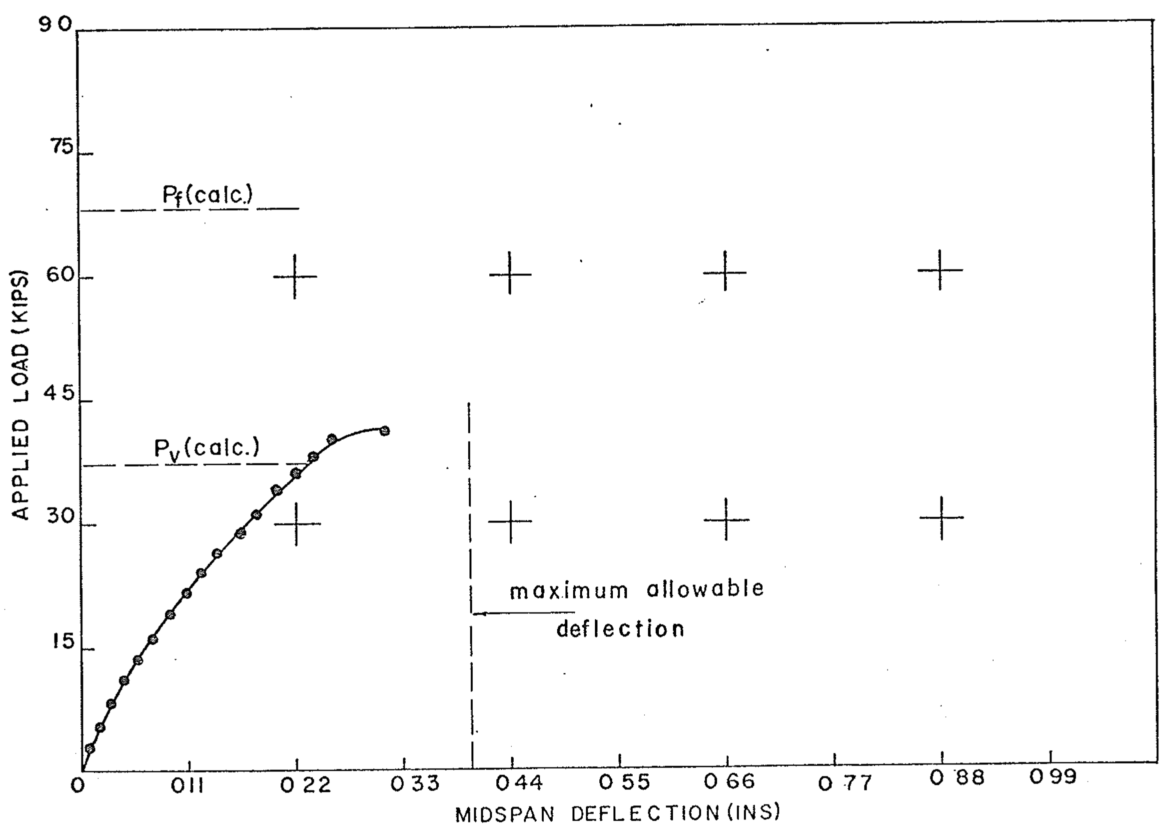

figure 64: details and load-deflection curve for beam 18

122

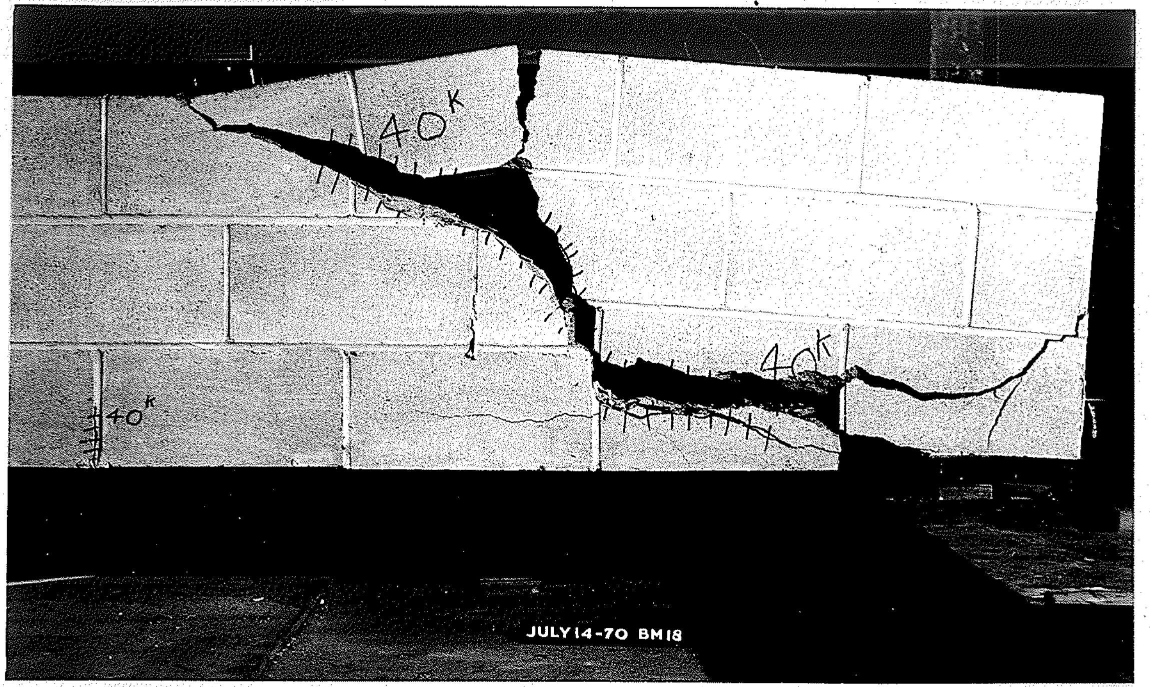

BEAM 18 SHOWING SHEAR FAILURE

FIGURE 65

TABLE XX

TEST DATA FOR BEAMS 13 AND 18
LOAD-MIDSPAN DEFLECTION RESULTS

Load (Bm.13) (kips)	Deflection (Bm.13) (inches)	Load (Bm.18) (kips)	Deflection (Bm.18) (inches)
0.0	0.0	0.0	0.0
0.5	0.005	1.0	0.004
1.0	0.010	2.0	0.008
1.5	0.015	3.0	0.010
2.0	0.024	4.0	0.014
2.5	0.032	5.0	0.019
3.0	0.045	6.0	0.024
3.5	0.058	7.0	0.027
4.0	0.070	8.0	0.031
4.5	0.082	9.0	0.035
5.0	0.095	10.0	0.040
5.5	0.110	11.0	0.045
6.0	0.120	12.0	0.051
6.5	0.135	13.0	0.056
7.0	0.150	14.0	0.061
7.5	0.165	15.0	0.068
8.0	0.180	16.0	0.074
8.5	0.195	17.0	0.080
9.0	0.210	18.0	0.085
9.5	0.228	19.0	0.092
10.0	0.245	20.0	0.099
10.5	0.260	21.0	0.105
11.0	0.285	22.0	0.111
11.5	0.308	23.0	0.118
12.0	0.333	24.0	0.124
12.5	0.355	25.0	0.131
15.0	0.370	26.0	0.138
13.5	0.390	27.0	0.145
14.0	0.405	28.0	0.153
14.5	0.430	29.0	0.180
15.0	0.450	30.0	0.170
15.5	0.482	31.0	0.180
16.0	0.495	32.0	0.188
16.5	0.510	33.0	0.195
17.0	0.532	34.0	0.202
17.5	0.555	35.0	0.210
18.0	0.572	36.0	0.220
18.5	0.592	37.0	0.230
19.0	0.612	38.0	0.238
19.5	0.635	39.0	0.248
20.0	0.665	40.0	0.257
20.5	0.695	41.0	0.312
21.0	0.840		

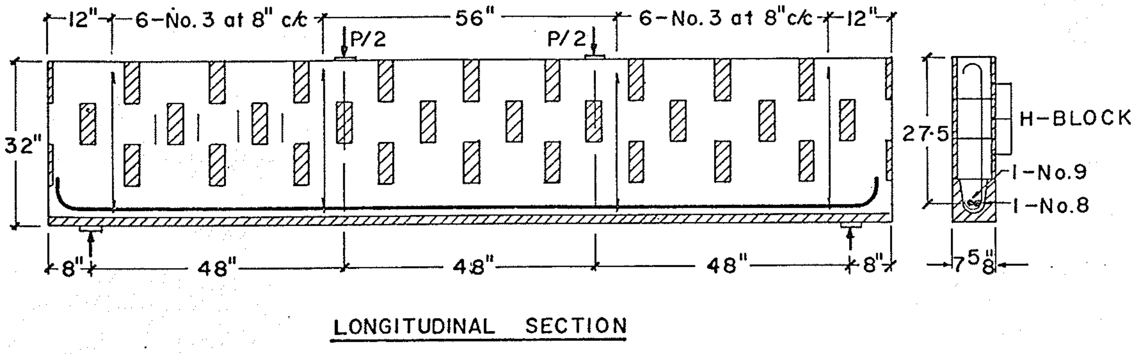

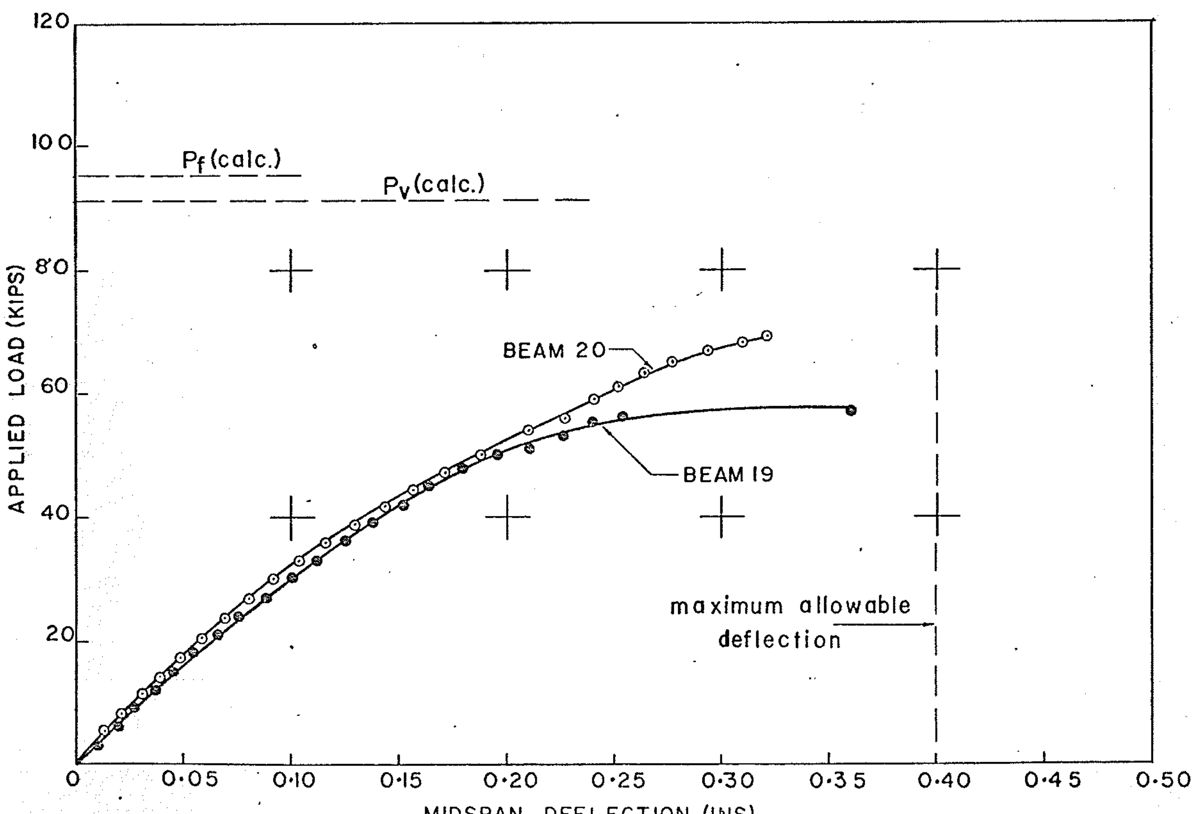

figure 66 details and load-deflection curves for beams 19 and 20

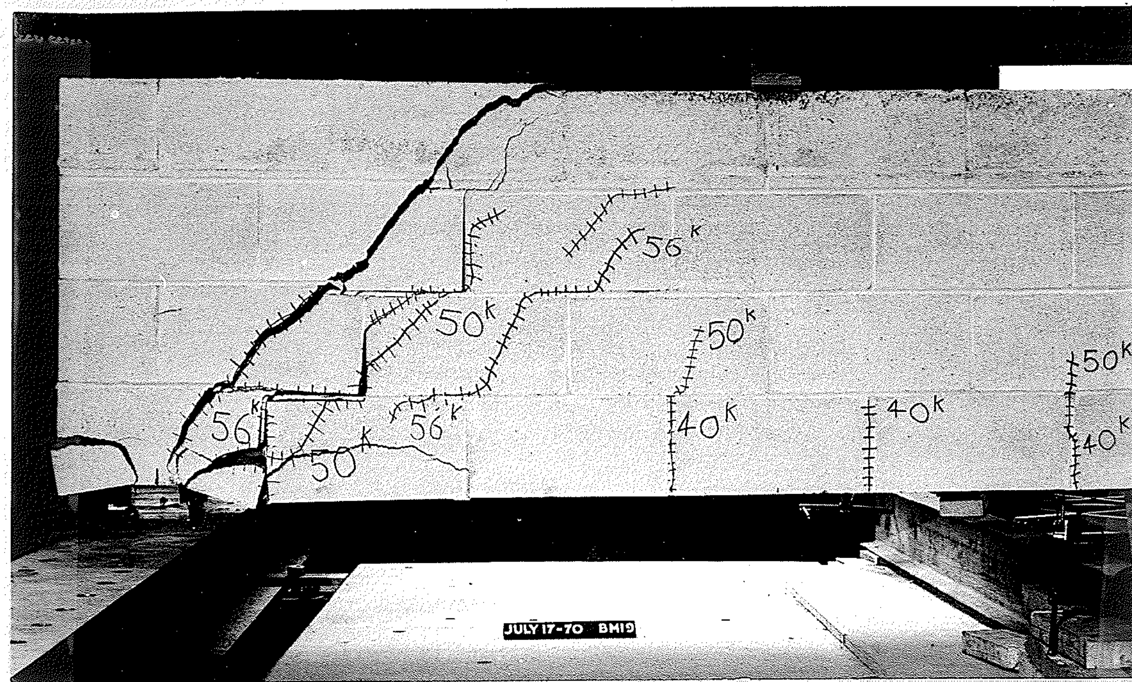

BEAM 19 SHOWING SHEAR FAILURE

FIGURE 67

BEAM 20 SHOWING SHEAR FAILURE

FIGURE 68

TABLE XXI

TEST DATA FOR BEAM 19
LOAD-MIDSPAN DEFLECTION RESULTS

Load (Bm.19) (kips)	Deflection (Bm.19) (inches)	Load (Bm.19) (kips)	Deflection (Bm.19) (inches)
0.0	0.0	29.0	0.095
1.0	0.004	30.0	0.100
2.0	0.006	31.0	0.103
3.0	0.010	32.0	0.107
4.0	0.013	33.0	0.111
5.0	0.016	34.0	0.116
6.0	0.019	35.0	0.120
7.0	0.022	36.0	0.125
8.0	0.025	37.0	0.129
9.0	0.027	38.0	0.134
10.0	0.030	39.0	0.138
11.0	0.033	40.0	0.142
12.0	0.036	41.0	0.149
13.0	0.040	42.0	0.152
14.0	0.042	43.0	0.156
15.0	0.045	44.0	0.160
16.0	0.048	45.0	0.164
17.0	0.050	46.0	0.169
18.0	0.054	47.0	0.174
19.0	0.058	48.0	0.180
20.0	0.061	49.0	0.189
21.0	0.065	50.0	0.195
22.0	0.068	51.0	0.212
23.0	0.072	52.0	0.222
24.0	0.075	53.0	0.226
25.0	0.079	54.0	0.233
26.0	0.083	55.0	0.240
27.0	0.088	56.0	0.254
28.0	0.091	57.0	0.360

TABLE XXII

TEST DATA FOR BEAM 20
LOAD -MIDSPAN DEFLECTION RESULTS

Load (Bm.20) (kips)	Deflection (Bm.20) (inches)	Load (Bm.20) (kips)	Deflection (Bm.20) (inches)
0.0	0.0	35.0	0.114
1.0	0.001	36.0	0.118
2.0	0.004	37.0	0.122
3.0	0.007	38.0	0.130
4.0	0.010	39.0	0.133
5.0	0.013	40.0	0.137
6.0	0.015	41.0	0.141
7.0	0.018	42.0	0.146
8.0	0.020	43.0	0.151
9.0	0.023	44.0	0.155
10.0	0.025	45.0	0.160
11.0	0.028	46.0	0.168
12.0	0.031	47.0	0.172
13.0	0.034	48.0	0.176
14.0	0.036	49.0	0.181
15.0	0.039	50.0	0.185
16.0	0.042	51.0	0.196
17.0	0.045	52.0	0.202
18.0	0.048	53.0	0.207
19.0	0.052	54.0	0.211
20.0	0.056	55.0	0.218
21.0	0.059	56.0	0.227
22.0	0.063	57.0	0.231
23.0	0.067	58.0	0.236
24.0	0.070	59.0	0.241
25.0	0.074	60.0	0.246
26.0	0.078	61.0	0.253
27.0	0,081	62.0	0.259
28.0	0.085	63.0	0.264
29.0	0.089	64.0	0.271
30.0	0.093	65.0	0.278
31.0	0.097	66.0	0.285
32.0	0.101	67.0	0.295
33.0	0.105	68.0	0.311
34.0	0.109	69.0	0.322

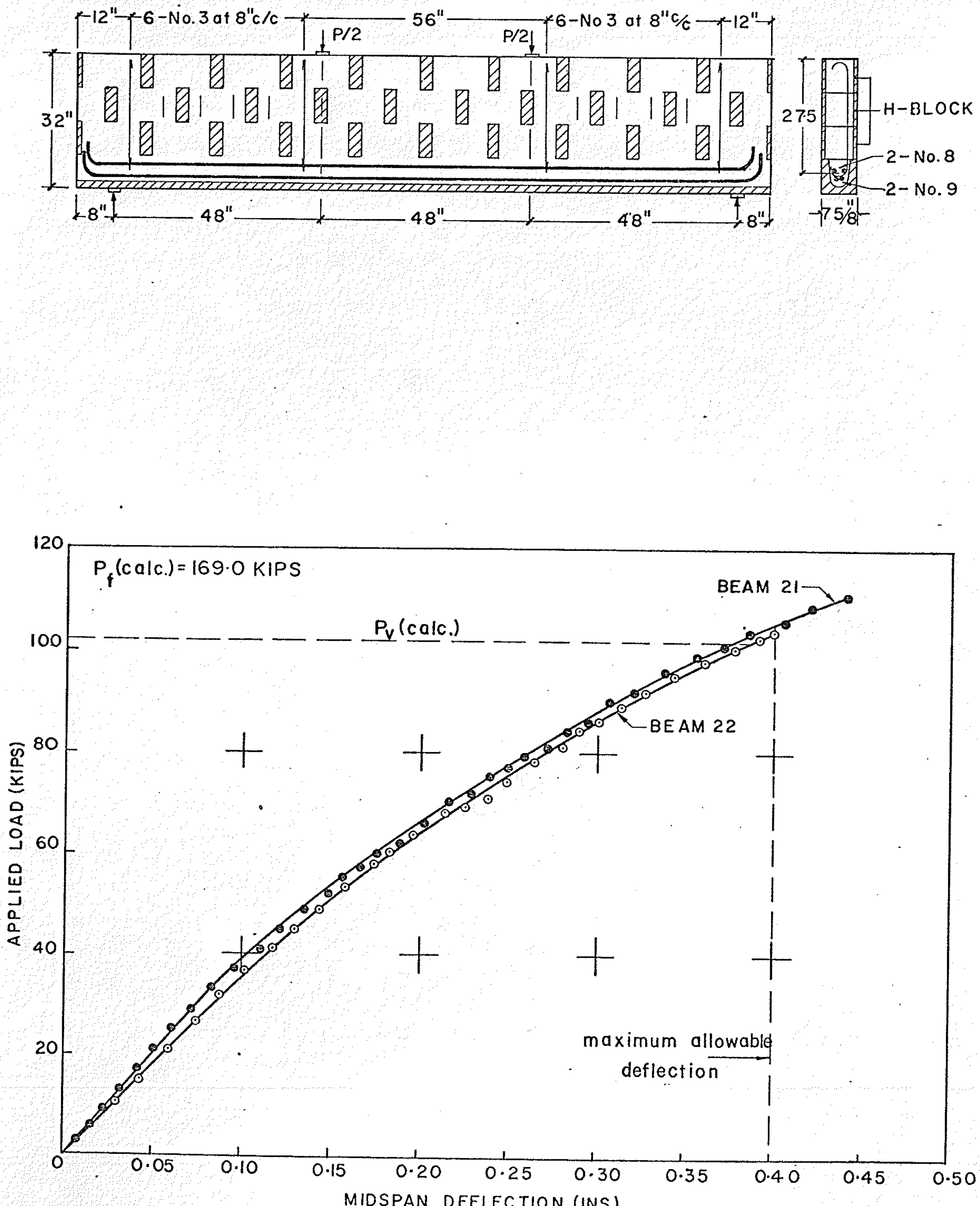

figure 69: details and load-deflection curves for beams 21 and 22

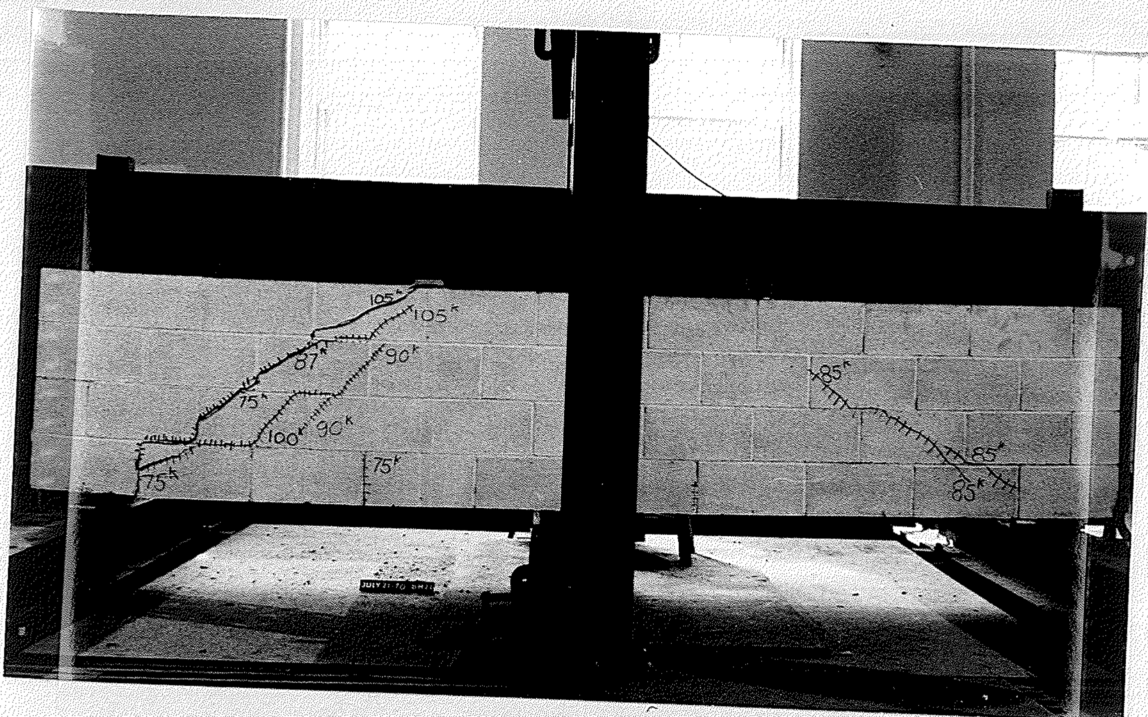

BEAM 21 SHOWING SHEAR FAILURE

FIGURE 70

BEAM 22 SHOWING SHEAR FAILURE

FIGURE 71

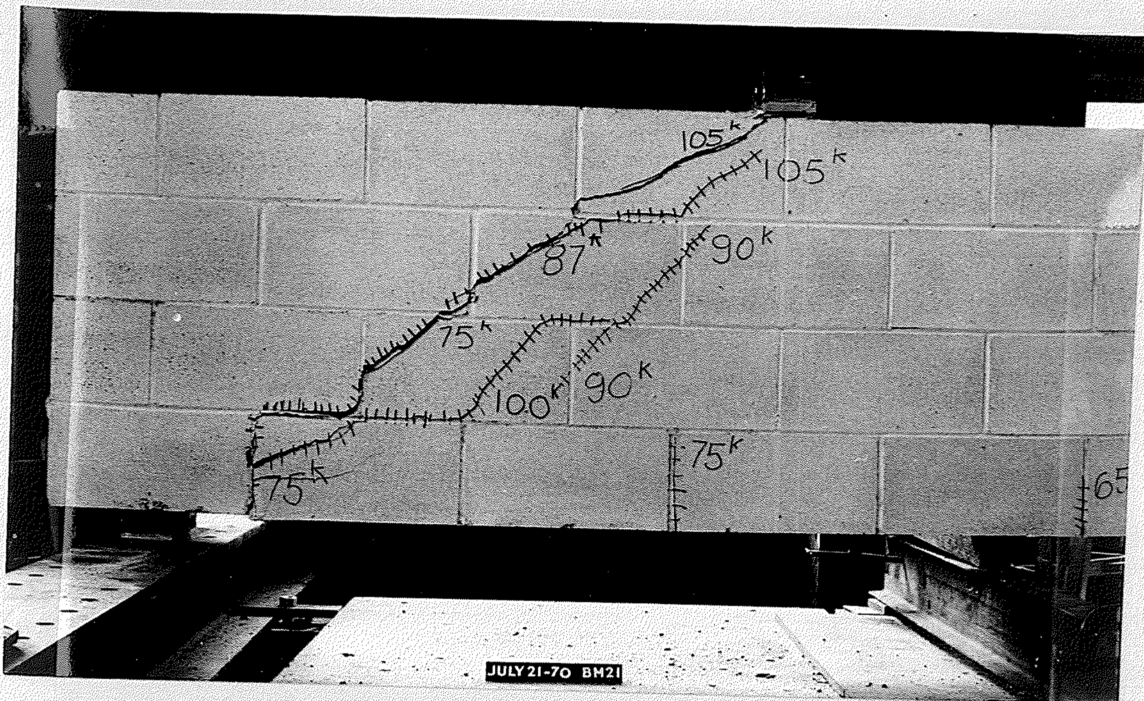

BEAM 21 SHOWING DIAGONAL TENSION CRACK

FIGURE 72

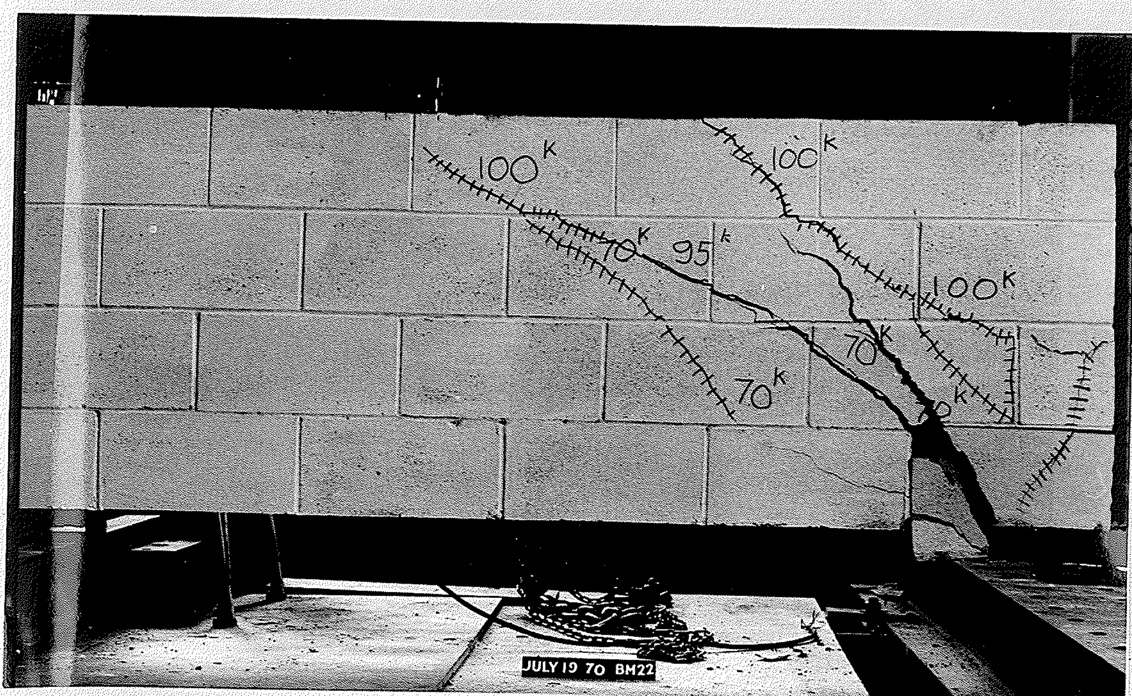

BEAM 22 SHOWING DIAGONAL TENSION CRACK

FIGURE 73

TABLE XXIII

TEST DATA FOR BEAM 21
LOAD-MIDSPAN DEFLECTION RESULTS

Load (Bm.21) (kips)	Deflection (Bm.21) (inches)	Load (Bm.21) (kips)	Deflection (Bm.21) (inches)
0.0	0.0	36.0	0.093
1.0	0.002	37.0	0.096
2.0	0.005	38.0	0.098
3.0	0.007	39.0	0.101
4.0	0.010	40.0	0.105
5.0	0.012	41.0	0.110
6.0	0.015	42.0	0.113
7.0	0.017	43.0	0.116
8.0	0.020	44.0	0.119
9.0	0.022	45.0	0.122
10.0	0.025	46.0	0.127
11.0	0.027	47.0	0.130
12.0	0.030	48.0	0.133
13.0	0.032	49.0	0.136
14.0	0.035	50.0	0.140
15.0	0.037	51.0	0.146
16.0	0.039	52.0	0.149
17.0	0.042	53.0	0.152
18.0	0.044	54.0	0.155
19.0	0.047	55.0	0.157
20.0	0.049	56.0	0.164
21.0	0.051	57.0	0.167
22.0	0.054	58.0	0.170
23.0	0.056	59.0	0.174
24.0	0.059	60.0	0.177
25.0	0.061	61.0	0.186
26.0	0.064	62.0	0.189
27.0	0.067	63.0	0.192
28.0	0.070	64.0	0.195
29.0	0.072	65.0	0.198
30.0	0.075	66.0	0.203
31.0	0.078	67.0	0.206
32.0	0.081	68.0	0.209
33.0	0.083	69.0	0.213
34.0	0.086	70.0	0.216
35.0	0.089	71.0	0.223

TABLE XXIII CONT'D.

TEST DATA FOR BEAM 21
LOAD-MIDSPAN DEFLECTION RESULTS

Load (Bm.21) (kips)	Deflection (Bm.21) (inches)	Load (Bm.21) (kips)	Deflection (Bm.21) (inches)
72.0	0.228	92.0	0.320
73.0	0.232	93.0	0.324
74.0	0.235	94.0	0.328
75.0	0.239	95.0	0.333
76.0	0.246	96.0	0.338
77.0	0.249	97.0	0.344
78.0	0.252	98.0	0.349
79.0	0.258	99.0	0.354
80.0	0.264	100.0	0.360
81.0	0.272	101.0	0.369
82.0	0.276	102.0	0.374
83.0	0.279	103.0	0.378
84.0	0.282	104.0	0.385
85.0	0.287	105.0	0.391
86.0	0.294	106.0	0.405
87.0	0.298	107.0	0.409
88.0	0.300	108.0	0.414
89.0	0.304	109.0	0.420
90.0	0.307	110.0	0.426
91.0	0.312	111.0	0.440

TABLE XXIV

TEST DATA FOR BEAM 22
LOAD-MIDSPAN DEFLECTION RESULTS

Load (Bm.22) (kips)	Deflection (Bm.22) (inches)	Load (Bm.22) (kips)	Deflection (Bm.22) (inches)
0.0	0.0	36.0	0.100
1.0	0.001	37.0	0.103
2.0	0.003	38.0	0.106
3.0	0.006	39.0	0.109
4.0	0.010	40.0	0.112
5.0	0.013	41.0	0.116
6.0	0.016	42.0	0.120
7.0	0.019	43.0	0.124
8.0	0.022	44.0	0.127
9.0	0.025	45.0	0.130
10.0	0.028	46.0	0.134
11.0	0.032	47.0	0.137
12.0	0.035	48.0	0.140
13.0	0.037	49.0	0.144
14.0	0.040	50.0	0.148
15.0	0.043	51.0	0.152
16.0	0.046	52.0	0.155
17.0	0.048	53.0	0.158
18.0	0.051	54.0	0.161
19.0	0.054	55.0	0.164
20.0	0.056	56.0	0.169
21.0	0.059	57.0	0.172
22.0	0.062	58.0	0.175
23.0	0.064	59.0	0.178
24.0	0.067	60.0	0.181
25.0	0.070	61.0	0.188
26.0	0.072	62.0	0.190
27.0	0.075	63.0	0.192
28.0	0.077	64.0	0.195
29.0	0.080	65.0	0.199
30.0	0.083	66.0	0.206
31.0	0.085	67.0	0.210
32.0	0.088	68.0	0.213
33.0	0.090	69.0	0.226
34.0	0.093	70.0	0.230
35.0	0.096	71.0	0.238

TABLE XXIV CONT'D.

TEST DATA FOR BEAM 22
LOAD-MIDSPAN DEFLECTION RESULTS

Load (Bm.22) (kips)	Deflection (Bm.22) (inches)	Load (Bm.22) (kips)	Deflection (Bm.22 (inches)
72.0	0.240	89.0	0.314
73.0	0.243	90.0	0.318
74.0	0.248	91.0	0.324
75.0	0.252	92.0	0.327
76.0	0.256	93.0	0.332
77.0	0.260	94.0	0.338
78.0	0.264	95.0	0.343
79.0	0.268	96.0	0.351
80.0	0.272	97.0	0.355
81.0	0.280	98.0	0.360
82.0	0.284	99.0	0.366
83.0	0.287	100.0	0.373
84.0	0.290	101.0	0.380
85.0	0.296	102.0	0.387
86.0	0.302	103.0	0.392
87.0	0.305	104.0	0.400
88.0	0.310		

TABLE XXV

TEST DATA FOR BEAMS 21 AND 22
LATERAL DEFLECTION OF COMPRESSION ZONE

Beam No.	Load (kips)	Top Left (Gauge 1)	Top Centre (Gauge 2)	Top Right (Gauge 3)
21	0	0	0	0
	10	0.003	0.010	0.012
	20	0.012	0.025	0.022
	25	0.020	0.031	0.031
	30	0.027	0.039	0.040
	35	0.034	0.049	0.049
	40	0.041	0.058	0.057
	45	0.048	0.067	0.064
	50	0.050	0.074	0.068
	55	0.054	0.078	0.071
	60	0.055	0.086	0.076
	65	0.055	0.095	0.081
	70	0.057	0.100	0.085
	75	0.056	0.106	0.089
	80	0.057	0.118	0.087
	85	0.058	0.127	0.089
	90	0.060	0.134	0.094
	95	0.062	0.145	0.102
	100	0.062	0.155	0.111
	105	0.055	0.170	0.121
	110	0.055	0.185	0.129
22	0	0	0	0
	10	0.069	0.069	0.075
	20	0.082	0.087	0.100
	30	0.081	0.092	0.110
	35	0.080	0.096	0.112
	40	0.077	0.100	0.115
	50	0.073	0.106	0.119
	60	0.070	0.111	0.125
	70	0.055	0.122	0.143
	80	0.045	0.124	0.152
	85	0.042	0.129	0.154
	95	0.037	0.135	0.160

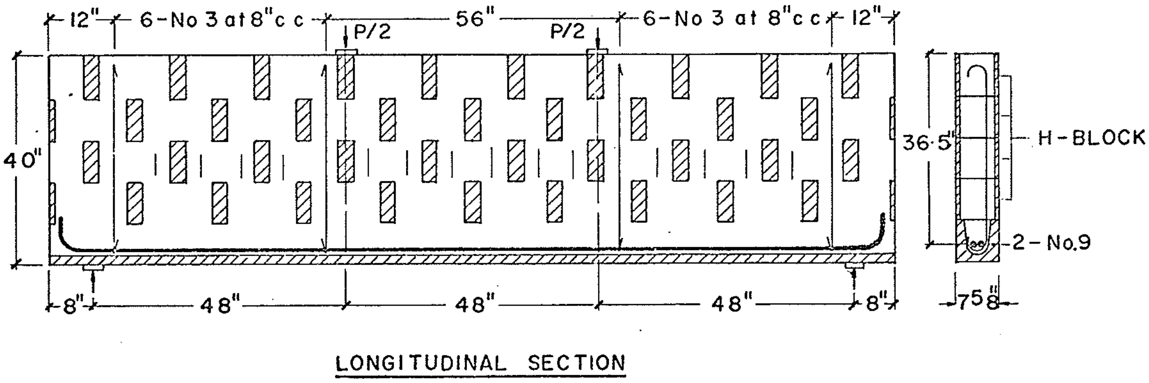

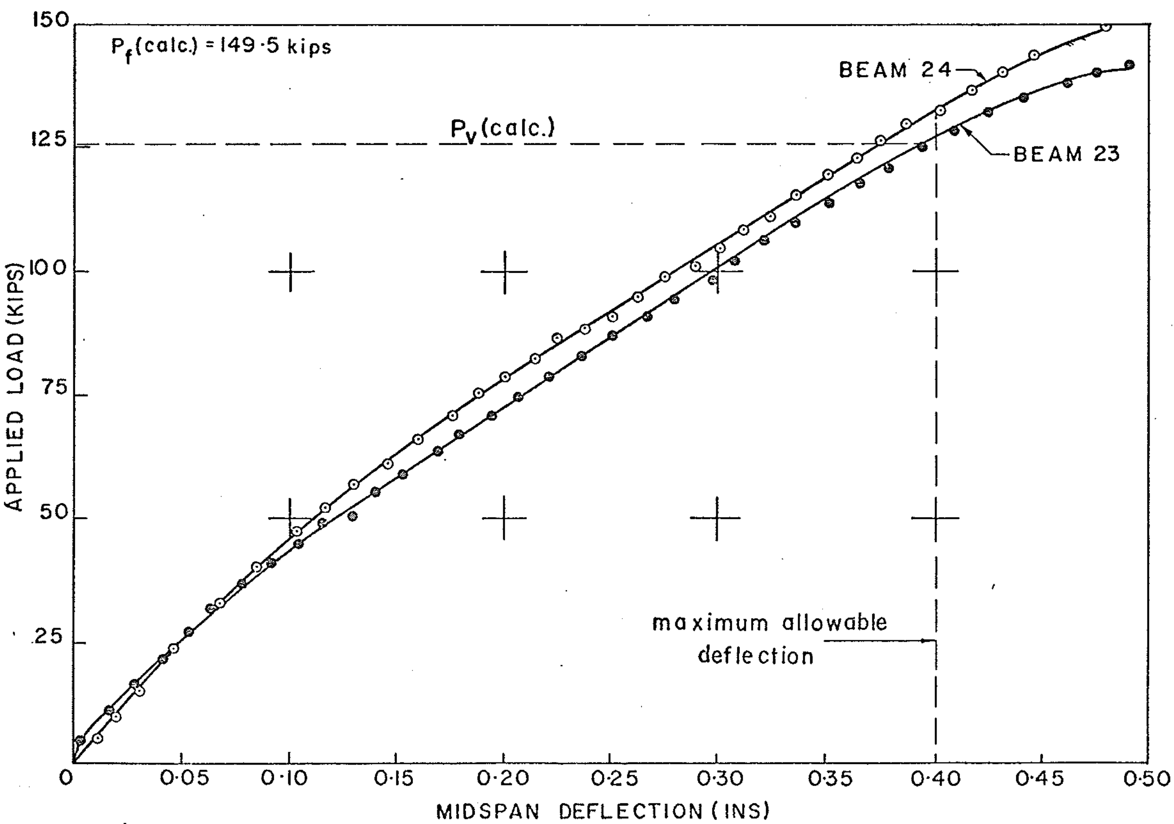

figure 74: details and load-deflection curves for beams 23 and 24

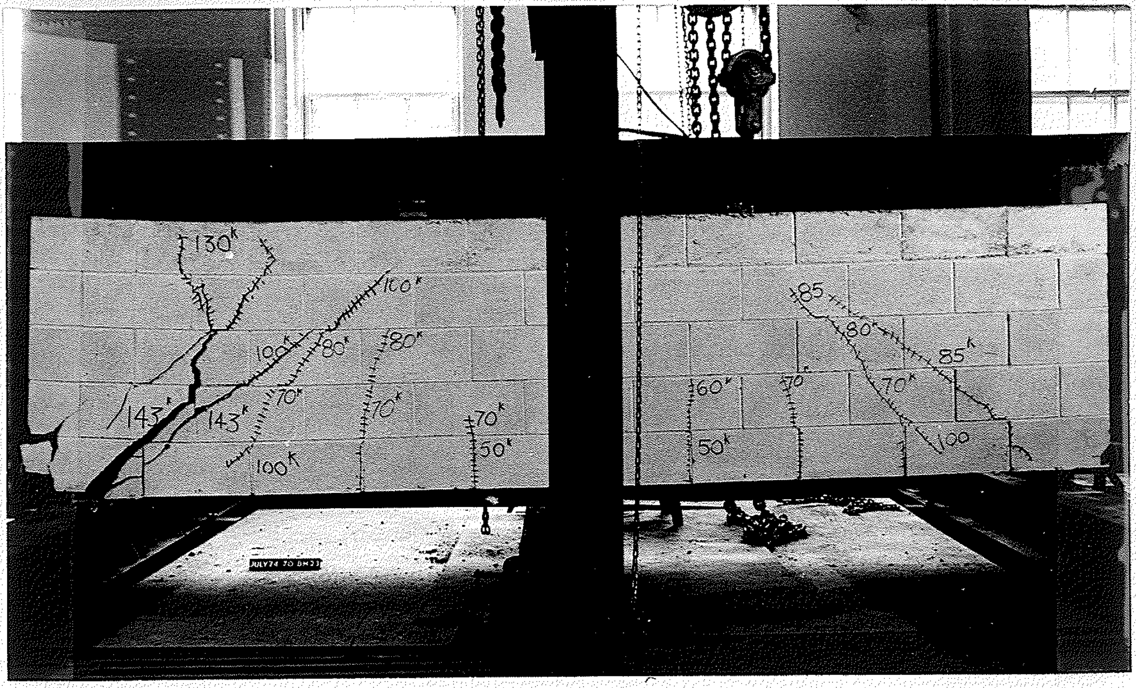

BEAM 23 SHOWING SHEAR FAILURE

FIGURE 75

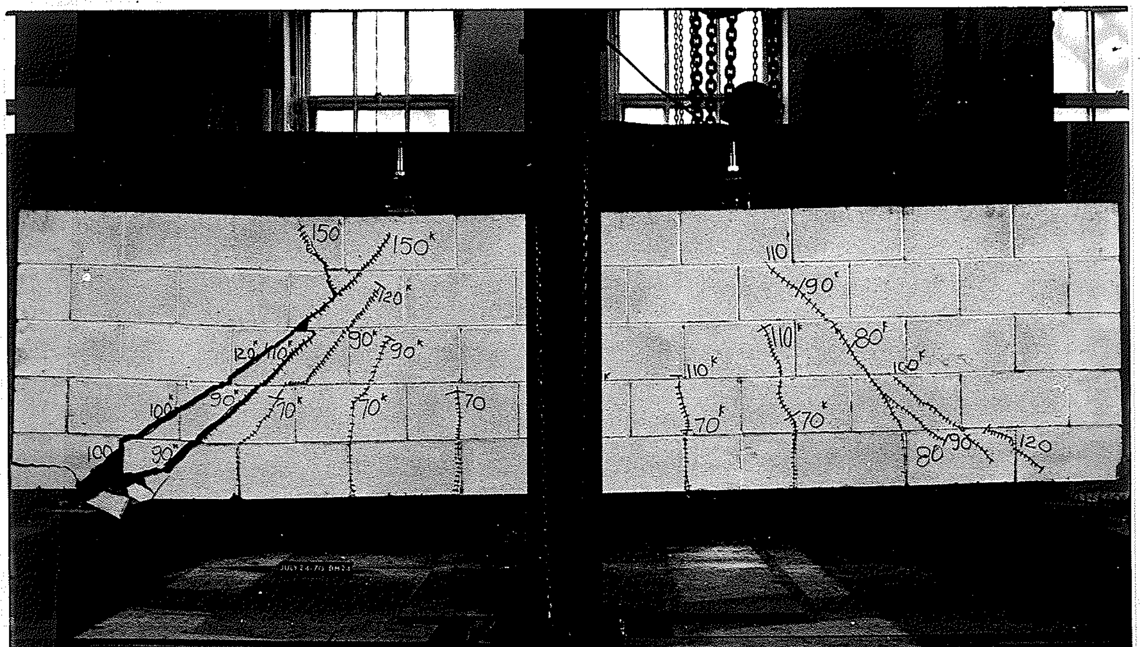

BEAM 24 SHOWING SHEAR FAILURE

FIGURE 76

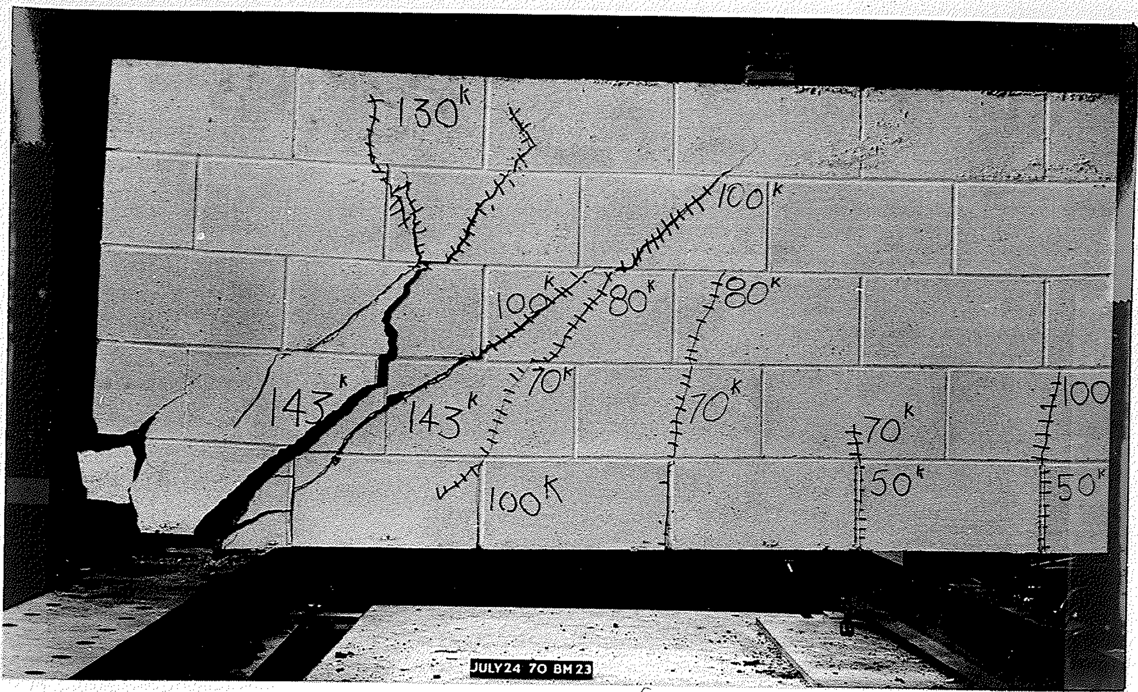

BEAM 23 SHOWING DIAGONAL TENSION CRACK

FIGURE 77

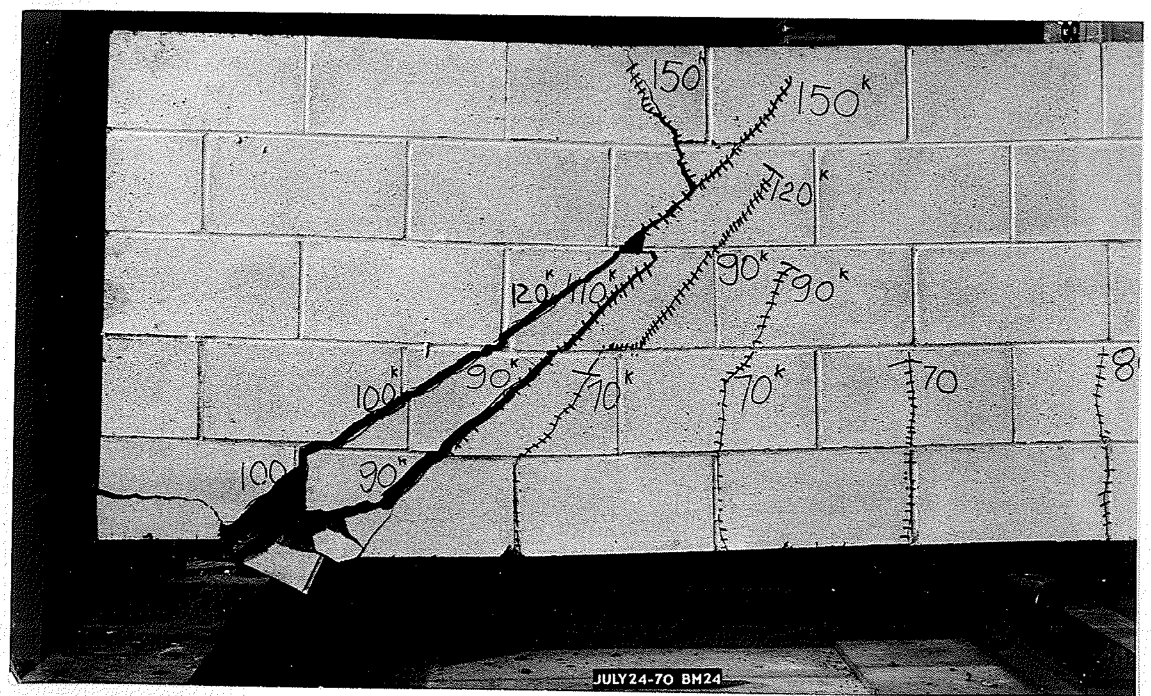

BEAM 24 SHOWING DIAGONAL TENSION CRACK

FIGURE 78

TABLE XXVI

TEST DATA FOR BEAM 23
LOAD-MIDSPAN DEFLECTION RESULTS

Load (Bm.23) (kips)	Deflection (Bm.23) (inches)	Load (Bm.23) (kips)	Deflection (Bm.23) (inches)
0.0	0.0	42.0	0.094
1.0	0.0	43.0	0.097
2.0	0.0	44.0	0.100
3.0	0.0	45.0	0.104
4.0	0.001	46.0	0.107
5.0	0.003	47.0	0.110
6.0	0.005	48.0	0.113
7.0	0.007	49.0	0.116
8.0	0.009	50.0	0.120
9.0	0.011	51.0	0.129
10.0	0.014	52.0	0.131
11.0	0.016	53.0	0.134
12.0	0.019	54.0	0.138
13.0	0.021	55.0	0.141
14.0	0.024	56.0	0.144
15.0	0.026	57.0	0.147
16.0	0.028	58.0	0.149
17.0	0.030	59.0	0.152
18.0	0.032	60.0	0.156
19.0	0.035	61.0	0.161
20.0	0.037	62.0	0.164
21.0	0.040	63.0	0.167
22.0	0.042	64.0	0.170
23.0	0.044	65.0	0.173
24.0	0.046	66.0	0.176
25.0	0.048	67.0	0.179
26.0	0.050	68.0	0.182
27.0	0.053	69.0	0.185
28.0	0.055	70.0	0.188
29.0	0.057	71.0	0.194
30.0	0.060	72.0	0.197
31.0	0.062	73.0	0.200
32.0	0.064	74.0	0.203
33.0	0.066	75.0	0.206
34.0	0.069	76.0	0.211
35.0	0.072	77.0	0.213
36.0	0.075	78.0	0.217
37.0	0.078	79.0	0.220
38.0	0.081	80.0	0.224
39.0	0.084	81.0	0.230
40.0	0.087	82.0	0.234
41.0	0.091	83.0	0.236

TABLE XXVI CONT'D.

TEST DATA FOR BEAM 23
LOAD-MIDSPAN DEFLECTION RESULTS

Load (Bm.23) (kips)	Deflection (Bm.23) (inches)	Load (Bm.23) (kips)	Deflection (Bm.23) (inches
84.0	0.239	114.0	0.350
85.0	0.242	115.0	0.354
86.0	0.247	116.0	0.358
87.0	0.250	117.0	0.362
89.0	0.259	118.0	0.365
90.0	0.262	119.0	0.370
91.0	0.267	120.0	0.374
92.0	0.270	121.0	0.378
93.0	0.273	122.0	0.382
94.0	0.278	123.0	0.386
95.0	0.287	124.0	0.390
96.0	0.290	125.0	0.392
97.0	0.293	126.0	0.400
98.0	0.296	127.0	0.404
99.0	0.299	128.0	0.408
100.0	0.302	129.0	0.412
101.0	0.305	130.0	0.416
102.0	0.307	131.0	0.421
103.0	0.310	132.0	0.424
104.0	0.314	133.0	0.430
105.0	0.317	134.0	0.435
106.0	0.320	135.0	0.440
107.0	0.324	136.0	0.450
108.0	0.326	137.0	0.455
109.0	0.330	138.0	0.462
110.0	0.335	139.0	0.468
111.0	0.340	140.0	0.475
112.0	0.344	141.0	0.482
113.0	0.347	142.0	0.490

TABLE XXVII

TEST DATA FOR BEAM 24
LOAD-MIDSPAN DEFLECTION RESULTS

Load (Bm.24) (kips)	Deflection (Bm.24) (inches)	Load (Bm.24) (kips)	Deflection (Bm.24) (inches)
0.0	0.0	42.0	0.090
1.0	0.001	43.0	0.093
2.0	0.003	44.0	0.095
3.0	0.005	45.0	0.098
4.0	0.007	46.0	0.100
5.0	0.010	47.0	0.103
6.0	0.012	48.0	0.105
7.0	0.014	49.0	0.108
8.0	0.016	50.0	0.110
9.0	0.018	51.0	0.114
10.0	0.020	52.0	0.117
11.0	0.023	53.0	0.119
12.0	0.025	54.0	0.122
13.0	0.027	55.0	0.125
14.0	0.029	56.0	0.128
15.0	0.031	57.0	0.131
16.0	0.033	58.0	0.134
17.0	0.035	59.0	0.137
18.0	0.037	60.0	0.142
19.0	0.039	61.0	0.147
20.0	0.041	62.0	0.150
21.0	0.043	63.0	0.153
22.0	0.045	64.0	0.155
23.0	0.047	65.0	0.158
24.0	0.049	66.0	0.161
25.0	0.051	67.0	0.164
26.0	0.053	68.0	0.167
27.0	0.055	69.0	0.170
28.0	0.057	70.0	0.173
29.0	0.059	71.0	0.178
30.0	0.061	72.0	0.180
31.0	0.063	73.0	0.183
32.0	0.065	74.0	0.185
33.0	0.067	75.0	0.188
34.0	0.069	76.0	0.191
35.0	0.071	77.0	0.194
36.0	0.074	78.0	0.198
37.0	0.076	79.0	0.202
38.0	0.078	80.0	0.205
39.0	0.081	81.0	0.211
40.0	0.084	82.0	0.213
41.0	0.087	83.0	0.216

TABLE XXVII

TEST DATA FOR BEAM 24
LOAD-MIDSPAN DEFLECTION RESULTS

Load (Bm.24) (kips)	Deflection (Bm.24) (inches)	Load (Bm.24) (kips)	Deflection (Bm.24) (inches)
84.0	0.218	118.0	0.345
85.0	0.221	119.0	0.348
86.0	0.224	120.0	0.351
87.0	0.227	121.0	0.357
88.0	0.235	122.0	0.361
89.0	0.239	123.0	0.364
90.0	0.242	124.0	0.367
91.0	0.252	125.0	0.370
92.0	0.255	126.0	0.373
93.0	0.257	127.0	0.376
94.0	0.260	128.0	0.380
95.0	0.263	129.0	0.383
96.0	0.267	130.0	0.386
97.0	0.270	131.0	0.396
98.0	0.274	132.0	0.400
99.0	0.277	133.0	0.403
100.0	0.280	134.0	0.406
101.0	0.290	135.0	0.410
102.0	0.292	136.0	0.414
103.0	0.295	137.0	0.418
104.0	0.298	138.0	0.423
105.0	0.301	139.0	0.426
106.0	0.304	140.0	0.431
107.0	0.307	141.0	0.434
108.0	0.310	142.0	0.438
109.0	0.313	143.0	0.442
110.0	0.316	144.0	0.447
111.0	0.323	145.0	0.452
112.0	0.326	146.0	0.457
113.0	0.329	147.0	0.462
114.0	0.332	148.0	0.467
115.0	0.335	149.0	0.474
116.0	0.338	150.0	0.480
117.0	0.342		

TABLE XXVIII

TEST DATA FOR BEAMS 23 AND 24
LATERAL DEFLECTION OF COMPRESSION ZONE

Beam No.	Load (kips)	Top Left (Gauge 1)	Top Centre (Gauge 2)	Top Right (Gauge 3)
23	0	0	0	0
	10	0.001	0	0
	20	0.002	0	0
	30	0.003	0.001	0
	40	0.004	0.001	0
	50	0.005	0.002	0.001
	60	0.005	0.002	0.001
	70	0.005	0.002	0.001
	80	0.005	0.002	0.001
	90	0.005	0.002	0.001
	110	0.005	0.002	0.025
	125	0.005	0.002	0.028
24	0	0	0	0
	25	0.021	0.026	0.014
	50	0.036	0.036	0.014
	60	0.043	0.042	0.012
	70	0.052	0.047	0.008
	80	0.060	0.051	0.012
	90	0.070	0.054	0.014
	100	0.077	0.061	0.020
	110	0.084	0.066	0.029
	120	0.092	0.069	0.035
	130	0.100	0.073	0.044

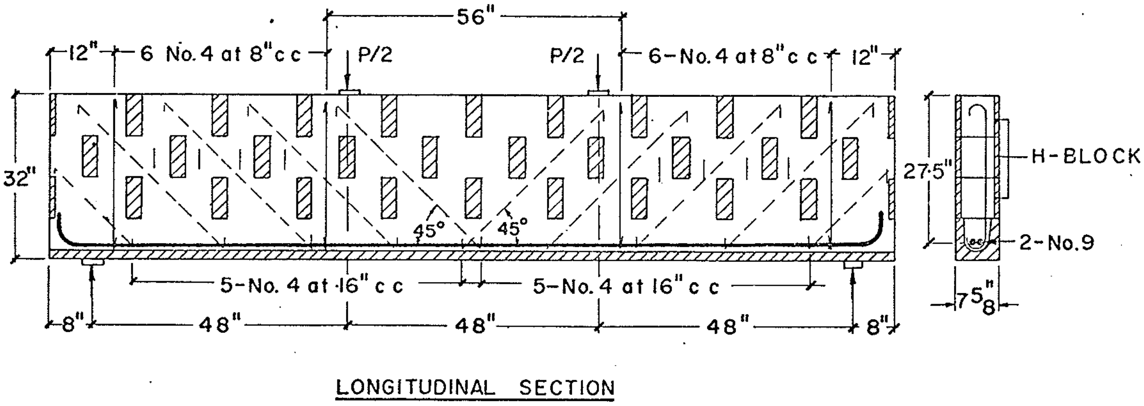

BEAM 25 – vertical steel

BEAM 26 – diagonal steel

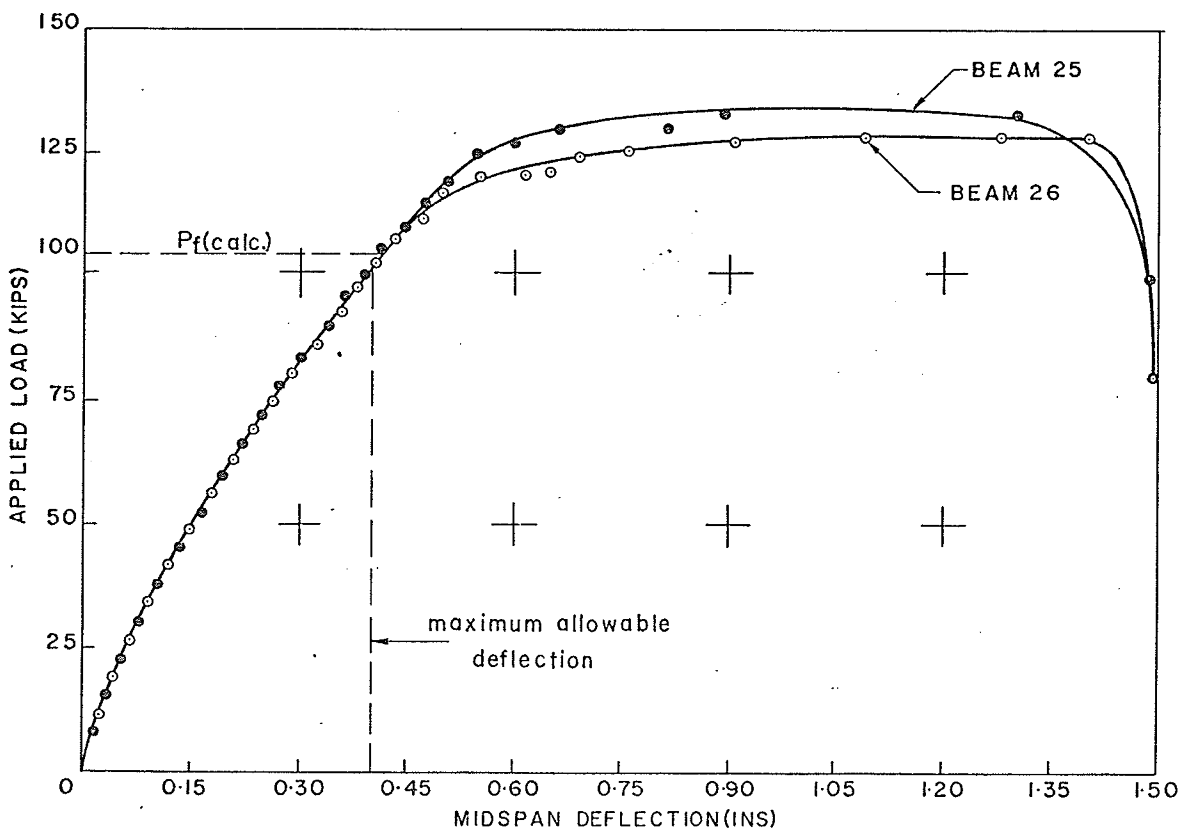

figure 79 details and load-deflection curves for beams 25 and 26

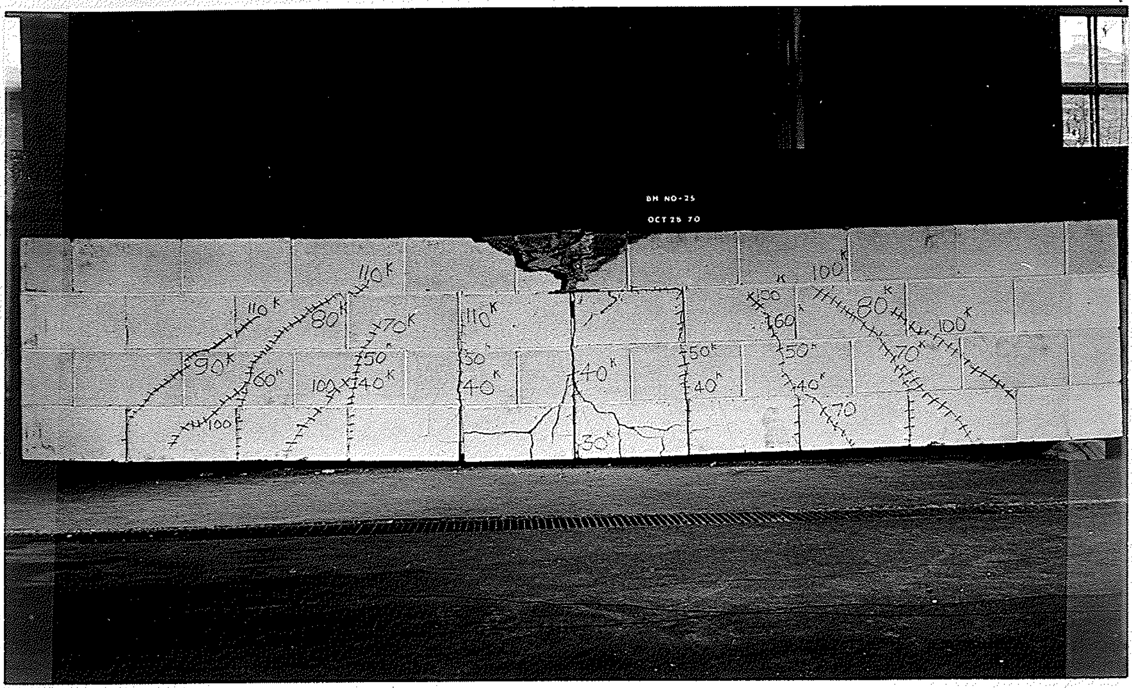

BEAM 25 SHOWING FLEXURAL FAILURE

FIGURE 80

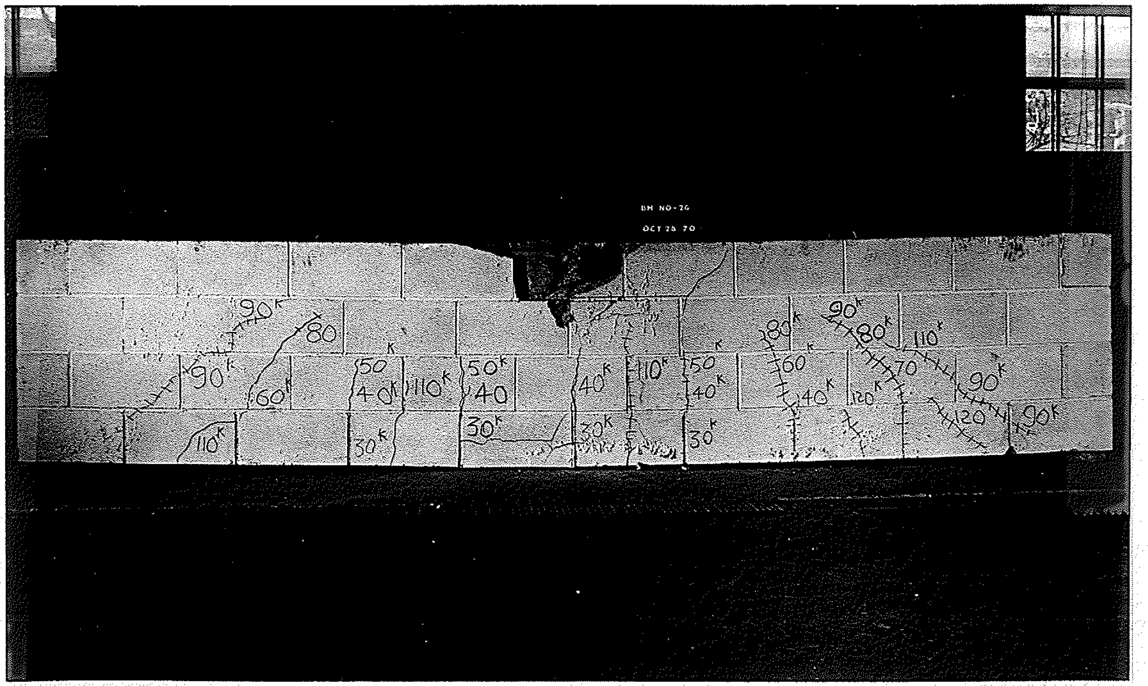

BEAM 26 SHOWING FLEXURAL FAILURE

FIGURE 81

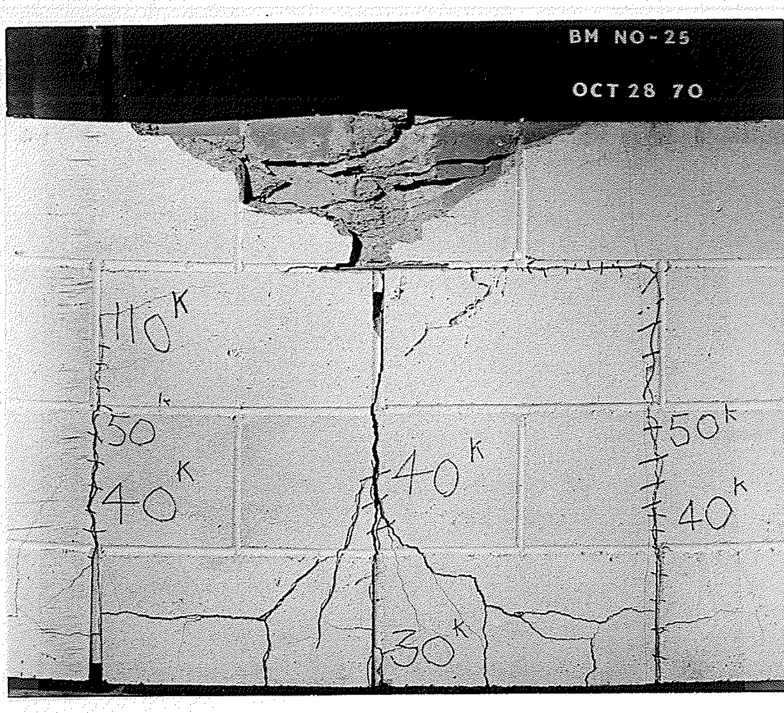

BEAM 25 SHOWING TENSION CRACKS

FIGURE 82

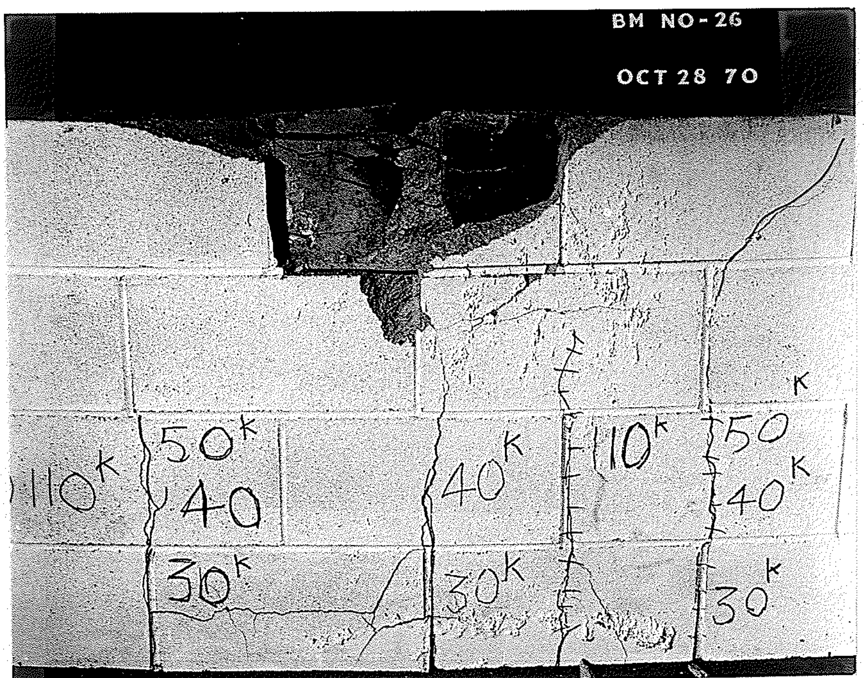

BEAM 26 SHOWING TENSION CRACKS

FIGURE 83

TABLE XXIX

TEST DATA FOR BEAM 25
LOAD-MIDSPAN DEFLECTION RESULTS

Load (Bm.25) (kips)	Deflection (Bm.25) (inches)	Load (Bm.25) (kips)	Deflection (Bm.25) (inches)
0.0	0.0	96.0	0.361
2.5	0.005	98.0	0.370
5.0	0.011	100.0	0.379
7.5	0.017	100.0	0.389
10.0	0.023	101.0	0.392
12.5	0.029	102.0	0.395
15.0	0.034	103.0	0.399
17.5	0.040	104.0	0.403
20.0	0.046	105.0	0.410
22.5	0.053	106.0	0.413
25.0	0.061	107.0	0.418
27.5	0.070	108.0	0.425
30.0	0.079	109.0	0.430
32.5	0.087	110.0	0.438
35.0	0.095	110.0	0.447
37.5	0.105	111.0	0.452
40.0	0.115	112.0	0.457
42.5	0.126	113.0	0.460
45.0	0.134	114.0	0.465
47.5	0.144	115.0	0.472
50.0	0.154	115.0	0.482
52.5	0.166	116.0	0.486
55.0	0.175	117.0	0.490
57.5	0.185	118.0	0.494
60.0	0.194	119.0	0.501
62.0	0.205	120.0	0.508
64.0	0.212	121.0	0.518
66.0	0.220	122.0	0.522
68.0	0.228	123.0	0.531
70.0	0.236	124.0	0.536
72.0	0.247	125.0	0.544
74.0	0.254	126.0	0.552
76.0	0.262	127.0	0.569
78.0	0.270	127.0	0.600
80.0	0.280	128.0	0.610
82.0	0.295	129.0	0.629
84.0	0.302	130.0	0.658
86.0	0.313	130.0	0.814
88.0	0.325	131.0	0.830
90.0	0.334	132.0	0.843
90.0	0.340	133.0	0.890
92.0	0.347	133.0	1.300
94.0	0.354	100.0	1.500

TABLE XXX

TEST DATA FOR BEAM 26
LOAD-MIDSPAN DEFLECTION RESULTS

Load (Bm.26) (kips)	Deflection (Bm.26) (inches)	Load (Bm.26) (kips)	Deflection (Bm.26) (inches)
0.0	0.0	82.5	0.310
2.5	0.005	85.0	0.320
5.0	0.011	87.5	0.332
7.6	0.017	90.0	0.346
10.0	0.023	92.5	0.360
12.5	0.029	95.0	0.370
15.0	0.035	97.5	0.381
17.5	0.041	100.0	0.393
20.0	0.048	100.0	0.399
22.5	0.055	102.0	0.407
25.0	0.063	104.0	0.415
27.5	0.072	106.0	0.426
30.5	0.080	108.0	0.439
32.5	0.089	110.0	0.452
35.0	0.097	110.0	0.466
37.5	0.105	112.0	0.474
40.0	0.113	114.0	0.483
42.5	0.124	116.0	0.496
45.0	0.133	118.0	0.510
47.5	0.144	120.0	0.557
50.0	0.154	120.0	0.615
52.5	0.165	120.0	0.636
55.0	0.175	121.0	0.650
57.5	0.185	122.0	0.660
60.0	0.197	123.0	0.674
62.5	0.210	124.0	0.690
65.0	0.220	125.0	0.759
67.5	0.231	126.0	0.786
70.0	0.241	127.0	0.910
72.5	0.253	128.0	1.090
75.0	0.269	128.0	1.280
77.5	0.275	128.0	1.400
80.0	0.287	80.0	1.500
80.0	0.292		

TABLE XXXI

TEST DATA FOR BEAMS 25 AND 26
LATERAL DEFLECTION OF COMPRESSION ZONE

Beam No.	Load (kips)	Top Left (Gauge 1)	Top Centre (Gauge 2)	Top Right (Gauge 3)
25	0	0	0	0
	10	0.068	0.065	0.064
	20	0.074	0.063	0.063
	30	0.080	0.072	0.069
	40	0.086	0.078	0.073
	50	0.091	0.084	0.077
	60	0.099	0.088	0.082
	70	0.100	0.099	0.089
	80	0.121	0.110	0.095
	90	0.130	0.120	0.104
	100	0.138	0.130	0.109
	110	0.144	0.147	0.113
	120	0.151	0.164	0.115
26	0	0	0	0
	10	0.035	-0.002	0.008
	20	0.033	0.004	0.013
	30	0.031	0.013	0.017
	40	0.032	0.021	0.025
	50	0.030	0.032	0.032
	60	0.030	0.043	0.039
	70	0.028	0.054	0.050
	80	0.027	0.065	0.060
	90	0.024	0.082	0.066
	100	0.028	0.097	0.061
	110	0.026	0.110	0.072
	120	0.025	0.048	0.082

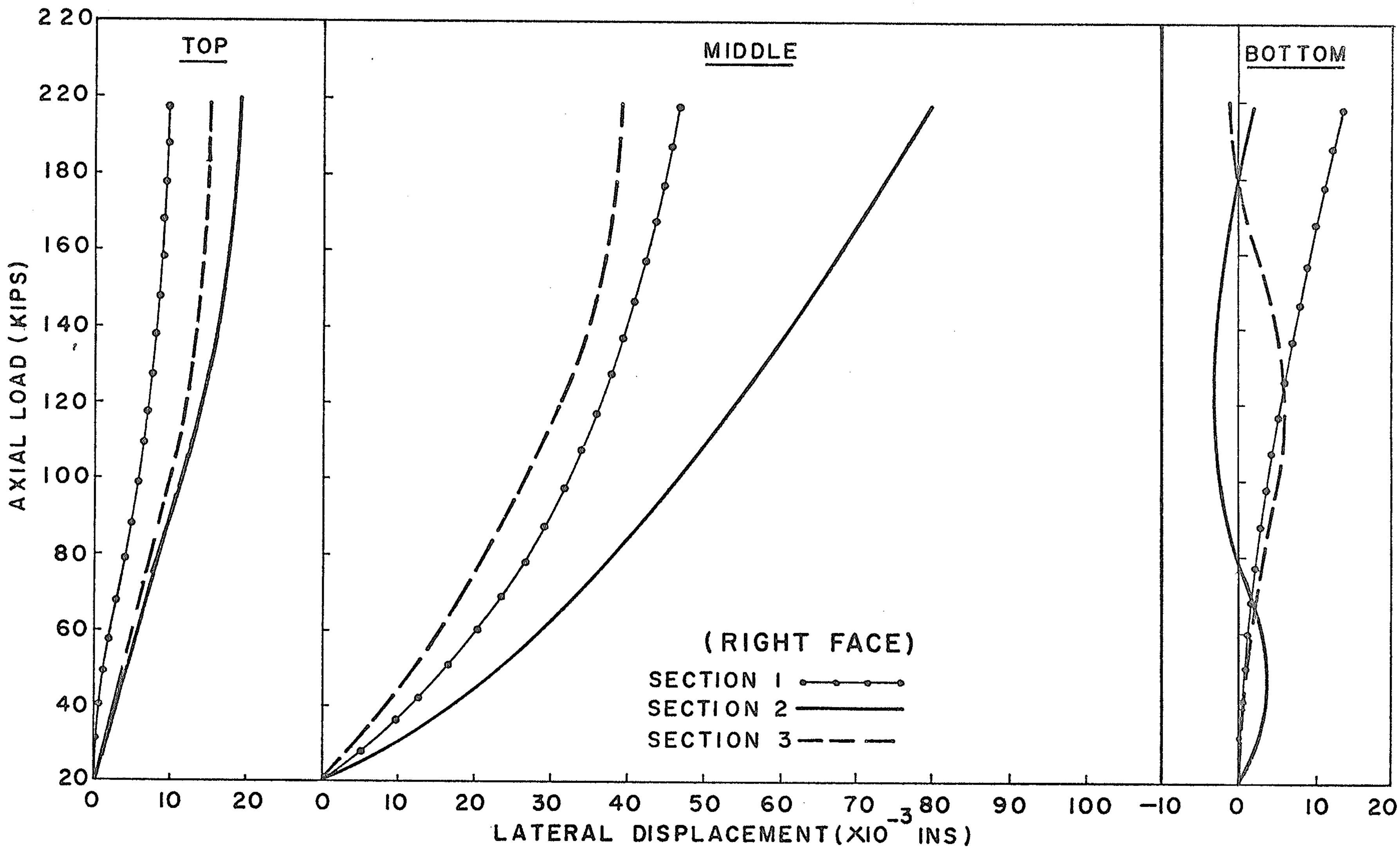

figure 84: load-lateral displacement curves for wall sections 1, 2, and 3

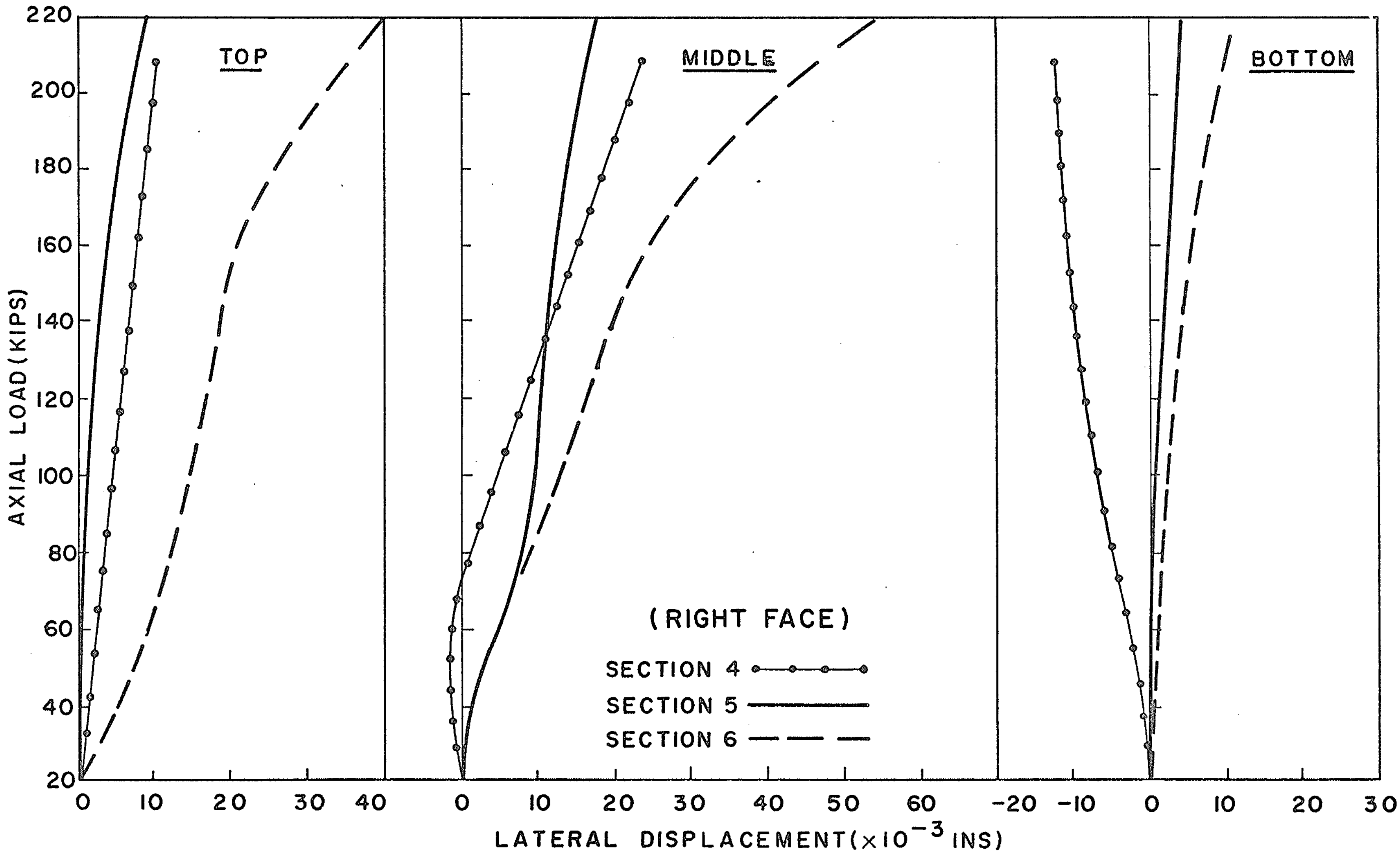

figure 85: load lateral displacement curves for wall sections 4, 5 and 6

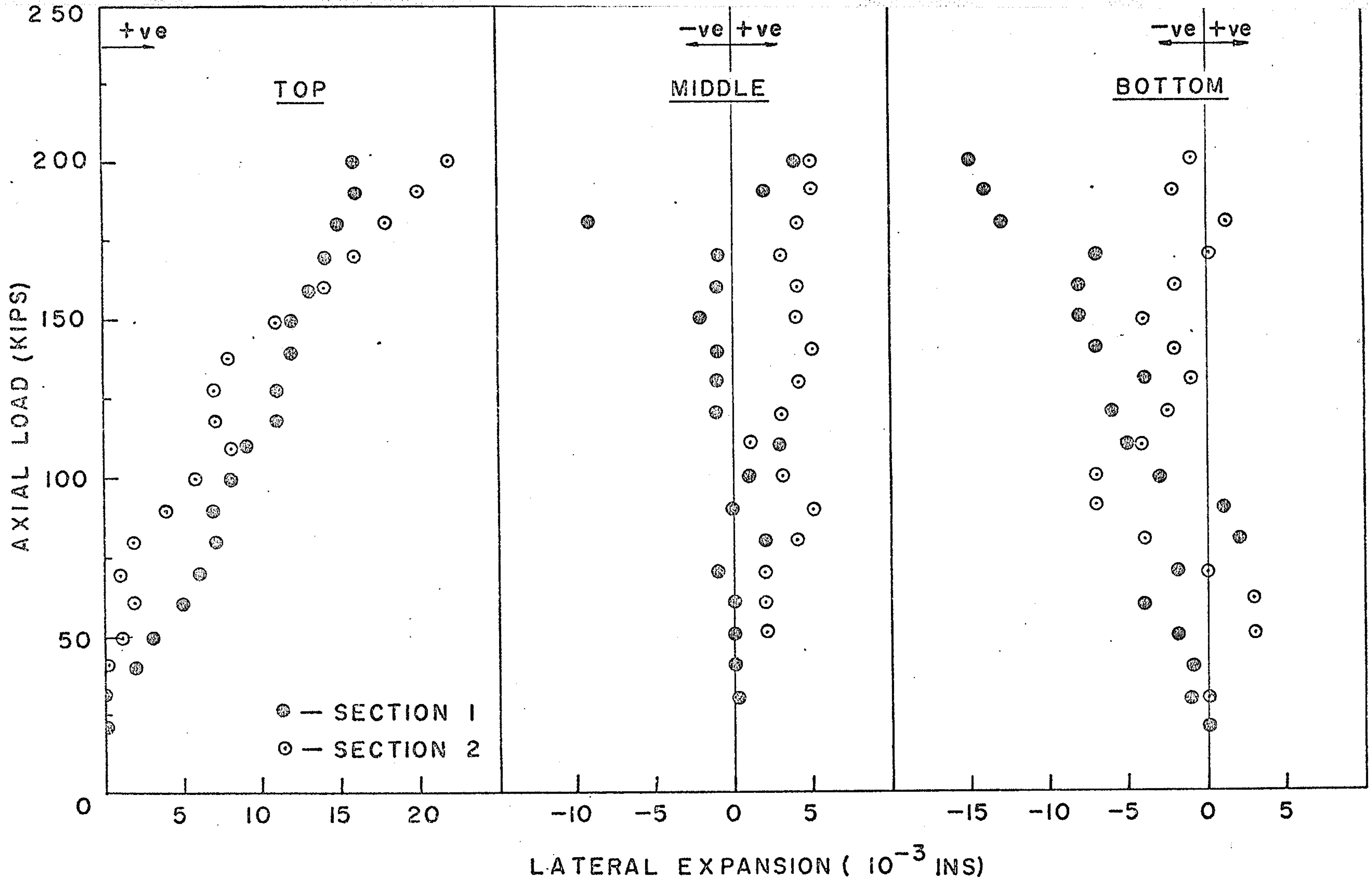

figure 86: load – lateral expansion curves for wall sections 1 and 2

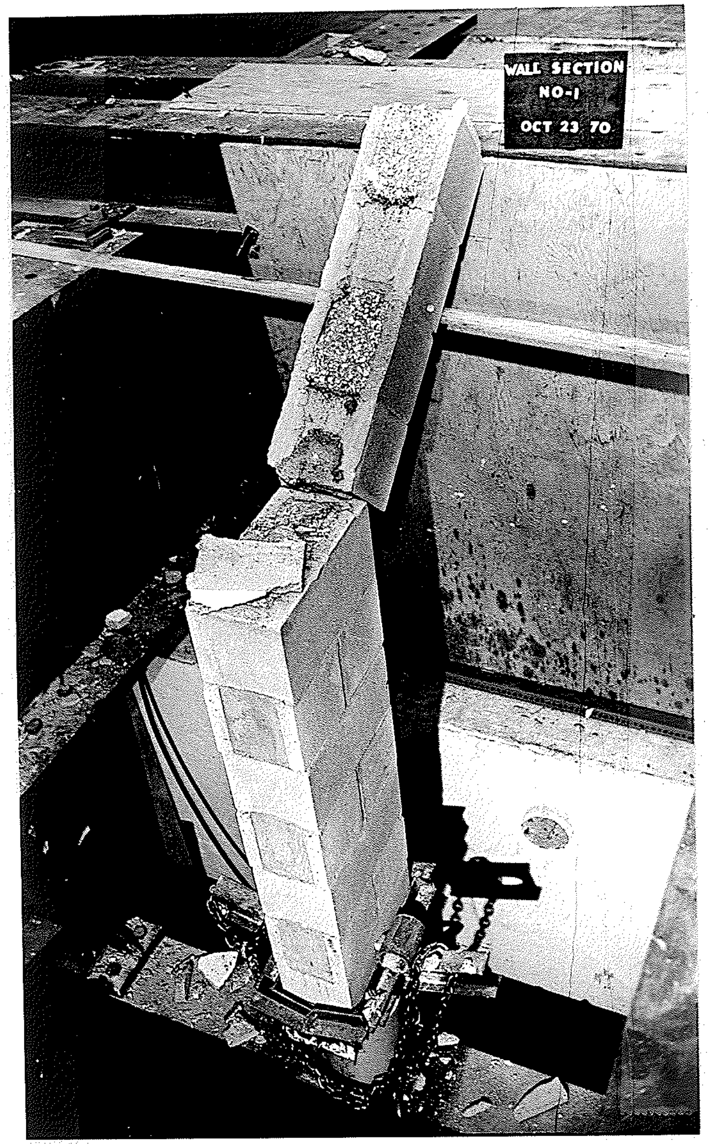

WALL SECTION 1 AT FAILURE

FIGURE 87

TABLE XXXII

TEST DATA FOR WALL SECTION 1

LATERAL DISPLACEMENT AND EXPANSION AGAINST LOAD

LOAD		LATERAL DISPLACEMENT (ins) Right Face			LATERAL DISPLACEMENT (ins) Left Face			LATERAL EXPANSION (ins)		
Gauge (p.s.i.)	Eqv. Load (kips)	Top (Gauge 1)	Middle (Gauge 2)	Bottom (Gauge 3)	Top (Gauge 4)	Middle (Gauge 5)	Bottom (Gauge 6)	Top Gauge1&4	Middle Gauge2&5	Bottom Gauge3&6
500	19.8	0	0	0	0	0	0	0	0	0
750	29.6	0	0.005	0.001	-0	-0.005	-0.002	0	0	-0.001
1000	39.5	0.001	0.010	0.001	0.001	-0.010	-0.002	0.002	0	-0.001
1250	48.9	0.002	0.016	0.001	0.001	-0.016	-0.003	0.003	0	-0.002
1500	58.4	0.002	0.020	0.001	0.003	-0.020	-0.005	0.005	0	-0.004
1750	68.4	0.004	0.024	0.003	0.002	-0.023	-0.005	0.006	-0.001	-0.002
2000	78.5	0.005	0.027	0.005	0.002	-0.025	-0.003	0.007	0.002	0.002
2250	88.4	0.005	0.029	0.007	0.002	-0.029	-0.006	0.007	0	0.001
2500	98.4	0.006	0.032	0.007	0.002	-0.031	-0.010	0.008	0.001	-0.003
2750	108.0	0.006	0.033	0.005	0.003	-0.033	-0.010	0.009	0.003	-0.005
3000	118.2	0.008	0.034	0.005	0.003	-0.035	-0.011	0.011	-0.001	-0.006
3250	127.0	0.008	0.036	0.008	0.003	-0.037	-0.012	0.011	-0.001	-0.004
3500	137.8	0.008	0.039	0.008	0.004	-0.040	-0.015	0.012	-0.001	-0.007
3750	148.0	0.008	0.040	0.008	0.004	-0.042	-0.016	0.012	-0.002	-0.008
4000	158.0	0.009	0.043	0.008	0.004	-0.044	-0.016	0.013	-0.001	-0.008
4250	167.8	0.009	0.044	0.012	0.005	-0.045	-0.019	0.014	-0.001	-0.007
4500	177.5	0.010	0.045	0.014	0.005	-0.054	-0.027	0.015	-0.009	-0.013
4750	187.5	0.010	0.045	0.014	0.006	-0.043	-0.028	0.016	+0.002	-0.014
5000	197.5	0.010	0.047	0.014	0.006	-0.043	-0.029	0.016	+0.004	-0.015

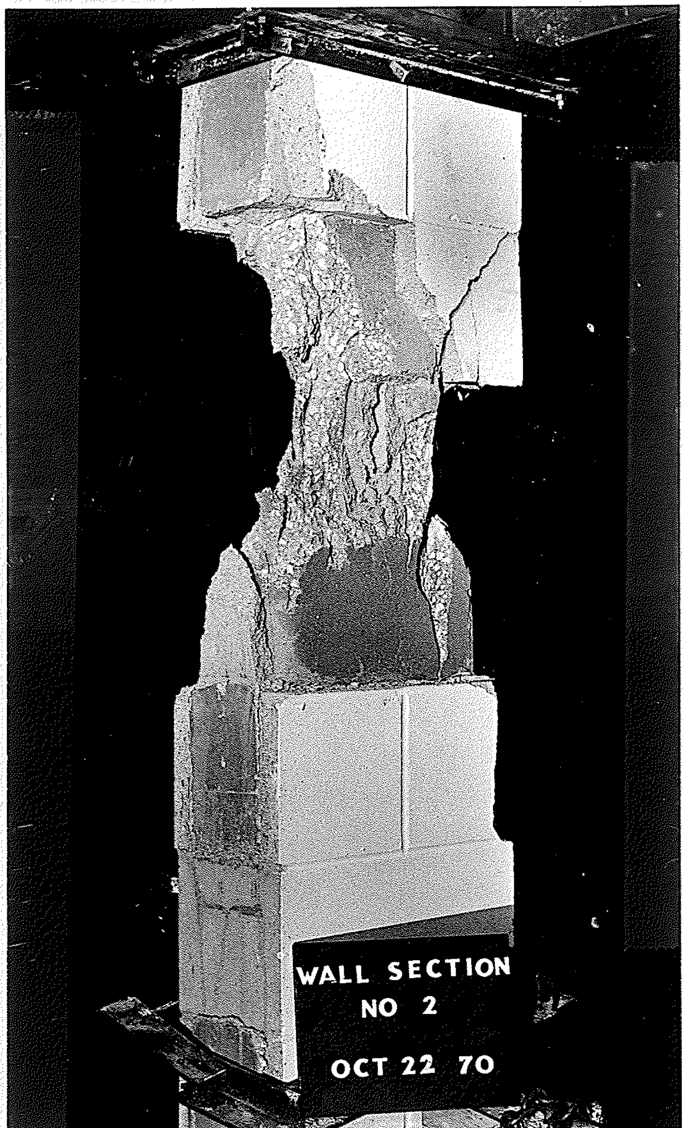

WALL SECTION 2 AT FAILURE

FIGURE 88

TABLE XXXIII

TEST DATA FOR WALL SECTION 2

LATERAL DISPLACEMENT AND EXPANSION AGAINST LOAD

LOAD		LATERAL DISPLACEMENT (ins) Right Face			LATERAL DISPLACEMENT (ins) Left Face			LATERAL EXPANSION (ins)		
Gauge (p.s.i.)	Eqv.Load (kips)	Top (Gauge 1)	Middle (Gauge2)	Bottom (Gauge3)	Top (Gauge4)	Middle (Gauge5)	Bottom (Gauge6)	Top (Gauge1&4)	Middle (Gauge2&5)	Bottom (Gauge3&6)
500	19.8	0	0	0	0	0	0	0	0	0
750	29.6	0.001	0.009	0.001	-0.001	-0.009	-0.001	0	0	0
1000	39.5	0.003	0.016	0.001	-0.003	-0.016	-0.002	0	0	-0.001
1250	48.9	0.004	0.022	0.004	-0.003	-0.020	-0.001	0.001	0.002	0.003
1500	58.4	0.006	0.027	0.004	-0.004	-0.025	-0.001	0.002	0.002	0.003
1750	68.4	0.006	0.031	0.001	-0.005	-0.029	-0.001	0.001	0.002	0
2000	78.5	0.007	0.034	0.001	-0.005	-0.030	-0.005	0.002	0.004	-0.004
2250	88.4	0.009	0.036	0.0	-0.005	-0.031	-0.007	0.004	0.005	-0.007
2500	98.4	0.010	0,040	-0.003	-0.004	-0.037	-0.004	0.006	0.003	-0.007
2750	108.0	0.013	0.052	-0.003	-0.005	-0.051	-0.001	0.008	0.001	-0.004
3000	118.2	0.014	0,060	-0.002	-0.007	-0.057	0	0.007	0.003	-0.002
3250	127.0	0.015	0.068	-0.001	-0.064	0		0.004	-0.001	
3500	137.8	0.016	0.073	0.0	-0.008	-0.068	-0.002	0.008	0.005	-0.002
3750	148.0	0.017	0.067	-0.004	-0.006	-0.063	0	0.011	0.004	-0.004
4000	158.0	0.017	0.070	-0.002	-0.003	-0.066	0	0.014	0.004	-0.002
4250	167.8	0.018	0.071	-0.001	-0.002	-0.068	0.001	0.016	0.003	0
4500	177.5	0.018	0.073	0.0	0.0	-0.069	0.001	0.018	0.004	0.001
4750	187.5	0.019	0.076	0.001	0.001	-0.071	-0.003	0.020	0.005	-0.002
5000	197.5	0.019	0.080	0.002	0.003	-0.075	-0.003	0.022	0.005	-0.001

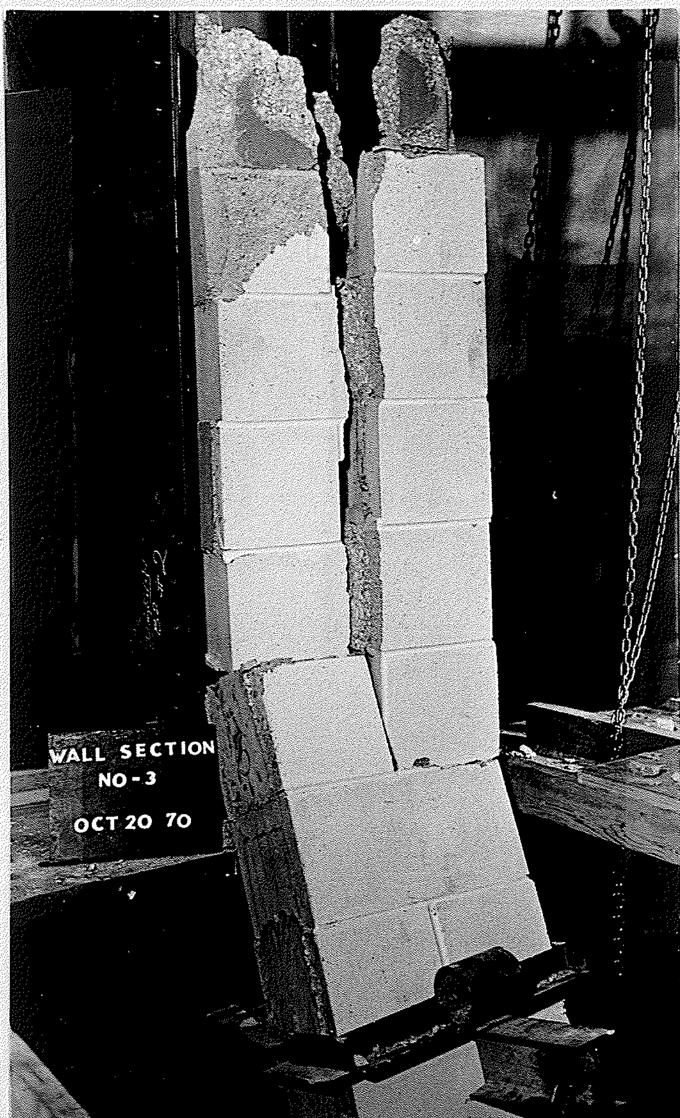

WALL SECTION 3 AT FAILURE

FIGURE 89

TABLE XXXIV

TEST DATA FOR WALL SECTION 3
LATERAL DISPLACEMENT AGAINST LOAD

Load		Lateral Displacement (ins.) Right Face		
Gauge Reading (p.s.i.)	Eqv. Load (kips)	Top (gauge 1)	Middle (gauge 2)	Bottom (gauge 3)
500	19.8	0	0	0
750	29.6	0.002	0.007	0.002
1000	39.5	0.003	0.008	0.002
1250	48.9	0.005	0.012	0.001
1500	58.4	0.006	0.014	0.001
1750	68.4	0.007	0.017	0.002
2000	78.5	0.008	0.021	0.003
2250	88.4	0.009	0.024	0.004
2500	98.4	0.010	0.027	0.004
2750	108.0	0.011	0.028	0.005
3000	118.2	0.012	0.031	0.005
3250	127.0	0.013	0.033	0.006
3500	137.8	0.013	0.035	0.006
3750	147.9	0.014	0.035	0.003
4000	158.0	0.014	0.036	0.003
4250	167.8	0.014	0.040	0.000
4500	177.5	0.015	0.040	0.000
4750	187.5	0.015	0.039	-0.001
5000	197.5	0.015	0.039	-0.001
5800	228.0	-	-	-

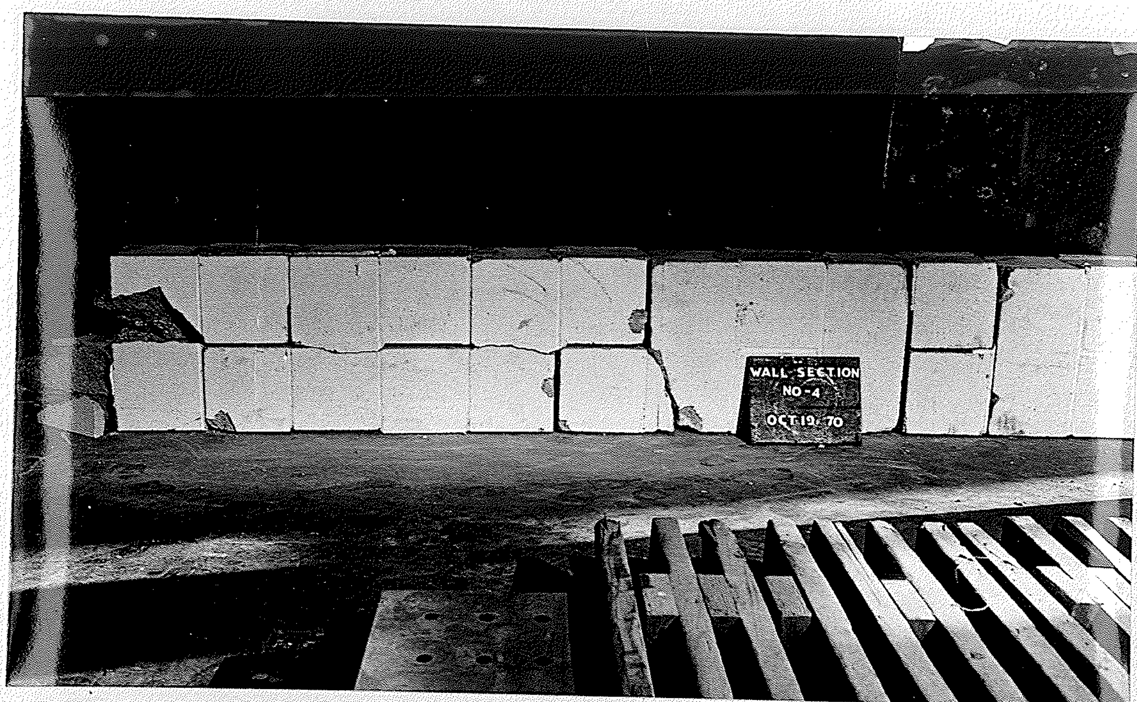

WALL SECTION 4 AT FAILURE

FIGURE 90

TABLE XXXV

TEST DATA FOR WALL SECTION 4
LATERAL DISPLACEMENT AGAINST LOAD

Load		Lateral Displacement (ins.) Right Face		
Gauge Reading (p.s.i.)	Eqv. Load (kips)	Top (gauge 1)	Middle (gauge 2)	Bottom (gauge 3)
500	19.8	0	0	0
1000	39.5	0.001	-0.001	0
1250	48.9	0.002	-0.001	-0.001
1500	58.4	0.002	-0.001	-0.001
1750	68.4	0.003	-0.001	-0.002
2000	78.5	0.003	-0.001	-0.004
2250	88.4	0.004	0.000	-0.005
2500	98.4	0.005	0.002	-0.005
2750	108.0	0.005	0.005	-0.007
3000	118.2	0.006	0.007	-0.008
3250	127.0	0.006	0.009	-0.009
3500	137.8	0.007	0.010	-0.008
3750	149.9	0.007	0.010	-0.008
4000	158.0	0.008	0.014	-0.008
4256	167.8	0.009	0.017	-0.008
4500	177.5	0.009	0.018	-0.010
4750	187.5	0.009	0.018	-0.010
5000	197.5	0.010	0.020	-0.010
5250	2070	0.011	0.022	-0.012
5500	2175	0.011	0.024	-0.013
5750	228.0	-	0.027	-
6000	237.5	-	0.029	-
6250	247.0	-	0.030	-
6500	257.0	-	0.032	-
7400	292.0	-	-	-

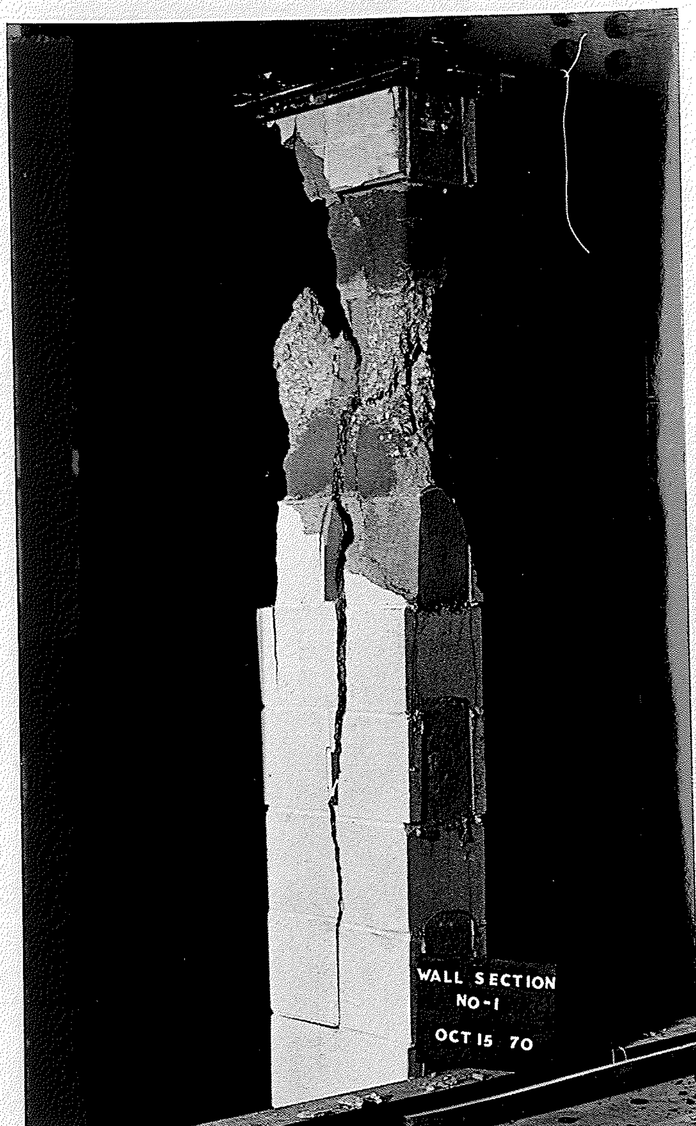

WALL SECTION 5 AT FAILURE

FIGURE 91

TABLE XXXVI

TEST DATA FOR WALL SECTION 5
LATERAL DISPLACEMENT AGAINST LOAD

Load		Lateral Displacement (ins.) Right Face		
Gauge Reading (p.s.i.)	Eqv. Load (Kips)	Top (gauge 1)	Middle (gauge 2)	Bottom (gauge 3)
500	19.8	0	0	0
750	29.6	0	0	0
1000	39.5	0	0	0
1250	48.9	0	0	0
1500	58.4	0.001	0.005	0
1750	68.4	0.001	0.007	0
2000	78.5	0.002	0.009	0
2250	88.4	0.002	0.009	0.001
2500	98.4	0.002	0.010	0.001
2750	108.0	0.003	0.010	0.001
3000	118.2	0.003	0.010	0.002
3250	127.0	0.084	0.011	0.002
3500	137.8	0.004	0.012	0.002
3750	148.0	0.005	0.012	0.002
4000	158.0	0.006	0.012	0.002
4250	167.8	0.006	0.012	0.003
4500	177.5	0.007	0.014	0.003
4750	187.5	0.007	0.016	0.003
5000	197.5	0.008	0.016	0.003
5250	207.0	0.008	0.016	0.004
5500	217.5	0.009	0.017	0.004
5750	228.0	0.009	0.023	0.004
6000	237.5	0.010	0.025	0.004
6200	245.0	-	-	-

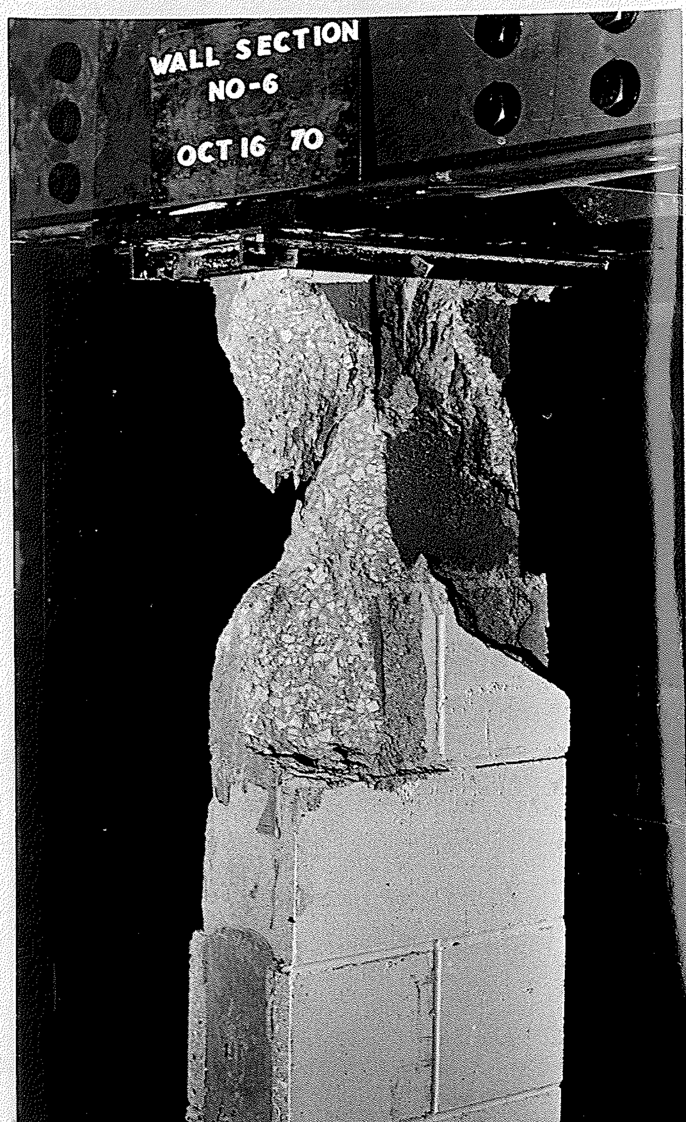

WALL SECTION 6 AT FAILURE

FIGURE 92

TABLE XXXVII

TEST DATA FOR WALL SECTION 6
LATERAL DISPLACEMENT AGAINST LOAD

Load		Lateral Displacement (ins.) Right Face		
Gauge Reading (p.s.i.)	Eqv. Load (kips)	Top (gauge 1)	Middle (gauge 2)	Bottom (gauge 3)
500	19.8	0	0	0
750	29.6	0.005	0	0.007
1000	39.5	0.007	0	0.005
1250	48.9	0.009	0.003	0.003
1500	58.4	0.010	0.005	0.002
1750	68.4	0.011	0.008	0.004
2000	78.5	0.013	0.008	0.004
2250	99.4	0.014	0.015	0.004
2500	98.4	0.015	0.017	0.002
2750	108.0	0.016	0.015	0.002
3000	118.2	0.017	0.015	0.002
3250	127.0	0.018	0.017	0.003
3500	137.8	0.018	0.017	0.005
3750	148.0	0.019	0.019	0.005
4000	158.0	0.025	0.027	0.005
4250	167.8	0.027	0.024	0.006
4500	177.5	0.029	0.028	0.006
4750	187.5	0.032	0.037	0.007
5000	197.5	0.034	0.043	0.008
5250	207.5	0.039	0.047	0.008
5500	217.5	0.039	0.053	0.010
5750	228.0	0.043	0.056	0.014
6000	237.5	0.044	0.058	0.015
7100	280.0	-	-	-